Master Thesis

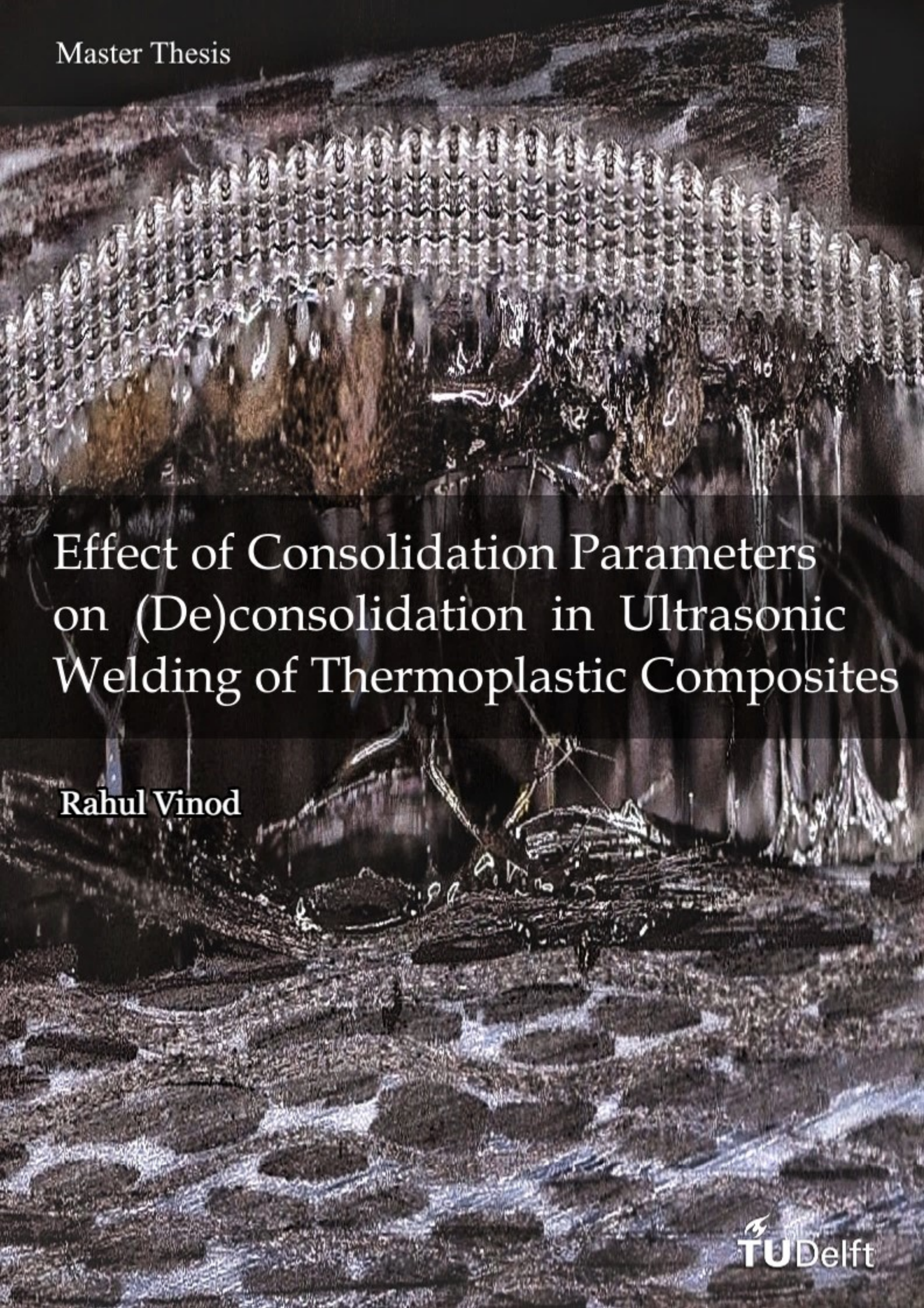

Effect of Consolidation Parameters on (De)consolidation in Ultrasonic Welding of Thermoplastic Composites

Rahul Vinod

TUDelft

Master's Thesis

Effect of Consolidation Parameters on (De)consolidation in Ultrasonic Welding of Thermoplastic Composites

by

Rahul Vinod

to obtain the degree of Master of Science

at the Delft University of Technology,

to be defended publicly on Tuesday, 25th August 2020 at 02:00 PM.

Student number: 4888758

Thesis Committee:

Dr. Irene Fernandez Villegas,	TU Delft, Chairperson and Supervisor
Dr. Sergio Turteltaub,	TU Delft, Examiner
Dr. Julie Teuwen,	TU Delft, Examiner
Ir. Bram Jongbloed,	TU Delft, Daily Supervisor

TU Delft Delft University of Technology

Acknowledgement

First and foremost, I would like to thank my thesis supervisor, Dr. Irene Fernandez Villegas, who inspired me to pursue a thesis in composite welding. Thank you for all your patience, enthusiasm and assistance and all the freedom you've given me during this thesis work. It was your constant feedback and positive criticism that pushed this thesis to the level that it is now.

I would like to express my deepest gratitude to Ir. Bram Jongbloed for supervising me in this thesis. You have been a great source of inspiration - both as a friend and as a scholar. Thank you for sharing your knowledge and technical know-how on the subject. If it weren't for your constant guidance and tips, this thesis would have been far lesser in content and significance.

I am also grateful to all the members of the composite welding group for putting up with my constant barrage of questions. I spend a great deal of time and effort at the Delft Aerospace Structures and Materials Laboratory (DASML). I would like to extend my gratitude particularly to Durga Mainali, Victor Horbowiec, Dave Ruijtenbeek, and Marlies Nijemeisland for their tips, suggestions and help. I would like to thank Ellen Meijvogel-de Koning and Wim Verwaal from the Geoscience and Engineering Laboratory, Department of Civil engineering and Geosciences, for their help on the micro-CT scans.

I would also like to express my sincere gratitude to Dr. Julie Teuwen and Dr. Sergio Turteltaub for taking time out of their schedule to review my work and agreeing to be on my thesis committee.

I would like to thank all my professors, both in my master's and bachelor's, who had to put up with me. I would also like to express my gratitude to my fellow ASM classmates and all my colleagues in NB 1.07. I loved the long discussions and camaraderie of working with you all. A special shout out to Abhas for taking time out to review my report and all the brainstorming sessions we've had throughout my research. A very special word of appreciation to Tanya for providing me with the confidence and support for the past year throughout this journey. Also, thank you for all the inputs on my presentations.

I would also like to thank all my former colleagues at TAML. I would also like to acknowledge all KSA members, for their constant support and for making my life at Delft a very memorable and truly enjoyable experience. A big shout-out to Abhijith Kamath for his regular assistance and Govind for helping me with the front cover of the report. I would like to extend my gratitude to all my comrades at RIT MH for motivating me and shaping me to the individual that I am today. You guys have been awesome and a great source of encouragement.

I'll forever be indebted to my parents, Vinod and Prasanthi, and my brother, Vimal, and my grandparents and relatives for their constant encouragement, love and unwavering support without which I would not have been able to pursue my dreams and ambitions.

And finally, for all those who weren't pestering me with the "when will you finish your Master's" question - a big thank you!!

Rahul Vinod
Delft, August 2020

Executive Summary

Thermoplastic composites are gaining prominence in the aerospace industry owing to their higher damage tolerance, cost-efficient means of manufacturing, and the possibility to be recycled. One of the major benefits of thermoplastics compared to thermosets is their ability to be welded, and one of the most promising welding techniques for thermoplastic composites is ultrasonic welding. Ultrasonic welding is the fastest welding technique currently known, with typical weld times of a few hundred milliseconds.

Studies have been conducted in plenty regarding static ultrasonic welding of thermoplastic composites. But the industrialisation of the process involves the development of a robust continuous ultrasonic welding process which can weld the entire span of the joints, thus enabling higher load transfer and reduced stress concentrations. However, the state-of-the-art continuous ultrasonic welded joints contain voids at various locations within the weld which are assumed to appear due to a lack of consolidation during the welding process. Unlike the static ultrasonic welding, where the sonotrode can both transfer the vibrational energy to the adherends being weld and provide consolidation force, the continuous ultrasonic welding requires a separate consolidation device to provide consolidation pressure application. This makes it necessary to expand the understanding of the consolidation process to improve the weld quality and increase the Technology Readiness Level (TRL) of the ultrasonic welding process before it can be industrially used. While a lot of research to date focused on the vibration phase of the process, not much information is available regarding the consolidation phase. This research project thus explores the effect of consolidation pressure and time on (de)consolidation in ultrasonic welding of thermoplastic composites.

An experimental study was carried out on the consolidation in static welding of CF/PPS test coupons, and the knowledge obtained was extended to the continuous ultrasonic welding process. The consolidation in the continuous ultrasonic welding process was provided by a separate consolidation device or ”consolidator” placed behind the sonotrode. Various characterisation techniques including lap shear strength, void content assessment and fracture surface analysis were used to analyse the results obtained. The experiments revealed that for semi-crystalline polymer PPS, consolidation should start when the polymer is in its melt state and extend until the interface temperature of the weld drops below the crystallisation temperature of the polymer. The results obtained indicated that the voids in ultrasonic welding were formed due to a combination of shrinkage due to crystallisation, fibre decompaction, the choice of the clamps used and excessive squeeze out of the resin. In continuous ultrasonic welding, the location of the consolidator behind the sonotrode and the consolidation pressure was found to influence the weld quality.

The research conclusions serve as a first step towards developing a robust consolidation process in continuous ultrasonic welding of thermoplastic composites.

Rahul Vinod
Delft, August 2020

Contents

List of Figures

List of Tables

Acronyms

ACARE Advisory Council for Aviation Research and Innovation in Europe.

CF carbon fibre.

CT computed tomography.

CUW continuous ultrasonic welding.

DSC differential scanning calorimetry.

ED energy director.

HAZ heat affected zone.

LSS lap shear strength.

PEEK Polyetheretherketone.

PEI Polyetherimide.

PPS polyphenylene sulfide.

Tc crystallisation temperature.

Tg glass transition temperature.

Tm melting temperature.

TRL technology readiness levels.

USW ultrasonic welding.

1

Introduction

1.1. Background

Empowering humans with the ability to fly was one of the most phenomenal achievements of the 20th century. The initial aircrafts of the 1900-20s, made of wood, could not sustain long periods of service. Not long after that, aluminium replaced wood in the manufacture of aerospace structures. The military advancements and the need to develop materials that were lighter and cheaper, more resistant to fatigue and corrosion, and improve tolerances to damage pushed the aircraft industry to seek new materials. Soon the age of composites in the aerospace industry began. Composites are materials obtained by combining two or more physically and chemically different constituents to produce a new material with properties different from the individual constituents. The superior strength to weight ratio, fatigue properties, and chemical resistance compared to metals and the ability to tailor properties by effectively orienting the fibres within the material made fibre-reinforced composites an ideal candidate for aircraft structures.

Various types of fibres are used in aerospace composites, including carbon, glass, and aramids. Similarly, the matrix can be classified into thermosets and thermoplastics. The thermosets can only be cured once due to the cross-linking of the polymer chains. On the contrary, thermoplastics can be recycled by melting into soft materials by heating above a specific temperature and solidifying on cooling since they do not form a 3D-cross sectional structure after processing. The appeal for thermoplastics hence stems from this advantage, a requirement that has gained prominence in the last few decades due to increased societal emphasis on green materials and technology. Additionally, the widely used thermoset composite prepregs have limited shelf life, and the production cycle time of thermosets are much longer than thermoplastics. As the manufacturing industry is expanding and highly complicated structures are being designed, it is vital that processes that can manufacture parts at high production rates and are cost-effective are developed. The advantages of thermoplastics can hence be widely taken advantage of, in both manufacturing and repair of structures. Though thermoplastics are currently not as widespread as thermosets in the aerospace industry, the said characteristics of the material serve a great potential to revolutionise the aerospace materials market.

1.2. Evolution of the joining technologies

It is considered that humans first started producing metals chemically for their needs almost 6000 years ago [1]. Ever since the number of new materials discovered and used in the manufacturing of various parts has increased profoundly. The development of new materials also propelled the need to develop new manufacturing technologies. From using fire and stones to make tools for their regular use, humans have come far a,s technology advanced over time. Soon enough, humans realised the difficulty in making larger, intricate parts and thus the joining technologies advanced. From a basic concept of tying stones to wooden handles to make spears, humans have advanced far in manufacturing and joining techniques. It was soon understood that manufacturing multiple parts and joining them together is a more suitable way of manufacturing rather than the manufacture of a

complete part. This realisation is quite exemplified by the fact that a single B747-8 is comprised of 6 million parts in total [2]. At the same time, the realisation of the assembly process meant an increase in the manufacturing cost and time, broader supply chain systems and increase in part weight. Thus, the design of a new joining solution involved producing joints with sufficient strength, reducing further part weight, and reducing the time and cost involved for the assembly. The traditional methods that have been employed in joining metals (and thermosets) in the aircraft industry are adhesive bonding and mechanical assembly. However, employing these joining techniques for thermoplastics is not ideal considering the unique properties of the thermoplastic composites. Mechanical fastening creates stress concentration in the material, delaminations, galvanic corrosions, increases man-material-machine costs and process time. Adhesive bonding requires considerable surface preparation, can degrade over time and has long curing times. While adhesive bonding is in widespread use for joining thermoset composites, the chemical inertness of thermoplastics prevents it from being bonded together via adhesives. This is where thermoplastic ultrasonic welding (USW), a joining technique that stems from the ability of thermoplastic to be recycled, serves as a potential alternative.

Welding is one of the prominent methods of permanently joining two parts, along with mechanical and adhesive joints. Welding makes the joint leak proof and hence is a valuable joining method where water or gas must be sealed. Since there is no incorporation of extra parts like in the case of mechanical assembly in the form of rivets or bolts, there is no mass or weight increase. Welding makes it possible to join dissimilar parts as well. Welding of metals has been at the forefront of joining technologies for decades now. But the use of welding to join thermoplastic components is a relatively new concept. It was not until induction welding was employed on the tail section of the Gulfstream G650 [3] that thermoplastic welding was employed in the critical control surface of a commercial aircraft. The J-nose of the A380 (resistance welded) is another example where welded thermoplastic composite structures are being used in the aircraft industry [4].

1.3. Motivation

One of the main goals of the FlightPath 2050 goals of the Advisory Council for Aviation Research and Innovation in Europe (ACARE) in the environment and energy sector is to design and manufacture aircrafts that are recyclable. A few requirements laid down include the development of new materials with improved mechanical and assembly characteristics, design of new manufacturing and assembly processes, improvement of repair technologies to improve the ecological footprint and optimisation of material re-utilisation [5]. The higher damage tolerance, cost-efficient means of manufacturing, possibility to be recycled and the ability to be welded together makes thermoplastics an excellent choice over metals and thermoset composites. Thermoplastic composites are thus a potential futuristic option for structural and semi-structural components in both the automotive industry (requiring high production rates) and the aerospace industry (complex and high-performance parts) [6]. This is slowly leading to a shift of focus from the current traditional aircraft materials (metals and thermoset composites) towards thermoplastic composites. Based on the requirements laid out by ACARE, one of the leading research towards developing thermoplastic composite aircraft structures is the Next Generation Multi-functional Fuselage Demonstration (MFFD) project, under Cleansky project. The Cleansky project strives to manufacture a full-scale fuselage demonstrator integrated with all functionalities made entirely of thermoplastics [7]. The expected increase in the usage of thermoplastic composites in the Aerospace and Defence sectors in the next four years is shown in Figure 1.1.

One of the significant advantages of thermoplastic composites that contribute to reducing the manufacturing and assembly costs and time is the weldability of thermoplastic composites. Welding operation is usually classified based on the source of heat. There are numerous ways to provide heat at the interface for welding operations. The source of heating can be via direct heat input (heated press, hot gas, laser heating, focused infrared) or via electromagnetic means (induction, resistance, microwave, dielectric) or due to friction (ultrasonic, spin). From the multiple methods of welding available, the techniques that have been generally considered to have the highest potential for carbon fibre thermoplastic composites currently are resistance, induction and ultrasonic welding (USW).

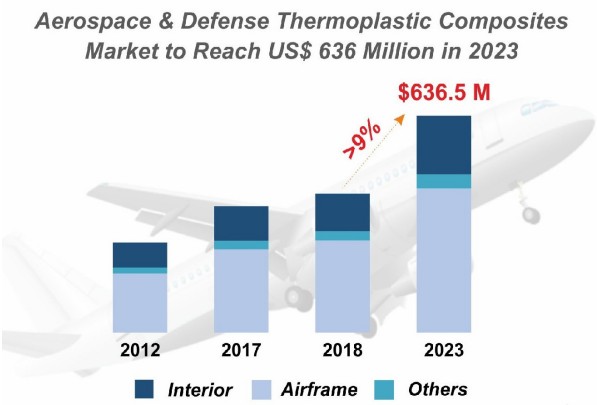

Figure 1.1: Evolution of thermoplastic composites over the years in the Aerospace Industry [8]

USW is the fastest among all three [9], and hence the process parameters play a significant role in developing a strong weld. Studies have shown that the thermoplastic laminates are prone to thermal deconsolidation and squeezed flow of the matrix [10–13] if the process is not properly controlled. This leads to an increase in the porosity and may affect the strength of the weld. Hence it is crucial to understand the phenomenon of thermal deconsolidation during USW.

While USW of thermoplastic composites have typically been a spot welding technique, USW in aerospace structural components demands the development of advanced welding techniques like continuous ultrasonic welding (CUW) process and sequential spot welding techniques. Sequential spot welding has been found to be similar to mechanically fastened joints in strength, and other characteristics [6] but is not the focus of this study. The development of a CUW allows welding the entire span of the joint, thus allowing a higher load transfer than in static welding and reduced stress concentrations [14]. Studies are underway in developing a robust CUW process. The state of the art in CUW of thermoplastic composites still contain voids at various locations in the weld. The elimination of these voids is one of the primary requirements to improve the quality of welds. Hence it is important to understand the formation of these voids and how the consolidation parameters in CUW influence the weld quality. Thus, it is necessary to define consolidation parameters but within the constraints in the vibration phase. This can be realised by initially determining the effect of consolidation parameters on the (de)consolidation of ultrasonic welding procedure in static welding and then extending the understanding to CUW process. This is a step towards increasing the technology readiness levels (TRL) levels of this technology. This knowledge is, hence, key in developing a robust process for the ultrasonic welding of thermoplastics.

1.4. Outline

The report thus summarises the various experimental activities that were carried out, the results from those tests and discussions, and further conclusions on the effect of consolidation parameters on the deconsolidation of ultrasonically welded thermoplastic composites. This report is divided into five parts.

- Part I: ”Literature Review” discusses the current understanding of the ultrasonic welding of thermoplastic composites and identifies the state of the art in the welding process. The gaps in knowledge regarding the welding process are identified, which is followed by the research questions, which will be answered in this research.
- Part II: ”Static ultrasonic welding” discusses the effect of various consolidation parameters on the static ultrasonic welding process. Multiple studies that were carried were critically discussed.
- Part III: ”Continuous ultrasonic welding” probes the effect of consolidation parameters in CUW based on the understanding from the static ultrasonic welding process.

- Part IV: ”Conclusions and Recommendations” sums up the outcomes of the research and their relevance in the development of a robust CUW process. Recommendations for further work is also presented.
- Part V: ”Appendix” consist of supplementary data and observations from the tests carried out during the research that further supports the conclusions of the research.

I

Literature Review

2

Ultrasonic Thermoplastic Welding

Ultrasonic welding (USW) is a fusion bonding technique used to join both thermoplastics and thermoplastic composites. The USW process entails three phases - (i) initial build-up phase, where a sonotrode (or horn) first touches the adherends and start the application of force until a trigger force is reached; (Steps 1,2 and 3 of Figure 2.1) (ii) a vibration phase wherein heat is generated by high-frequency, low amplitude vibrations applied transverse to the substrate being weld under a defined force; The frequency of vibration is usually between 20-50 kHz, while the amplitude of vibration is between 10-250 μm [6] (Steps 4 of Figure 2.1) and (iii) a consolidation phase, wherein the weld is allowed to cool down under pressure to achieve consolidation (Step 5 of Figure 2.1).

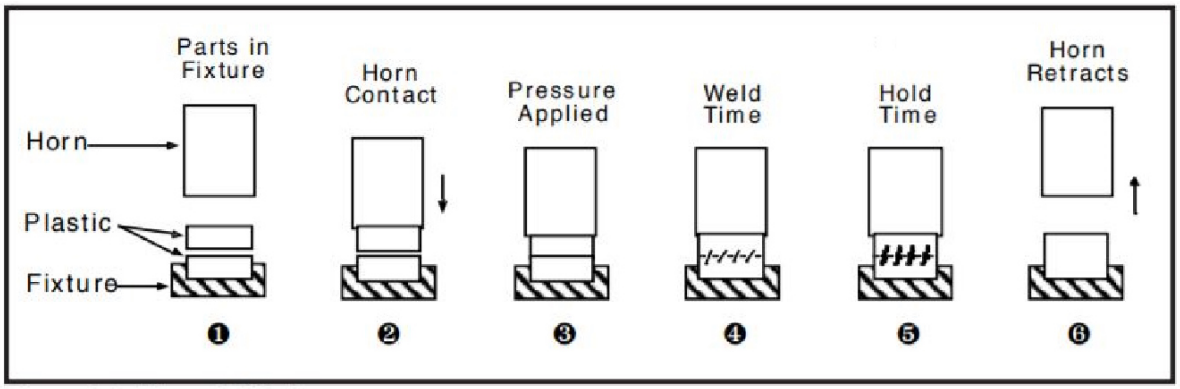

Figure 2.1: Basic ultrasonic welding process [15]

The welding time in USW is very short due to which it is widely used in mass production of thermoplastic polymers. Studies have shown that in-plane mechanical and failure performances and shear load carrying capacities of USW are comparable to that of mechanical joints [16, 17]. On a similar note, the mechanical strength and fatigue performances of USW were comparable to both resistance and induction welding [9]. Research is also progressing towards joining thermosets using thermoplastics as a coupling layer [18] and joining a thermoplastic composite to a thermoset composite [19].

2.1. Energy Director

An energy director (ED) is a resin film or a resin protrusion that is usually sandwiched between the two adherends to heat the interface of the two parts preferentially by serving as an asperity between the two adherends. The relative movement between the ED and the adherend ensure heating via surface friction while the lower stiffness of the energy director compared to the adherends ensure heating via viscoelastic heating. Inspired by the plastic industry, the initial energy directors were

triangular, rectangular or semi-circular ridges. During the vibration phase, the ED undergo cyclic strains and hence heat up faster than the adherends [20]. The higher cyclic strain from the decreased cross-sectional area ensures that the heating and melting first occurs at the tip of the triangles and then progresses towards the base [21]. The disadvantage with such a configuration was the need to define several factors - the number of ridges, their location and spacing, shape and orientation- that played a significant role in the generation of heat and the flow of resin in the interface. This resulted in undesired weld quality, if not well controlled. The disadvantages of the traditional ED led to modifications to suit for use in the USW of thermoplastics by adapting a flat ED [20, 22–24]. Flat ED was found to preferentially heat up due to its low compressive stiffness which led to large scale deformations during vibration, thus enabling the ED to melt and flow evenly across the interface [20].

2.2. Heating Mechanisms

When two adherends are placed together on top of each other, the contact is initially between the asperities on the surface of the adherends. During the vibration phase of the USW process, the dynamic vibrations, coupled with the welding pressure, ensures that these asperities undergo cyclic deformation, which in turn produces heat. This heat melts the interface resulting in inter-molecular diffusion and polymer macro-molecular entanglements [25]. The static pressure increases the concentration of the mechanical energy in the welding interface while the dynamic pressure due to the mechanical vibrations ensures that the required temperature is build up in the interface [26]. The main contributor to heating the ED before the temperature reaches the Tg is thus interfacial friction and thermal conduction. The contribution of this heating is dependent on the relative displacement between the adherends, welding force, welding amplitude and the nature of the energy director.

Once the temperature reaches Tg, viscoelastic heating takes over. The heat affected zone (HAZ) now increases drastically due to viscoelastic heating and thermal conduction. This raises the temperature of the energy director to above its processing temperature [27]. The generation of viscoelastic heat is affected by stress and strain while [28] the presence of an interface will not influence its generation rate. However, the frictional heat generation relies on the presence of this interface [28]. The vibrations thus lead to a combination of inter-molecular and boundary friction heating, interfacial heating, inter-molecular diffusion and polymer chain entanglements, which is then left to consolidate under pressure [25]. This diffusion of the polymer chains across the interface that results in polymer entanglements or bonds at elevated temperatures is termed as autohesion [29]. All these processes take place in a few hundred milliseconds!

The average dissipated energy per unit time or the viscoelastic frictional heating rate can be given as [21]

$$\dot{Q}_{\text{avg}} = \frac{\omega \epsilon_0^2 E''}{2} \tag{2.1}$$

where ω is the frequency of vibration, ε_o is the cyclic strain of the polymer and E'' is the loss modulus of the polymer.

2.3. Equipment

The basic construction of an USW machine consists of a power supply, sonotrode, booster, piezoelectric transducer, actuator, and a fixture or base (see Figure 2.2). The vibration is provided by the sonotrode which is connected via a booster to the piezoelectric transducer. The power supply converts line voltage to a high voltage. It houses an automatic tuning unit, an amplitude regulator and an overload circuit breaker. The automatic tuning unit allows the power supply unit to work at the resonant frequency while the amplitude regulator keeps the amplitude constant throughout the process by modulating the power consumption. A controller is also housed along with the power supply unit that includes the microprocessor which enables in situ measurement and recording of parameters [25]. The electrical energy is transformed into mechanical vibrations by the piezoelectric transducer, which is amplified by the booster before it is transmitted to the adherends via the

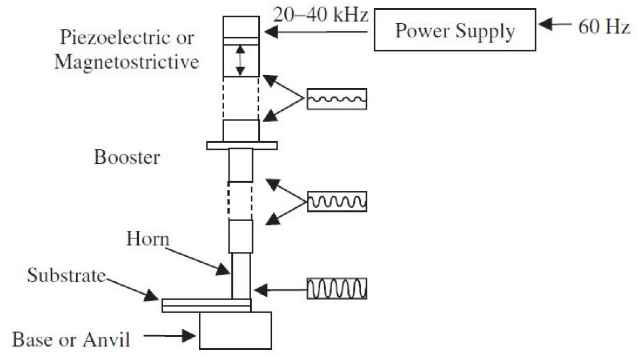

Figure 2.2: Basic schematic of an ultrasonic welding machine [30]

sonotrode. The actuator controls the vertical movement of the sonotrode, booster and the piezoelectric transducer (collectively called the ultrasonic stack) during the welding process.

2.4. Welding parameters

The vibration phase of the USW process is controlled by two parameters - the amplitude of vibration and welding force or pressure. Both these factors indirectly control the vibration time. In general, longer welding duration increases the energy dissipated and subsequently, increase the weld strength. However, increasing beyond a limit is unnecessary as it might cease to produce any more increase in weld quality. Beyond this, the increase in temperature at the weld line and through-thickness heat conduction might increase the depth of the melt zone. Longer welding duration can even lead to local degrading of the polymer as the extended exposure to the vibration amplitudes will result in an increase of temperature at the weld interface.

2.4.1. Amplitude of vibration

The amplitude of vibration controls the generation of heat at the welding interface. As the amplitude of vibration increases, the rate of heat generation also goes up, which in turn reduces the processing time and lead to an increase in the overall dissipated power. Thus, higher amplitude reduces the time it takes for the maximum power to be achieved [31]. This is because the power peak is obtained through a combined effect of interfacial heating and viscoelastic heating and the energy dissipation due to viscoelastic forces is proportional to the square of the amplitude [21] (Refer equation 2.1). Hence the higher the amplitude, the higher the rate of energy dissipation and higher will be the heating rate.

2.4.2. Welding force

The welding force has four major roles in the USW of thermoplastic composites [32, 33]

- Provide a good contact between the adherends and the energy director
- Provide a good contact between the sonotrode and the adherend to minimise the effect of hammering
- Act as a static load during the application of the vibrations or the cyclic loading
- To force the ED to flow during the welding process

Since interfacial friction results in the nucleation of new hot spots during the welding process, a high welding force results in a shorter weld time. This reduction in the welding time when the welding force is increased can be attributed to the heat generation in the initial stages that mostly relies on surface friction [25]. On the contrary, a low welding force will result in an increased hammering or loss

of contact between the sonotrode and the adherend [34] during welding. The hammering can result in a low energy transmission thus reducing the overall efficiency of the process [35]. This, combined with poor contact between the adherends and the energy director, might result in a slow heat generation and an incomplete melting and flow of the ED [31]. Contrarily, an unnecessarily high welding force can result in a squeeze flow of the matrix along the adherend edges [13]. Similar phenomena have also been noted in induction welding where high forces have resulted in fibre buckling and flashes at the edges [36].

2.5. Consolidation parameters

The consolidation phase of USW process is controlled by two parameters - consolidation time and consolidation pressure. If the specimens are not re-consolidated post welding, it deconsolidates which severely hamper the weld quality. Hence, knowledge of the deconsolidation mechanisms is pivotal in developing a robust USW process.

Despite the influence of consolidation parameters on the consolidation quality, much work has not been done especially since the influence of consolidation parameters on the final weld quality is far less compared to the welding parameters. Consolidation time (or holding time) was reported to have a minimal effect on the weld strength provided it is sufficiently long [32]. Villegas hypothesised that the consolidation should extend until the interface temperature drops below glass transition temperature of the polymer [6]. However, no further information on parameters such as how long or short this phase can be, how much consolidation force should be provided or how the consolidation phase can be controlled are available.

Koutras et al. investigated the effect of welding parameters on the cooling rate at the weld interface of CF/PPS and analysed the degree of crystallinity at the weld interface [37]. A higher welding force and amplitude, courtesy to its shorter welding time and consequently a smaller heat affected zone, exhibited a higher cooling rate. Despite the cooling rate exhibited during the consolidation phase being higher than the critical cooling rate of PPS under quiescent conditions, the weld interface of PPS revealed a semi-crystalline structure. This was attributed to crystallisation that was strain-induced [37].

2.6. Stages of thermoplastic ultrasonic welding

Benatar and Gutowki had shown in the late 1980s, from their tests on CF/PEEK [21] that the sub-processes of USW was similar to the division of processes for the polymer crack healing that was earlier proposed by R.P Wool and K.M.O'Connor [38].

Building on these studies, Villegas investigated the USW process using CF/PEI and a flat ED and proposed the below five stages of USW (refer Figure 2.3). These five stages were then utilised to define a displacement-based process control for the USW process [31], which will be discussed in the following section.

- **Stage 1 - Heating up of the energy director**
  The power increases almost linearly in this stage along with an initial retraction of the sonotrode to accommodate the vibrations [31]. During this stage, the energy director heats up until the heating progresses from the edge to the overlap. The welding interface does not undergo any observable physical changes. The predominant heating phenomenon in this stage is surface friction.
- **Stage 2 - Local melting of the flat energy director**
  The power decreases in this stage while the displacement of the sonotrode does not vary significantly. The ED starts to melt with melt sites nucleating in various parts of the ED. This nucleation of hot spots is driven by interfacial friction.
- **Stage 3 - Entire melting of the flat energy director**
  There is an increase in the displacement of the sonotrode in the downward direction due to the melting and flow of the ED. The weld line thickness decreases continually until the end of the vibration phase. There is a sudden rise in the power curve, due to the sudden spike in the mechanical impedance when the different melt front converges [21].

- **Stage 4 - Local melting of the upper matrix layers**
  A power plateau is formed, and the displacement continues to rise. The resin in the adherend now starts to flow as the heat is now transferred from the molten ED to the adherend.
- **Stage 5 - Matrix melting of the adherend**
  The dissipated power decreases while the sonotrode displacement continues to rise. The matrix in the adherend melts during this stage.

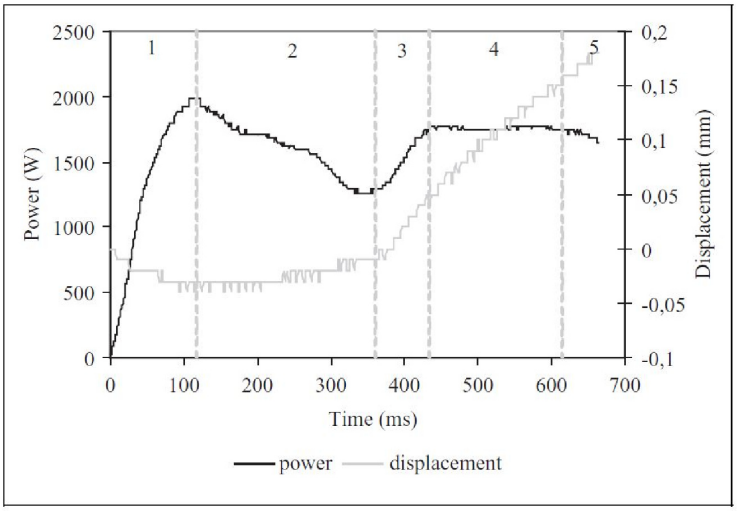

Figure 2.3: Typical dissipated power-displacement curve for CF/PEI as reported by Villegas; Vibration amplitude : 86.2 µm, welding force : 500 N [31]

2.7. Process Control

The USW process is an extremely fast process with welding time of a few milliseconds to a few seconds. If the temperature at the interface does not build up to Tm (or Tg in case of amorphous polymers), the energy directors will not melt, and a proper weld will not be formed. Similarly, if the temperature at the interface is not controlled, it might lead to excessive polymer flow and distortion of the fibres in the adherends or even degradation of the polymers. Therefore, it is important that the welding process is efficiently controlled. To ensure welds producing consistent strength and performing optimally, various control methods have been developed over time.

Controlling the welding time, which dictates how long the vibration phase should continue for is a direct way to control the welding process. However, the quality of specimens welded with similar welding time was found to be inconsistent [39]. Welded joints were seen to be more consistent in other means of process control than direct time control of the vibration phase.

Two main indirect control methods were developed to control welding processes indirectly - (i) sonotrode vertical displacement and (ii) welding energy.

Benatar and Gutowski established a relation between the impedance of the ultrasonically welded composite and the molten ED flow, which is in turn related to the weld quality [21]. They showed how there was a spike in the dynamic impedance when the melt fronts meet and proposed this as a theoretical means of controlling ultrasonic weld. Due to the difficulties in measurements of dynamic impedance at high frequencies, they also suggested using other parameters such as power and acceleration of the base as a controlling factor [21]. They showed that as the impedance of the interface changes when all the melt front meets and ED starts to flow, the dissipated power and acceleration of the base also changes [21].

Building along these studies, Villegas et al. came up with the method of monitoring the welding process in-situ using a displacement-controlled approach from the power-displacement data from the microprocessor [20, 31, 40, 41]. Displacement control meant welding until the sonotrode moved a predefined distance in the vertical direction during welding aided by the melting of the ED. Multiple experiments 2.3 have led to the conclusion that the maximum weld strength is obtained when welded to stage 4 of the welding process. Welding to stage 4 can be effectively controlled by designing the microprocessor to terminate the welding procedure after a predefined value of sonotrode displacement, which can be determined from the power-displacement curves. This procedure is also effective in reducing the dispersion in the lap shear strength as the displacement control-based welding is insensitive to fluctuations in vibration amplitude and welding force [40].

An alternate control method using weld energy as a control procedure was shown by Harras et al. [39]. The welding energy is the area under the dissipated power curve and hence is the sum of energy used to create the weld and the energy dissipated in the fixture and the adherends as well [42]. Hence any change in the boundary condition can affect the energy required as well. Nevertheless, welding at lower energies implied inadequate weld energy resulting in unwelded EDs while welding at higher energies showed deterioration of properties due to overheating.

2.8. Continuous ultrasonic welding (CUSW)

Most of the studies on ultrasonic thermoplastic welding so far has been either on spot welding or static welding. The up scaling of the USW process is vital before the technology can be used in the industry as a manufacturing/joining method. Two methods that have the potential to be developed as such are the sequential ultrasonic spot welding [42] and the continuous ultrasonic welding [14]. This section deals with the studies carried out on continuous ultrasonic welding.

CUW involves the sonotrode continuously moving over the overlap to be welded, thus producing a continuous weld seam, as shown in Figure 2.4. The welding parameters in CUW are the welding pressure, vibration amplitude and welding speed. The welding speed in CUW is determined based on the optimum welding conditions during the static welding of adherends [43].

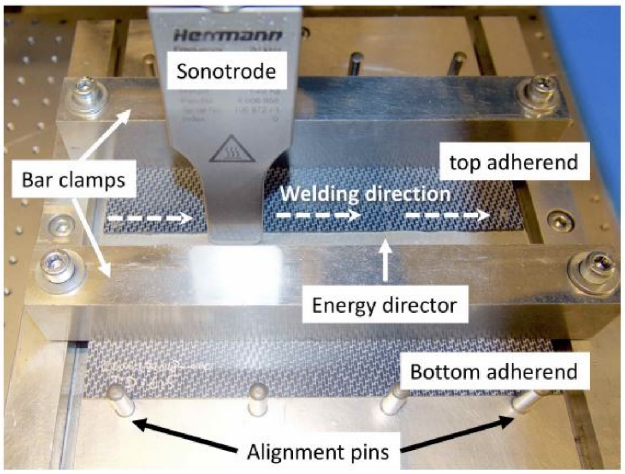

Figure 2.4: Depiction of the CUW process [44]

The selection of the energy director is critical in CUW of thermoplastic composites. To accommodate the squeeze flow of the ED in the CUW process during the sonotrode movement over the unwelded weld interface, at least one of the adherend should be flexible [45]. Senders et al. proposed using a very thin flat energy director (0.08 mm) which enables a near-zero flow of the energy director. The use of thin ED was reported to provide sufficient weld strength [45] while ensuring that the welding process does not stop or slow down the squeeze flow process. This is now

replaced by the state of the art in CUW of thermoplastics using polymer mesh (Refer Figure 2.5b). Jongbloed et al. proposed using a 0.20 mm thick woven mesh ED which was reported to provide higher compliance in the continuous welding of thermoplastic composites compared to a thin ED proposed by Senders et al. [46]. The polymer mesh allows for expansion and deformation at the beginning of the welding process as the mesh filament crossings established multiple areas of contact throughout the entire overlap experiencing high static and dynamic pressures [43]. This initial contact gives a uniform heat generation and distribution and expands within the open areas of the mesh, thus further expanding the contact area, wetting the entire adherend. (Refer Figure 2.5b).

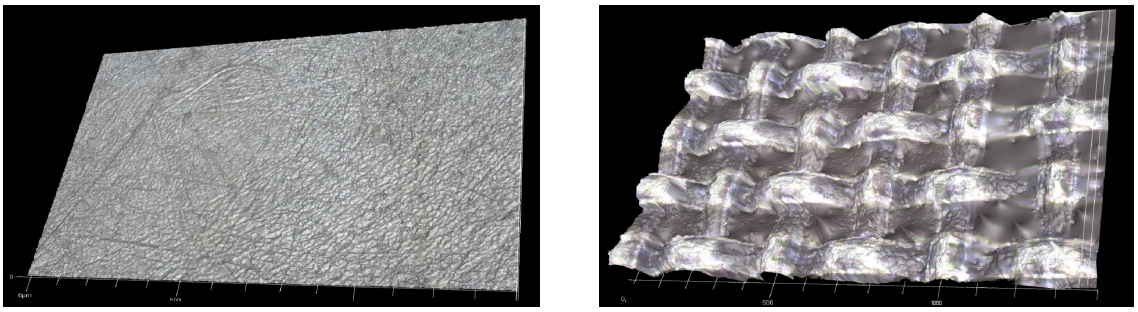

(a) Neat polymer ED **(b)** Mesh ED

Figure 2.5: PPS EDs when observed under an optical microscope (10x magnification)

The state of the art in CUW was as can be seen in Figure 2.6 [43]. The image shows a representative fracture surface of a continuously welded CF/PPS using a mesh energy director (ED) with a welding speed of 45 mm/s, welding force of 500N and a vibrational amplitude of 82.5 µm. The fracture surface exhibits voids at various locations within the weld.

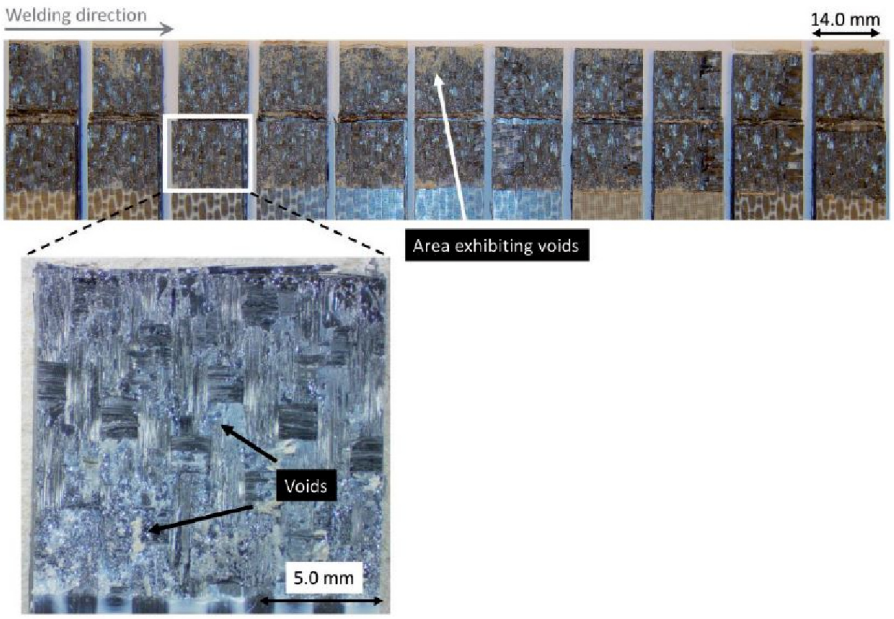

Figure 2.6: Fracture surface of a continuously welded CF/PPS plate with mesh energy director without consolidation device [43]

2.9. Thermal (de)consolidation - An overview

Thermal deconsolidation occurs when a well-consolidated structure subjected to reheating-cooling cycle, undergo an adverse change in their macro-performance or their mesostructure leading to an

unexpected loss of strength and stiffness [13]. Deconsolidation can lead to an increase in the void content [12, 13, 47, 48], increase in the thickness due to fibre decompaction [12] and buckling or changes in the surface roughness [12, 13, 49, 50].

A significant amount of research has focused on the deconsolidation of consolidated laminates which were reheated to above its processing temperatures and cooled down without external pressure. Four main mechanisms have been identified that contribute towards the deconsolidation of thermoplastic composite laminates when subjected to a reheating cycle. These mechanisms are briefly listed as [10, 12, 13, 51]:

1. Decompaction of fibre reinforcement network due to the release of the residual stresses or lack of adequate external pressure during consolidation
2. Viscoelasticity of the matrix medium resulting in thermal expansion
3. Thermal expansion of the voids
4. Coalescence of the smaller voids to form larger voids

Among the deconsolidation mechanisms in the growth of voids in the thermoplastic laminates, the traction induced by thermal deconsolidation (fibre reinforcement network decompaction) was reported as the dominant deconsolidation mechanism compared to other factors [13].

2.9.1. Deconsolidation mechanisms in thermoplastic laminates

Decompaction of fibre reinforcement network

When the dry fibre preform is impregnated with resin, the applied pressure and the flow of resin can exert stress on the dry fibre preform [52]. These compressive stresses are retained in the specimen when the composite is consolidated and cooled down in a press or an autoclave. These are usually termed as residual stresses and will remain in the specimen. During a reheating cycle, these residual locked-in stresses may be released, which results in deconsolidation of the laminates [12]. In other words, when reheated to above the melting temperature for crystalline and semi-crystalline polymer composites (Tg for amorphous polymer composites), the residual energy tends to release, leading to deconsolidation of laminates. There may be a change in the part dimensions and an increase of void content leading to a low-quality part. These are alleviated by either a reheating step for thermoplastics or a post-cure step for thermosets.

When initially preconsolidated glass mat polypropylene was heated for varying duration, deconsolidation was found to increase over time when there was no external pressure. This decompaction or the ”spring-back” of the fibre matrix configuration was found not only to increase the void content but also to increase the thickness of the laminate [12], as seen in Figure 2.7.

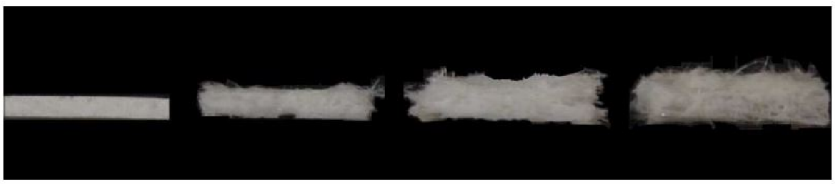

Figure 2.7: Change in thickness over time during deconsolidation; 0, 50, 200 and 500 s: glass mat [12]

Thermal expansion of the matrix medium

The viscoelastic properties of the thermoplastic matrix also play a significant role in void growth. It is known that an increase in temperature decreases the viscosity. On increasing the temperature above Tg but maintaining it below Tm for a semi-crystalline polymer means that it has both crystalline and amorphous phases in it. For amorphous polymer, the onset of a truly liquid melt can be roughly taken

as Tg + 60-100°C where the viscosity diminishes rapidly [13, 53, 54]. Therefore, at a temperature between the Tg and liquid melt temperature, where the polymer melt has both the properties of viscosity and elasticity, the polymer melt can store elastic energy that allows it to deform under stress. This rubber-like behaviour will cause the voids in the polymer matrix to grow due to traction and produce new voids via cavitation [13]. As this temperature reaches the melting temperature, the elastic properties diminish and void growth due to traction reduces.

The reheating process of thermoplastic composites were observed to cause a phenomenon known as ”void migration” where voids that were initially present disappear and reappear but at a different location along the direction of the heat flux [50]. Figure 2.8 shows a CF/PEI laminate, whose voids migrate from one location to another as the heating time increased.

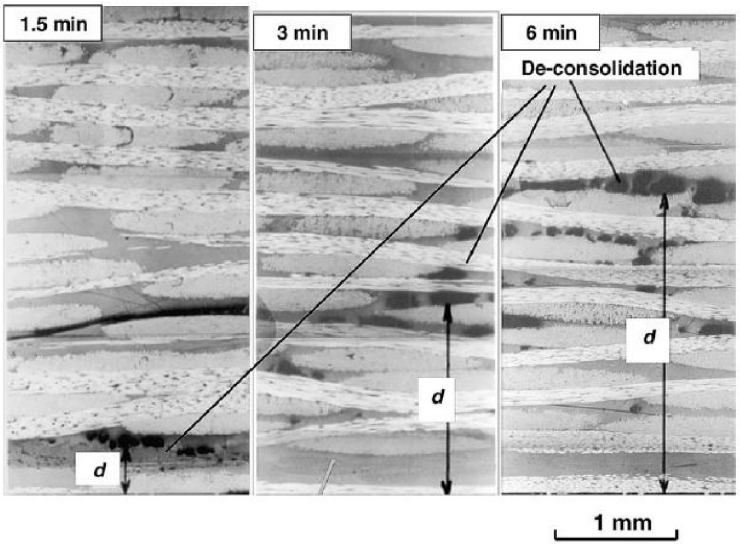

Figure 2.8: Void migration configurations at various heating times [50]

Thermal expansion of the voids

The high temperatures that the laminate is exposed to will result in thermal expansion of the voids within the laminate due to an increase in the internal void pressure. However, the influence of the thermal expansion of voids on the total increase in void content is considered trivial. The increase of the volume of the voids due to thermal expansion is only around 0.7 times its initial volume even at the upper bound of estimation where elasticity and surface tension effects were not taken into account [13]. Contrarily, the void content increase due to thermal deconsolidation is around 10-20% [13].

Coalescence of the smaller voids to form larger voids

This phenomenon reduces the total number of voids in the laminate but increases the size of the voids present. However, there is no perceivable increase in the global void content over time. [13].

2.9.2. Squeezed creep flow of the matrix melt

This process of reconsolidation can also result in squeezed creep flow of the matrix melt [50]. Squeezed creep flow of matrix melt occurs when high temperature and high-pressure results in the flow of the matrix from the free edges of the composite. This can lead to a reduction in the part thickness, fibre distortions and reduced strength due to inadequate reinforcement. In resistance welding, higher pressures were seen to lower the weld strength which was attributed to fibre distortions and matrix flow due to squeezed creep flow of the matrix melt [50, 55].

2.10. Consolidation in USW of thermoplastic composites

There is no study currently available regarding the deconsolidation mechanisms in USW. The time available for deconsolidation and reconsolidation during the welding process is extremely low when compared to composite laminates. One of the earliest mentions of consolidation time for USW of thermoplastic composites in literature was by A. Benatar in 1987 in his PhD. thesis who experimentally stated that the consolidation time (or holding time) has a minimal effect on the weld strength provided it is sufficiently long [56]. However, it was not stated what sufficiently long meant. Nor was it stated how much consolidation pressure was required. Villegas went a step ahead and stated that the consolidation pressure might have to be applied until the temperature of the weld stack drops below the Tg of the polymer [6].

However, experimental studies on resistance welds have revealed that a good quality weld can be obtained by a pressure as low as 0.2 MPa [49, 55, 57]. The formation of voids during resistance welding of CF/PEI is mainly due to fibre decompaction because of inadequate pressure applied and residual volatiles [58]. Interestingly, the effect of fibre decompaction was found to be easily overcome by increasing the applied welding pressure to around 0.4 MPa while a welding pressure of 1.5 MPa was required to prevent void formation due to the residual volatiles [58].

Despite the advancements in the understanding of the effect of consolidation on thermal deconsolidation in composite laminates, it is still a challenge that remains to be solved to identify how consolidation parameters influence the weld quality in USW. It is unknown if deconsolidation mechanisms for the laminates bear the same significance in deconsolidation of thermoplastic welding since the USW process is different from that of the consolidation of laminates and other forms of welding techniques.

3

Research Proposal

The preceding chapter detailed the ultrasonic welding (USW) process based on the available literature. It was thus identified that the understanding of deconsolidation during the USW process is lacking, especially regarding the process parameters (time and pressure) of the consolidation phase. The effects that the holding time and pressure have on deconsolidation behaviour in USW remains to be investigated. As stated in section 2.10, the influence of consolidation time and pressure is crucial in defining the process requirements of the continuous ultrasonic welding (CUW) process. It is critical to understand the consolidation time and pressure required to improve the weld quality in the current state of the art in the CUW process. It is also critical to determine the dimensions and placement of the consolidation device or ”consolidator” in the CUW process and gain more insight into the sources of thermal deconsolidation during the consolidation phase. This is a compelling field of study as it is a step towards developing a robust continuous ultrasonic process.

In static USW, the high-frequency low-amplitude vibrations are exerted by the sonotrode to the adherend stack, while in CUW, the sonotrode moves along the weld line producing a continuously welded seam. The definition of consolidation pressure and consolidation time in static USW have so far been via trials that gave satisfactory results but with no scientific backing. The effects of consolidation parameters in CUW have not been studied till date.

With no scientific backing, the simplest solution in static USW would be to use the same force as the welding force for consolidation and to apply pressure until the temperature drops well below Tg. In static or in spot welding, yes - it does seem a trivial solution. Moreover, it has stayed that way ever since. On the contrary, consolidation time is a critical element in the development of the CUW process. In CUW, a separate consolidation device is required since the sonotrode cannot provide consolidation like in static USW. Since in CUW, the consolidator also moves along with the sonotrode, the speed of the consolidator cannot be separately controlled. Also, the speed of the sonotrode movement is determined by the welding parameters which implies that the only parameters that can control the duration of consolidation in CUW are the consolidator length and its position behind the sonotrode. The welding speed in the state-of-the-art CUW process is around 35-45 mm/s. Assuming the state-of-the-art consolidation time of 4s [17, 22, 40–43, 59, 60] for static USW, the consolidator will be 140-180 mm long, if the specimens are to be consolidated in CUW for the same duration as in static USW. This is impractical during welding of small and curved plates, and it thus becomes necessary to understand and define efficient consolidation parameters for the development of a robust continuous ultrasonic welding process.

3.1. Research Questions

From the gaps identified in the literature, the primary research question that is expected to be answered by the end of the study is as below.

How do the consolidation pressure and time influence the (de)consolidation in the weld interface during the ultrasonic welding process of thermoplastic composites?

To solve the above-defined project goal, the following sub-questions are to be answered.

1. How is the consolidation of the weld interface influenced by the consolidation time in static ultrasonic welding of thermoplastic composites?
   (a) How can the consolidation time be defined based on the changes in the physical properties of the polymer around its glass transition temperature/melting temperature?
   (b) What is the effect on the consolidation of the weld interface when the application of consolidation pressure is stopped
      i. before the interface temperature drops below Tm,
      ii. when the interface temperature is between Tm and Tg,
      iii. after the interface temperature drops below Tg.
2. How is the consolidation of the interface influenced by the consolidation pressure in static ultrasonic welding of thermoplastic composites?
   (a) What is the minimum threshold for the consolidation pressure that can still provide a good consolidation at the interface?
   (b) Does a high consolidation pressure lead to an improved consolidation of the interface?
3. What is the effect of consolidation pressure and holding time on the cooling rate at the weld interface in static ultrasonic welding of thermoplastic composites?
   (a) How does the presence of sonotrode influence the rate of cooling at the weld interface during the consolidation phase?
4. Can the displacement data obtained from the microprocessor be used for in situ monitoring of the consolidation phase?
5. How can the knowledge obtained about the consolidation parameters in static ultrasonic welding be used to define consolidation parameters for continuous ultrasonic welding of thermoplastic composites?
   (a) Does the continuous ultrasonic welding process require the same consolidation pressure as that of static welding?
   (b) How far can the consolidator be placed away from the sonotrode such that a good consolidation is obtained?
   (c) How does the presence of the consolidator affect the cooling rates during continuous ultrasonic welding process of thermoplastic composites?

3.2. Hypotheses

Based on the discussions in the previous sections, it is apparent that there exist a few gaps in the understanding of deconsolidation process in USW of thermoplastic composites. Certain observations and hypotheses have been detailed below with backing from the literature which has assisted in formulating the research questions.

1. It is hypothesised that stopping the consolidation pressure application before the temperature reaches Tm will result in a deconsolidated weld. A good weld is expected when consolidation pressure is applied until the temperature drops below Tg.

2. Deconsolidation of laminates after welding is assumed to occur if the applied pressure is below a defined critical pressure. Possibly, a high consolidation pressure might provide higher strength but might lead to higher squeeze flow of the matrix.

3. The effect of consolidation pressure on cooling rate is assumed to be minimal. At the same time, the sonotrode contact on the adherend might influence the cooling rate, which implies that the consolidation time might influence the cooling rate.

4. The displacement of the sonotrode may show some variation during the phase change of the material which might aid in establishing a control method for the consolidation phase during the ultrasonic welding process.

5. It is hypothesised that the consolidation parameters required for continuous ultrasonic welding process might differ from that of the static USW process due to the differences in the boundary conditions of the process. Nevertheless, it is assumed that understanding from static USW will be pivotal to help define consolidation parameters in CUW.

    (a) The consolidation pressure required for continuous ultrasonic welding might differ due to the boundary conditions. Similar to static ultrasonic welding, a consolidation pressure application below a threshold value is assumed to lead to laminate deconsolidation. A high consolidation pressure is assumed to lead to excessive squeeze flow from the weld interface.

    (b) The distance of the consolidator from the sonotrode might depend on the temperature profiles at the weld line. Here again, the consolidator should be so placed that the consolidation extends until the interface temperature drops below Tg. Placing the consolidator too close to the sonotrode might result in damping of vibrations and thus a deconsolidated weld interface. Also placing the consolidator too far from the sonotrode was hypothesised to result in consolidation pressure application after the weld line solidified.

    (c) The presence of the consolidation device or the consolidator might affect the cooling rates in CUW. It is assumed that the consolidator might conduct heat from the adherends due to through-thickness heat dissipation which can reduce the cooling rates in the presence of the consolidator.

II

Research Activities

4

Static Ultrasonic Welding (USW)

4.1. Introduction

The consolidation quality of the weld is strongly influenced by several factors, which include the welding parameters, the consolidation parameters, and the clamping mechanism used. This study limits its study to the effect of consolidation parameters viz. consolidation or holding pressure and time during the consolidation phase of USW on the (de)consolidation in ultrasonically welded specimens. To evaluate the consolidation or weld quality, this study focuses on LSS, fracture surface analysis, resin squeeze out, weld line thickness and void content as the primary characterisation techniques.

This chapter set forth various methods that were employed to investigate the effect of consolidation parameters of time and pressure on (de)consolidation in static USW and discusses the results obtained. Section 4.2 explores the materials used in this research. The machines used for the specimen preparation and welding are detailed in 4.3 while the test methods and characterisation techniques are explained in section 4.4. This culminates in the study of the effect of consolidation time on (de)consolidation of the welded specimens in section 4.5 and the effect of consolidation pressure in section 4.6. The section concludes by listing the major understandings from the tests carried out.

4.2. Materials

4.2.1. Adherends

The adherend material used in this study was five harness satin weave carbon fibre reinforced polyphenylene sulfide (CF/PPS) fabric. The CF/PPS is a high-performance composite used in the aerospace industry owing to its high chemical and heat resistance. The laminates were manufactured using six powder-coated prepreg plies, which were supplied by TenCate Advanced Composites (product code: CF 0286 127 Tef4 43%). The prepreg roll was cut to sizes of 580 mm x 580 mm in a Gerber cutting machine. The cut prepreg layers were stacked in a $[0/90]_{3s}$ sequence and were then held together using a handheld ultrasonic welder by welding at the four corners of the stack. This prepreg stack was sandwiched between two stainless-steel plates, which were initially degreased with ethanol and then coated with Marbocote 227CEE release agent. The stack of prepreg, along with the stainless-steel plates were then sandwiched between two isolated graphite plates arrangement to facilitate a uniform distribution of heat over the entire laminate surface during laminate consolidation. The prepreg stack was then consolidated in a Joos flat hot plate press for 20 minutes at 320^{o}C and 1 MPa pressure. The laminate thus produced had a nominal thickness between 1.80 - 1.90 mm. The thermoplastic laminates were then cut to dimensions of 101.6 mm x 25.4 mm for static ultrasonic welding (USW) tests in a water-cooled Proth grinding machine.

4.2.2. Energy Director (ED)

The energy director (ED) used for the entirety of this study was a 0.20 mm thick plain-woven PPS mesh. This PPS mesh is state of the art in the continuous ultrasonic welding process and was

supplied by PVG GmbH, Germany, and comes by the product name PPS100. The glass transition temperature (Tg) of the material was reported to be 97°C, while the melting temperature (Tm) was reported as 283°C [43]. A degreasing agent - Hyso QD was used to degrease the adherends and ED before welding.

4.3. Machines and parameters

4.3.1. Ultrasonic Welding Machine

A VE20 Slimline dialog 6200 welder from Hermann Ultrasonics was used for thermoplastic welding, as shown in Figure 4.1. The shape of the sonotrode was rectangular with a contact area of 15 mm by 30 mm and operated at 20 kHz. The sonotrode gain was 1:1.7 and was capable of maximum peak-to-peak vibration amplitude of 94 µm. The welding machine was capable of peak-to-peak amplitude levels up to 90.4 µm. The microprocessor of the welding unit automatically adjusted the power requirements of the machine that enabled the amplitude to be kept constant throughout the welding process. The machine allowed welding and consolidation forces between 130 N and 1500 N. The machine also provided in-situ data regarding the vertical displacement of the sonotrode and the energy consumption during welding.

A welding fixture designed in-house at TU Delft, which will henceforth be called ”Spring Jig”, was used to clamp adherends in static USW (see Figure 4.1). This specially designed clamping tool allowed vertical movement of the top adherend thus preventing the top adherend from bending when the polymer of the ED melted and was squeezed out during the welding process. The tool also helped keep the top adherend parallel to the surface of the bottom adherend during the welding process, which was necessary for a uniform heat generation. The clamping ensured a weld overlap of 12.7 mm x 25.4 mm.

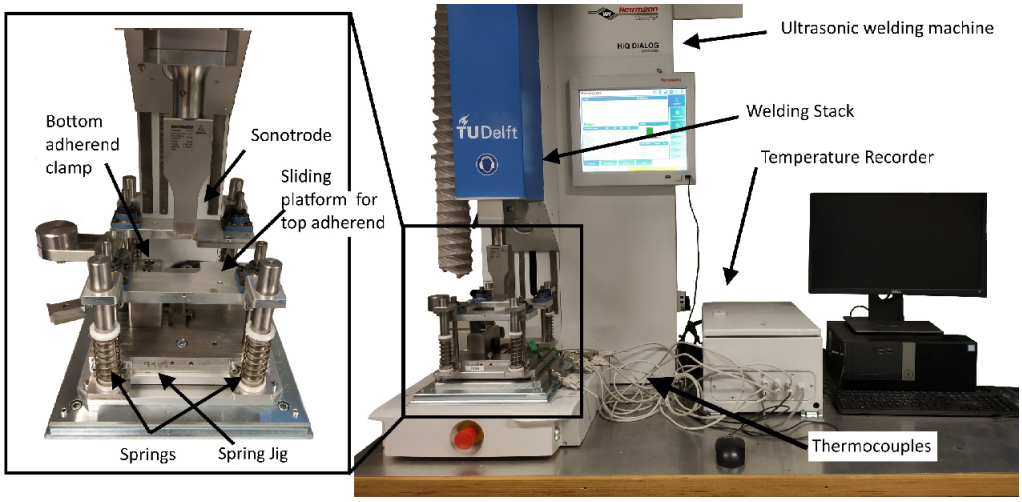

Figure 4.1: Static ultrasonic welding machine

The welding parameters used in this study were a welding force of 500 N (corresponding welding pressure of 1.6 MPa considering a weld area of 12.7 mm x 25.4 mm) and a vibrational peak-to-peak amplitude of 80 µm. The static welds in this project were ”displacement-controlled”. This meant that the vibration of the sonotrode was stopped once the sonotrode moved a predefined distance in the vertically downward direction. For the welds in this study, a vertical sonotrode displacement of 0.07 mm was used to control the welding process (refer Appendix A).

4.3.2. Temperature recording

The incorporation of thermocouples was deemed necessary at various stages of this study. A k-type thermocouple was used and was embedded within the weld interface as per the configuration shown in Figure 4.2. The thermocouple was placed between the bottom adherend and the energy director. More details on the choice of location of the thermocouple within the weld overlap is discussed in Appendix C.

Figure 4.2: Location of thermocouple in the weld

4.4. Characterisation Techniques

This section details the various machines and methods used to determine the consolidation or weld quality during this study. There is no defined ASTM standard to assess the quality of welded thermoplastic specimens. This uncertainty has led a significant part of the academic fraternity to rely on multiple methods to define the consolidation quality of a thermoplastic weld such as lap shear strength (LSS), fracture surface analysis and void content.

4.4.1. Lap shear strength (LSS) assessment

The lap shear strength tests were conducted in the Zwick/Roell 250kN universal testing machine. The grips were offset as deemed necessary to ensure that the load introductions were parallel to the overlap. The crosshead speed used was 1.3 mm/min. The single lap shear strength (LSS) of the weld was calculated by dividing the maximum load at failure with the overlap area (25.4 mm x 12.7 mm). The LSS was assessed and reported as the average of five individual LSS values for every configuration. Wherever this method deviated, it has been duly stated in the respective sections.

4.4.2. Fracture surface analysis

The fracture surface of the specimens (obtained after the LSS test) were analysed to determine the failure mode of the welded joint, presence of voids and to check if the ED melted entirely during the welding process. A Keyence VR-5000 Wide-Area 3D measuring system was used for observing the fracture surfaces in more detail.

4.4.3. Cross-sectional micrograph

One welded specimen per configuration was cut using a diamond cutter in a Secotom-10 cutting machine to obtain a cross-sectional view of the welded overlap. Figure 4.3 shows the plane along which the cut was made in the welded overlap. The cut specimens were then embedded in ”EpoFix Resin” and ”EpoFix Hardener” mixed in the ratio 25:3 and left to cure for more than 12 hours. Once cured, the embedded resins were ground and polished using a Struers Tegramin 20 Polishing machine using a cycle that consisted of grinding against SiC Foils of grain sizes 46 µm, 18 µm and 10 µm. These embedded specimens were then polished in a diamond suspension with particle sizes of 3 µm and 1 µm and later with a colloidal silica suspension (OP-S NonDry). The samples were then inspected using a Keyence VK-X1000 3D laser

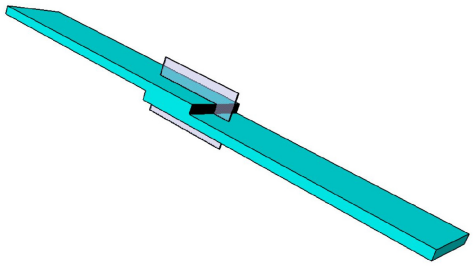

Figure 4.3: Plane along which cuts were made in the welded specimen for microscopy analysis

scanning microscope. The cross-sectional view was instrumental in obtaining information regarding the void content within the welded specimen, polymer squeeze flow from the welds and the thickness of the weld line.

4.4.4. Volumetric void content assessment

The limitation of the cross-sectional micrograph was that only one slice of the entire weld volume could be observed and analysed. This limitation was overcome by scanning the welded specimens in a 3D Phoenix NANOTOM high-resolution micro computed tomography (CT) scanner to assess the volumetric void content. The scanner uses an x-ray source with a maximum voltage of 180 kV and a maximum power of 15 W. The welded samples were inspected at a resolution of 14 µm. The data from the CT scan were subsequently analysed using a commercially available image analysis software ”Avizo” from ThermoFisher Scientific. An interactive threshold module calculates the volumetric void content in the welded specimen. The void volume was then rendered and presented for further understanding of the void distribution within the welded specimen.

4.4.5. Weld line thickness measurement

The thickness of the weld line was measured from the cross-sectional micrographs. The calculation was done using the analyser in the Keyence VK-X1000 3D laser scanning microscope software. A line was initially drawn along the top surface of the top adherend depicted by Line A in Figure 4.4. Line B was then drawn parallel to line A along the other edge of the top adherend. Similarly, line D and C were drawn on the bottom adherend. The distance between line B and C was measured at five different locations along the weld line. The average of this distance was reported as the weld line thickness. The weld line in Figure 4.4 is exaggerated for better clarity.

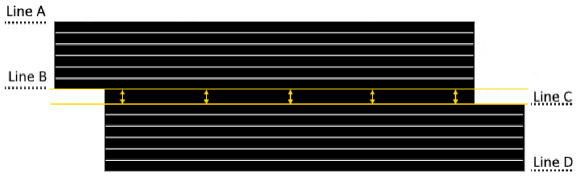

Figure 4.4: Schematic for the procedure adopted to measure the weld line thickness

4.4.6. Differential scanning calorimetry (DSC)

DSC measurements on the ED were studied using the Perkin Elmer DSC machine. For measurement of the degree of crystallinity of the ED after welding, the EDs were isolated from the adherends during welding. The isolation of the ED was done by sandwiching the ED between two 25 µm thick Kapton films before welding, which was held in place using tape. This methodology was used previously by Koutras et al. for the characterisation of crystallinity at the interface of ultrasonically welded CF/PPS joints [37]. A schematic of the arrangement is shown in Figure 4.5. The DSC specimens cut from the isolated EDs were then weighed and subsequently heated from 30 °C to 310 °C at 10 °C/min in a purge of nitrogen gas. The degree of crystallinity was defined as

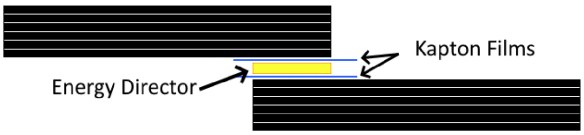

Figure 4.5: Schematic for isolation of ED for crystallisation tests

$$\text{Degree of Crystallinity} = \frac{\Delta H_m - \Delta H_c}{\Delta H_f{}^o} * 100 \tag{4.1}$$

where ΔH_m is the specific enthalpy at melting in J/g, ΔH_c is the specific enthalpy at the cold crystallisation peak in J/g and $\Delta H_f{}^o$ is the specific enthalpy of melting in J/g for an ideal 100%

crystalline sample. The value of ΔH_f^o is considered as 112 J/g [37], taking into account, the similarity between the PPS mesh and the flat ED [43].

4.5. Effect of consolidation time on the consolidation of the welds

4.5.1. Methodology

The research started by investigating the temperature profiles at the weld interface during the USW process by incorporating thermocouples in the weld interface, as stated in section 4.3.2. These temperature profiles were used to identify consolidation times that would best represent various stages of thermal physical changes in the polymer during the consolidation process. Specimens were then welded to investigate how the consolidation of the weld interface was influenced when the application of consolidation force was stopped (i) before the interface temperature drops below Tm, (ii) when the interface temperature was between Tm and Tg and (iii) after the interface temperature dropped below Tg. It was hypothesised that the consolidation should extend until the temperature at the weld line drops below Tg. Several characterisation techniques stated in section 4.4 were employed to help understand the effect of consolidation time on the consolidation of welds. The LSS was determined to understand the development of strength during the consolidation phase. The fracture surfaces revealed how the ultrasonic welds fractured during the LSS tests and provided information regarding the presence of voids. The cross-sectional micrographs and micro-CT scans enabled the visualisation and calculation of the void volume in the welded specimen after the welding process. A differential scanning calorimetry of the ED enabled the calculation of the degree of crystallisation of the ED after welding. This helped confirm if the weld interface still retained its semi-crystalline nature despite the high cooling rates in USW. Five specimens were tested for LSS and one each for cross-sectional micrographs and micro-CT scans.

Representative curves

Before the main research questions are answered, a representative power-displacement-force curve and a temperature profile curve are presented, which will aid in better understanding of the process and results presented in this section.

A representative power-displacement-force curve is shown in Figure 4.6a. Stage A represents the vibration phase, while stage B represents the consolidation phase. Stage A has been shown separately in Figure 4.6b and takes only about 300 ms. The displacement of the sonotrode at the end of vibration was 0.07 mm (refer Figure 4.6b), which after consolidation, increased to about 0.17 mm (refer Figure 4.6a). Since the welding and consolidation forces were the same, a constant 500 N force application can be seen throughout the process.

A typical temperature profile during a combined vibration and consolidation phase is shown in Figure 4.7. During the vibration phase, the interface temperature increased from room temperature to temperatures above 650 °C in roughly 300 ms. During the consolidation phase (the shaded region in Figure 4.7), the temperature dropped back to room temperature but at a rate slower than the heating rate during welding. In this representative curve, the temperature profile is only plotted for 2000 ms from the start of welding. Since the study focuses only on the effect of consolidation parameters on the (de)consolidation of welds, all temperature profiles depicted henceforth shall only be the temperature at the interface during the consolidation phase.

Choosing consolidation times for consolidation time trials

Research started by identifying various consolidation times that best represent various stages of thermal physical changes in the polymer during the consolidation process. At the onset of the consolidation phase, the temperature at the weld interface was above the melting temperature, which then cooled down under pressure as seen in Figure 4.7. Thus, the consolidation phase will see the polymer transition from a molten stage (above Tm) to a glassy state (between Tm and Tg) and finally

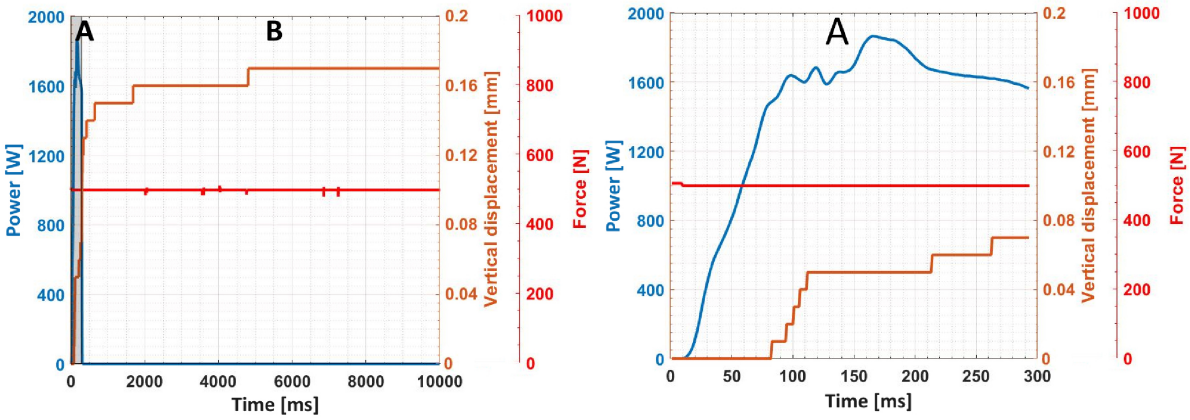

(a) Full weld sequence

(b) Close up of A from the full weld sequence

Figure 4.6: Power-displacement-force curves for a representative static ultrasonic weld; Vibration amplitude (peak-to-peak): 80 µm, welding pressure: 1.6 MPa (500 N), consolidation pressure: 1.6 MPa, consolidation time: 10000 ms, weld control - displacement to 0.07 mm

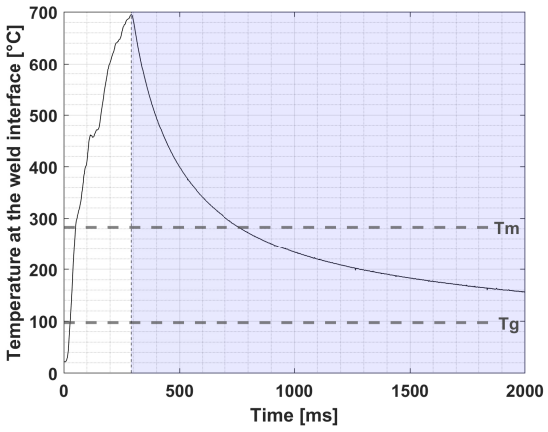

Figure 4.7: A typical temperature curve of a static ultrasonic weld (the consolidation phase is highlighted)

solidifying in due time (below Tg). To determine the temperature profile at the weld interface during consolidation, specimens were initially welded with a consolidation pressure of 1.6 MPa (corresponding welding force of 500 N) and a consolidation time of 10000 ms with thermocouples embedded in the interface as mentioned in section 4.3.2. Five specimens were welded, and the thermocouple readings were plotted, as shown in Figure 4.8. The mean temperature stated in the diagram is the average of the interface temperatures of five different welds measured during the consolidation phase.

Based on Figure 4.8, different consolidation times were identified and are as stated in Table 4.1.

4.5.2. Experimental Results - Effect of consolidation time

Based on the consolidation times defined in Table 4.1, specimens were welded with a peak-to-peak amplitude of 80 µm and a welding and consolidation pressure of 1.6 MPa (corresponding force - 500 N). The vibrations were stopped once the vertical displacement of the sonotrode reached 0.07 mm in the downward direction. The welded specimens were then tested for its LSS, void content, and weld line thickness.

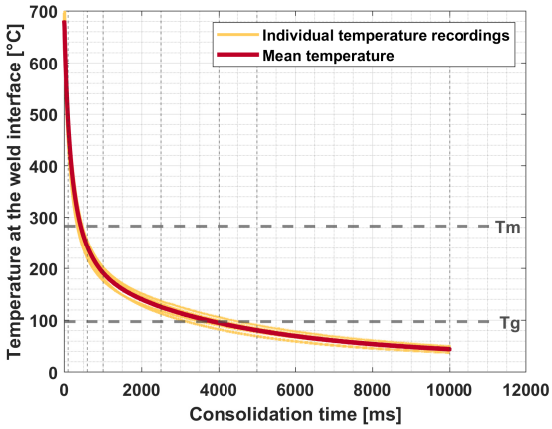

Figure 4.8: Variation of temperature during the consolidation phase in static ultrasonic welding; Vibration amplitude (peak-to-peak): 80 µm, welding pressure: 1.6 MPa (500 N), consolidation pressure: 1.6 MPa, consolidation time: 10000 ms, weld control - displacement to 0.07 mm

Table 4.1: Choice of consolidation time

Consolidation Time	Justification for choice
0 ms	Represents no consolidation
100 ms	Specimen interface temperature above Tm
600 ms	Specimen interface temperature between Tg and Tm, but closer to Tm
1000 ms	Specimen interface temperature midway between Tg and Tm
2500 ms	Specimen interface between Tg and Tm, but close to Tg
4000 ms	State of the art [17, 22, 40–43, 59, 60]
5000 ms	Specimen interface temperature below Tg
10000 ms	Specimen interface temperature close to room temperature

Lap shear strength

The results of the LSS tests of specimens welded at varying consolidation times are shown in Figure 4.9 and Table 4.2. The average temperature at the weld interface is also plotted in the figure for better clarity. When the application of consolidation pressure was stopped before the temperature at the weld interface dropped below the melting temperature (welds with consolidation time of 100 ms and welds without consolidation), the single LSS was low. Specimens welded without consolidation were not bonded when it was taken out of the welding jig (hence LSS of 0 MPa). The strength of the weld when consolidated for 100 ms averaged 2.5 MPa for the two welds, which was tested for LSS (three of the welds debonded when taken out of the welding jig). Consolidating for 600 ms and 1000 ms represented welds where the temperature of the interface dropped below Tm. At 600 ms of consolidation time, the temperature at the interface was between 220 °C and 260 °C and exhibited LSS of 18.7 ± 6.0 MPa. However, slightly increasing the consolidation time to 1000 ms, where the temperature dropped to less than 200 °C increased the LSS to 32.3 ± 1.7 MPa. The strength of the welds at consolidation times of 2500 ms, 4000 ms, 5000 ms, or 10000 ms is not statistically different from the specimens welded with a consolidation time of 1000 ms, even though the temperature at the weld interface only dropped below Tg at about 5000 ms. A one-way between subjects ANOVA conducted to compare the effect of consolidation time on single LSS for 1000, 2500, 4000, 5000 and 10000 ms revealed that there is no significant effect of consolidation time on single LSS at the $p < 0.05$ level for consolidation times above 1000 ms [$F(4, 15) = 2.65$, $p = 0.074$].

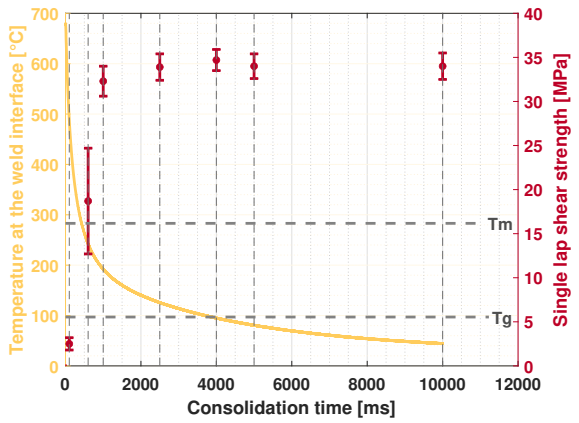

Consolidation time [ms]	LSS [MPa]
0	0
100	2.5 $\pm$ 0.7
600	18.7 $\pm$ 6.0
1000	32.3 $\pm$ 1.7
2500	33.9 $\pm$ 1.5
4000	34.7 $\pm$ 1.2
5000	34.0 $\pm$ 1.4
10000	34.0 $\pm$ 1.5

Figure 4.9 & Table 4.2: Effect of consolidation time on lap shear strength; Vibration amplitude (peak-to-peak): 80 µm, welding pressure: 1.6 MPa (500 N), consolidation pressure: 1.6 MPa, weld control - displacement to 0.07 mm

Fracture surface analysis

Figure 4.10 shows the fracture surfaces of specimens welded at varying consolidation times. The fracture surfaces, for specimens with consolidation times of 100 ms and 600 ms, and welds without consolidation showed a distinctive polymer accumulation in the weld interface. The texture of the fracture surfaces drastically changed when the consolidation time was increased to 1000 ms. The voids from the fracture surface at 1000 ms were more than that observed when consolidated for 2500 ms or 4000 ms. Voids can be seen in welds with consolidation time until 4000 ms. There was no intact ED observed in any of the welds. The failure occurred at the weld line for all specimens welded at varying consolidation times under the chosen welding parameters.

Cross-sectional micrographs

The cross-sectional micrographs of welds consolidated for different durations are shown in Figure 4.11. For specimens welded with no consolidation and a consolidation time of 100 ms, no welded joints were formed. For the specimen welded with a consolidation time of 600 ms, numerous voids were visible along the weld line. For the specimens welded at consolidation times of 1000 ms or above, voids were not visible in substantial quantities. Moreover, the voids in all cases were concentrated mainly in the weld interface and not within the adherends. Squeeze flow was observed, but these are mostly restricted to the polymer from the weld line.

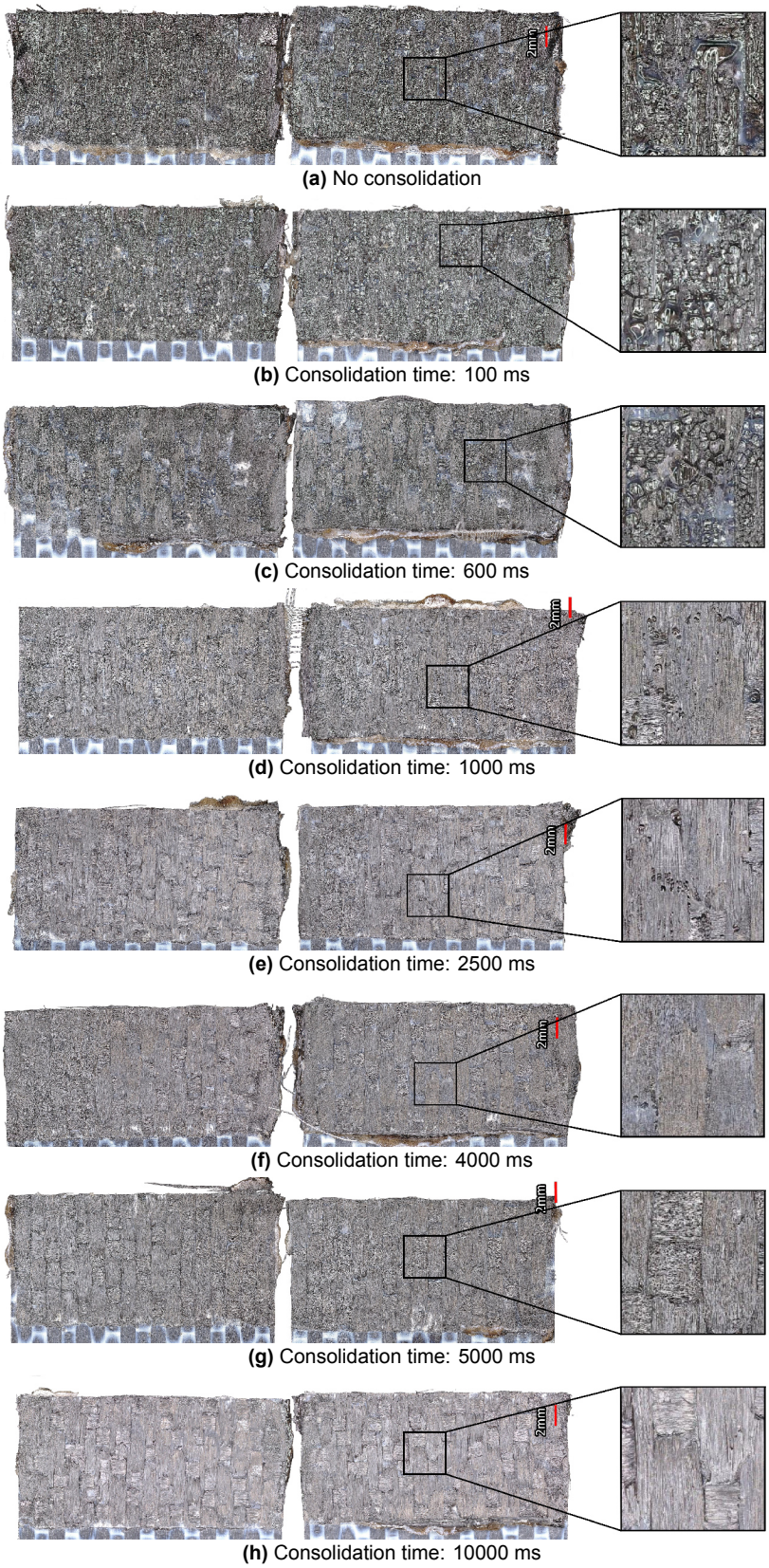

(a) No consolidation

(b) Consolidation time: 100 ms

(c) Consolidation time: 600 ms

(d) Consolidation time: 1000 ms

(e) Consolidation time: 2500 ms

(f) Consolidation time: 4000 ms

(g) Consolidation time: 5000 ms

(h) Consolidation time: 10000 ms

Figure 4.10: Fracture surface of samples welded at varying consolidation time; Vibration amplitude (peak-to-peak): 80 µm, welding pressure: 1.6 MPa (500 N), consolidation pressure: 1.6 MPa, weld control - displacement to 0.07 mm

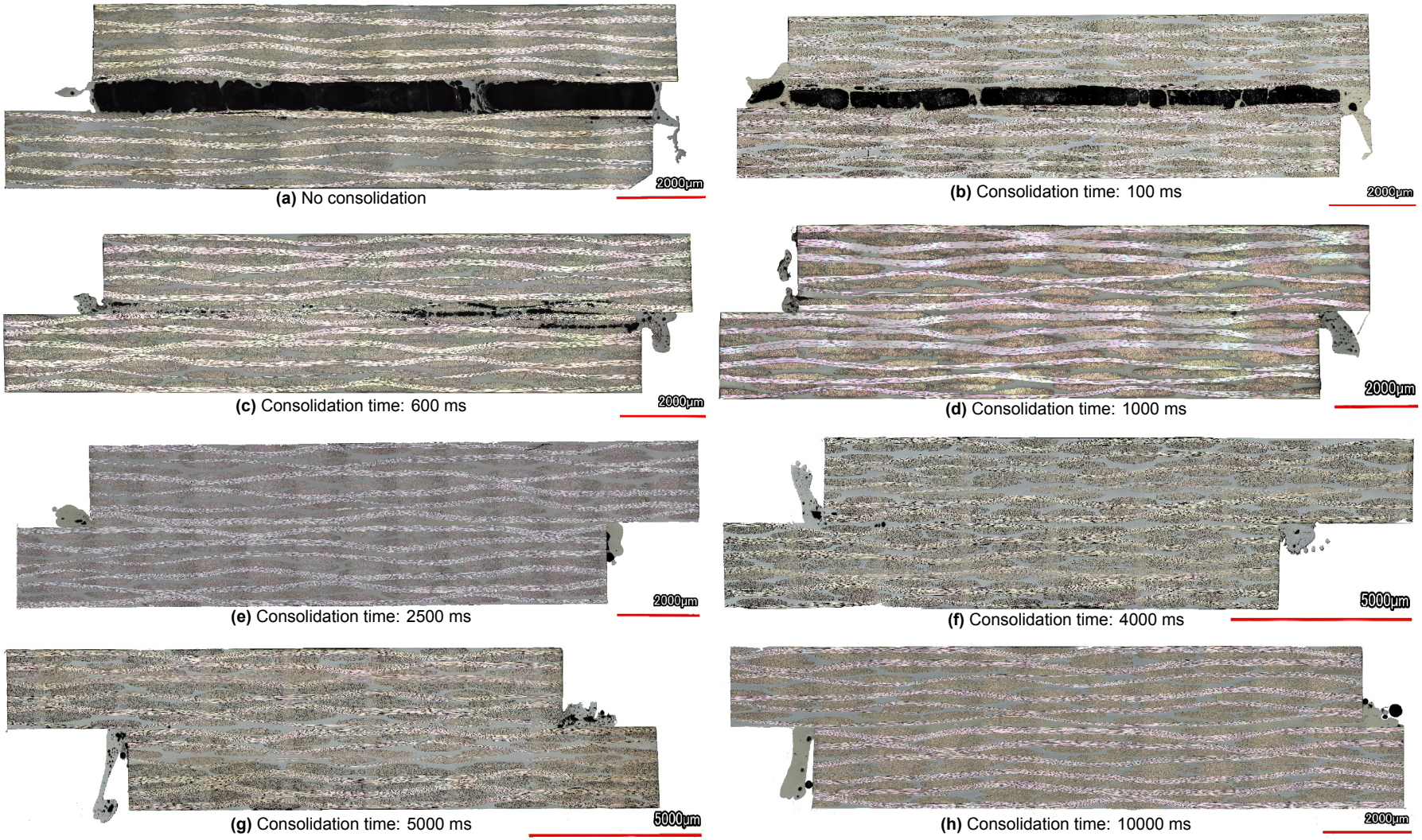

Figure 4.11: Cross-sectional micrographs of specimens welded at different consolidation time (observed at 10x magnification); The top adherend is on the top; Vibration amplitude (peak-to-peak): 80 µm, welding pressure: 1.6 MPa (500 N), consolidation pressure: 1.6 MPa, weld control - displacement to 0.07 mm

Micro-CT scans

The distribution of the voids was as shown in Figure 4.12. While the specimen consolidated for 600 ms had voids distributed throughout the weld line, the welds with consolidation time of 1000 ms or higher showed voids majorly at the edge of the welds. Appendix E includes additional images from the micro-CT scans for better clarification.

Table 4.3 shows the volumetric void content of the specimens welded at varying consolidation times obtained via micro-CT of the welded specimens. The specimens which were used for volumetric void content determination were further tested for its LSS, which is also reported in the table. The average LSS calculated earlier (from Table 4.2) have also been listed for further clarity. When consolidated for 600 ms, the void content was 0.61% compared to void content of 0.05-0.07 % for the welds consolidated for 1000 ms or more. The void content of the weld consolidated for 600 ms was more than ten times than when welded with a consolidation time of 1000 ms. None of the welds had a volumetric void content above 1%.

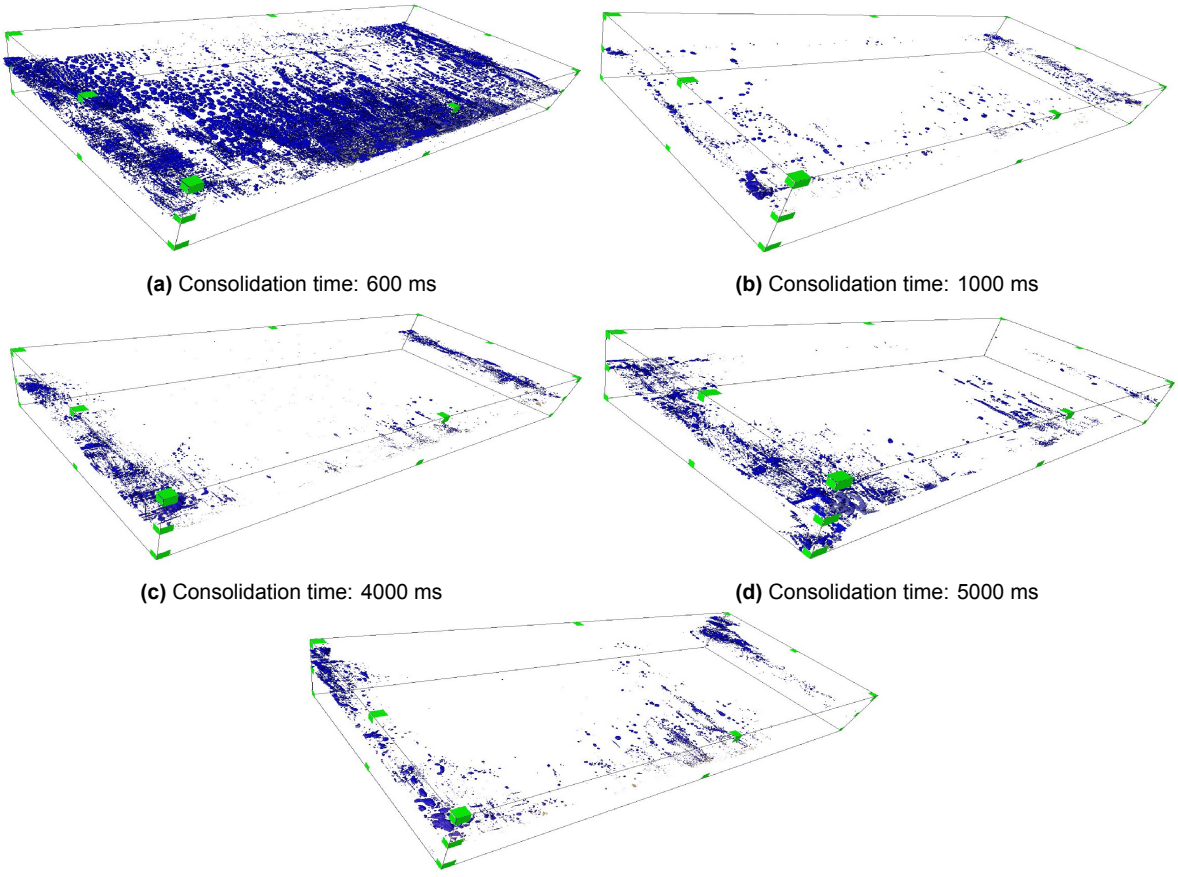

(a) Consolidation time: 600 ms

(b) Consolidation time: 1000 ms

(c) Consolidation time: 4000 ms

(d) Consolidation time: 5000 ms

(e) Consolidation time: 10000 ms

Figure 4.12: CT scan image of specimens welded with varying consolidation times depicting the distribution of voids within the welded specimens; Vibration amplitude (peak-to-peak): 80 µm, welding pressure: 1.6 MPa (500 N), consolidation pressure: 1.6 MPa, weld control - displacement to 0.07 mm

Degree of crystallinity assessment

Figure 4.13 and Table 4.4 shows the degree of crystallinity of the isolated ED when welded at varying consolidation times. The pristine ED had a degree of crystallisation of 38.4 ± 0.4 %. The crystallinity at a consolidation time of 600 ms and 1000 ms did not vary much from each other but showed a degree

Table 4.3: Volumetric void content of specimens welded at varying consolidation time; Vibration amplitude (peak-to-peak): 80 µm, welding pressure: 1.6 MPa (500 N), consolidation pressure: 1.6 MPa, weld control - displacement to 0.07 mm

Consolidation time [ms]	Volumetric void content [%]	LSS of the micro-CT specimen [MPa]	Average LSS from Table 4.2 (n=5) [MPa]
600	0.61	25.7	18.7 ± 6.0
1000	0.05	34.5	32.3 ± 1.7
4000	0.05	35.2	34.7 ± 1.2
5000	0.07	32.7	34.0 ± 1.4
10000	0.06	33.5	34.0 ± 1.5

of crystallinity of about 11-13%. When consolidation time was increased to 10000 ms, the crystallinity of the weld interface dropped to 6.2 ± 1.0 %.

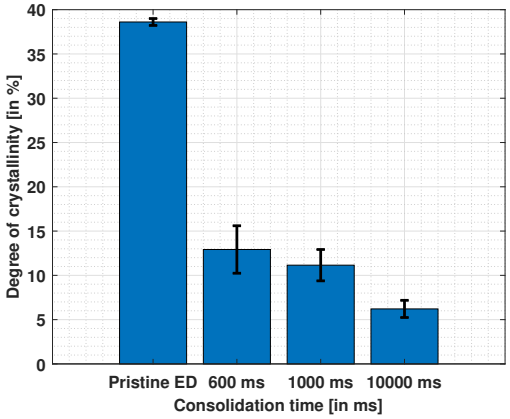

Consolidation Time [ms]	Degree of crystallisation (n=3) [%]
Pristine ED	38.6 ± 0.4
600	12.9 ± 2.7
1000	11.2 ± 1.8
10000	6.2 ± 1.0

Figure 4.13 & Table 4.4: Degree of crystallinity at the weld interface when welded with varying consolidation times; Vibration amplitude (peak-to-peak): 80 µm, welding pressure: 1.6 MPa (500 N), consolidation pressure: 1.6 MPa, weld control - displacement to 0.07 mm

Weld line thickness measurement

Figure 4.14 and Table 4.5 shows the weld line thickness of specimens welded with varying consolidation times. While 600 ms of consolidation force application resulted in an average weld line thickness of 55 ± 18 µm, the weld line thickness for welds with a consolidation time of 1000 ms and above only varied marginally between 20 µm to 6 µm.

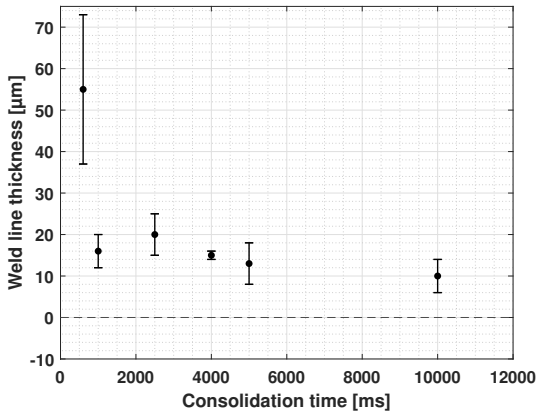

Consolidation time [ms]	Weld line thickness [µm]
600	55 ± 18
1000	16 ± 4
2500	20 ± 5
4000	15 ± 1
5000	13 ± 5
10000	10 ± 4

Figure 4.14 & Table 4.5: Weld line thickness for specimens welded at varying consolidation time; Vibration amplitude (peak-to-peak): 80 µm, welding pressure: 1.6 MPa (500 N), consolidation pressure: 1.6 MPa, weld control - displacement to 0.07 mm

4.5.3. Discussion - Effect of consolidation time

This section discusses the results obtained from tests performed to answer the first part of the research objective, i.e., the effect of consolidation times on the consolidation of the weld interface. The research began with the definition of certain consolidation times that corresponded to various thermal stages of the polymer during the consolidation phase, as shown in Table 4.1. The initial hypothesis was that the consolidation should continue until the temperature dropped below the glass transition temperature of the polymer. For the polymer chosen, the melting temperature was 283 °C, and the glass transition temperature was 97 °C [43].

The average temperature profile at the weld interface, as mentioned in Figure 4.8, is the average temperature recordings at the hottest part of the weld interface of five different welds. The mean temperature in Figure 4.8 has been used for all temperature-related discussions since it provides an estimate of the temperature at the weld interface at any given time during the consolidation phase despite the temperature at the start of consolidation being different for all five readings. Also, from Figure 4.8, it can be deduced that the temperature at the interface dropped from a peak temperature of above 600 °C to a temperature below glass transition temperature in a short span of 5 s during the consolidation phase. This meant that the polymer transitioned from being a melt to a glassy state and then finally solidified, all within a 10 s time frame.

Consolidation pressure stopped before the interface temperature drops below Tm

When the application of consolidation pressure was stopped before the interface temperature dropped below Tm (specimens welded without consolidation and specimens consolidated for 100 ms), no consolidated joints were formed as seen in Figure 4.11a and Figure 4.11b. The strength of the joints was negligible, and the fracture surfaces showed a resin-rich surface. The polymer melt was not capable of providing enough cohesive force to hold the adherends together due to a lack of external pressure when the temperature dropped below Tm resulted in deconsolidated welds. This deconsolidation of the weld was plausibly due to the traction of the sonotrode while it retracted that enabled fibre decompaction due to a lack of external consolidation pressure application when the interface temperature dropped below Tm. Appendix B details the effect of clamps on deconsolidation in USW when welded without external consolidation pressure application. It was seen that the specimens welded without clamps and held in place by tapes (no-clamp configuration) and specimens held in place by bar clamps (bar clamp configuration) produced joints with strengths of 6.6 ± 0.6 MPa and 15.2 ± 2.7 MPa respectively (see Appendix B). This confirms that the clamping mechanism does indeed affect the consolidation quality.

The LSS of specimens welded with a consolidation time of 100 ms (2.5 ± 0.7 MPa) was slightly higher than that of welds with no consolidation (0 MPa). This difference was presumably due to the polymer melt which solidified when the temperature dropped below Tm during the upward movement of the top adherend during deconsolidation. This solidified polymer holding the two adherends together can be observed in Figure 4.11a and Figure 4.11b.

Consolidation pressure stopped when the interface temperature was between Tm and Tg

The quality of the welded specimens in which the application of consolidation pressure was stopped when the interface temperature was between Tm and Tg improved significantly when compared to welded specimens whose consolidation pressure application was stopped before the interface temperature dropped below Tm.

The LSS of specimens consolidated for 600 ms was only 18.7 ± 6.0 MPa in comparison to welds consolidated for 1000 ms whose LSS was 32.3 ± 1.7 MPa, as seen in Figure 4.9. Additionally, the volumetric void content of specimens consolidated for 600 ms was more than ten times than that observed for specimens consolidated for 1000 ms. The deconsolidation of the specimen consolidated for 600 ms was further substantiated by a thicker weld line (55 ± 18 µm) as compared to a specimen consolidated for 1000 ms (16 ± 4 µm) as shown in Figure 4.14. This is interesting since the interface

temperature of the specimen at 600 ms was about 220-260 °C while at 1000 ms was about 170-200 °C (from Figure 4.8). Literature on polymer properties around this temperature revealed that the crystallisation temperature of the PPS polymer is assumed to lie between 160 °C and 190 °C [37]. Additionally, for amorphous polymers, a temperature of 60-100 °C above Tg is roughly assumed as the temperature of the onset of truly liquid melt [53] which would again fall in the range of 160-200 °C. At temperatures between Tg and Tc, a semi-crystalline polymer is known to retain both the viscous and elastic properties, giving it the characteristics of solids [13], since the chain mobility is hindered by the crystals [61, 62]. Hence tests were performed to determine if the ultrasonically welded specimens still retained a semi-crystalline structure despite the very high cooling rates. The results (see Figure 4.13) indicated that the weld interface crystallised (a degree of crystallinity between 6-13%), a possible reason being the high strain rates due to the high vibration frequencies used in the welding process [37]. This implied that the consolidation should be extended at least until the temperature at the weld interface drops below the crystallisation temperature to obtain a well-consolidated weld. This might also explain the high standard deviations in the LSS of welds consolidated for 600 ms. External factors like clamping of the adherends or slight changes in the welding parameters during welding might have resulted in variations in the cooling rate at the weld interface. This most likely would have resulted in a difference in the LSS of specimens consolidated for 600 ms.

Now that the consolidation time requirement for the semi-crystalline polymer was determined, it was imperative to investigate why the weld deconsolidates when the consolidation pressure application was stopped before the interface temperature dropped below Tc (welds whose consolidation pressure application was stopped after 600 ms). Hence the reasons behind the formation of voids in the weld interface were investigated. One of the major contributors to thermal deconsolidation is the decompaction of fibre reinforcement network [10, 12, 13, 51] during the reheating process of thermoplastic composites in the absence of external pressure application. In USW, if the consolidation pressure is not adequately applied, welds can deconsolidate as was seen in welds whose consolidation was stopped before the interface temperature dropped below Tm.

The springs of the spring jig can exert a retraction force on the adherend that can lead to deconsolidation if the consolidation force application is prematurely terminated. To test the effect of springs of the spring jig on the void formation and consolidation quality, specimens were welded in a no-clamp configuration (see Appendix B for further details) and consolidated for 600 ms. Cross-sectional micrographs were made, and the LSS was tested and compared against specimens welded with the spring jigs. The results of the LSS are as in Table 4.6, fracture surface analysis in Figure 4.15 and cross-sectional micrographs in 4.16. The LSS of specimens welded with no clamp configuration and consolidated for 600 ms was as high as that observed when consolidated for longer durations in the spring jig. The fracture surfaces and the cross-sectional micrographs indicate that the void content greatly reduced when the no clamp configuration was used. This is conclusive to ascertain that the springs of the spring jig played a major role in void formation during the USW process.

Table 4.6: LSS of specimens welded in different clamping configurations and consolidated for 600 ms; Vibration amplitude (peak-to-peak): 80 µm, welding pressure: 1.6 MPa (500 N), consolidation pressure: 1.6 MPa, weld control - displacement to 0.07 mm

Clamping mechanism	LSS (in MPa)
Spring Jig	18.70 ± 6.0 (n=5)
No clamp configuration	34.09 ± 1.2 (n=4)

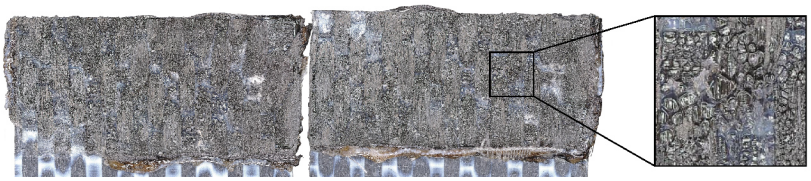

(a) Spring jig

(b) No clamp configuration

Figure 4.15: Fracture surface of specimens welded with different clamping configurations; Vibration amplitude (peak-to-peak): 80 µm, welding pressure: 1.6 MPa (500 N), consolidation time: 600 ms, consolidation pressure: 1.6 MPa, weld control - displacement to 0.07 mm

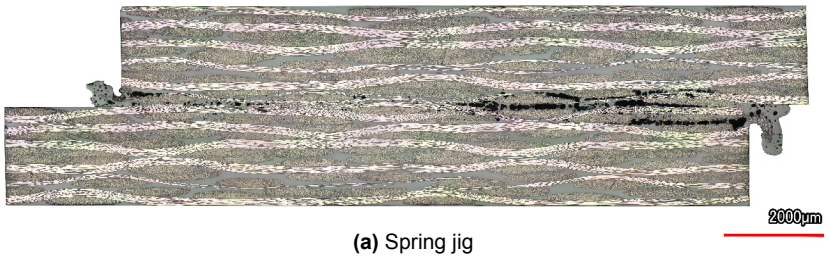

(a) Spring jig

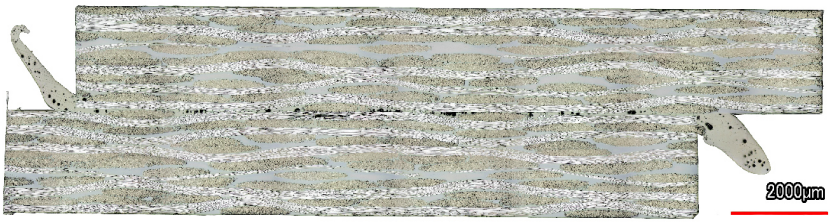

(b) No clamp configuration

Figure 4.16: Cross-sectional micrographs of specimens welded with different clamping configurations; Vibration amplitude (peak-to-peak): 80 µm, welding pressure: 1.6 MPa (500 N), consolidation time: 600 ms, consolidation pressure: 1.6 MPa, weld control - displacement to 0.07 mm

When specimens were welded with a consolidation time of 600 ms in the no-clamp configuration, the effect of the retraction forces of the springs in the spring jig was eliminated. But voids were still observed in the weld line as seen in Figure 4.16b. Since the interface temperature at 600 ms was close to Tc of the polymer, a likely reason for void formation might be the shrinkage induced by crystallisation. It was already seen in Figure 4.13 that specimens welded with a consolidation time of 600 ms crystallise despite the very high cooling rates. To test if the crystallisation of the polymer contributed to void formation, specimens were welded by consolidator placed12 mm froming the ED from the weld interface by placing it between two Kapton films before welding as defined in section 4.4.6. This methodology ensured that the ED was free from fibre decompaction induced voids while the no-clamp configuration ensured the retraction forces of the springs were eliminated from the study. Post welding, the isolated ED was separated from the weld line and was inspected under the microscope. The image thus obtained was as shown in Figure 4.17. Voids were still observed in the ED, indicating that the voids were most likely formed from the shrinkage in the polymer during crystallisation.

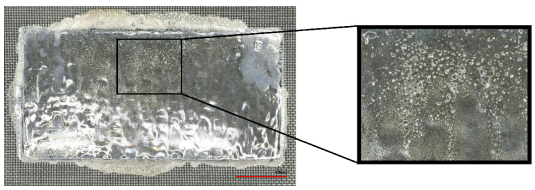

Figure 4.17: Isolated ED from specimens welded in the no clamp configuration; Vibration amplitude (peak-to-peak): 80 µm, welding pressure: 1.6 MPa (500 N), consolidation time: 600 ms, consolidation pressure: 1.6 MPa, weld control - displacement to 0.07 mm

The shrinkage due to crystallisation can also introduce cavitation voids [13, 63, 64], which are nanometre and micrometre sized voids but may require higher resolution microscopes to effectively detect and quantify and hence has not been considered here. Given the low moisture absorption rates of PPS [65, 66], it was assumed that the void formation due to residual volatiles in the polymer, which was a dominant mechanism for void formation in resistance welding of CF/PEI [58], is negligible.

Consolidation pressure stopped before the interface temperature drops below Tg

From Figure 4.12, the voids in the specimens consolidated for 1000 ms or more were observed to concentrate at the weld edges rather than in the weld interface. It can be assumed that the voids at the edges of the specimens were potentially due to the squeeze flow of the polymer. The strength and the volumetric void content for specimens consolidated when the consolidation pressure was stopped after the interface temperature drops below Tg (consolidation times of 4000 ms, 5000 ms and 10000 ms) were comparable to results obtained for specimens consolidated for 1000 ms (see Table 4.2 and Table 4.3). But the fracture surfaces in Figure 4.10 showed that the voids decreased slightly when the consolidation time was increased above 1000 ms. This difference in observation might be since the resolution of the micro-CT scan was only 14 µm which meant that smaller voids whose diameter were less than 14 µm were not observed. Additionally, the strength of specimens which were computed for micro-CT scans varied slightly from the average LSS as seen in Table 4.3.

Crystallinity at the weld interface under varying consolidation time

The degree of crystallisation at the weld line decreased with an increase in consolidation time. A reasonable explanation is that the removal of sonotrode resulted in a decrease in the cooling rates between Tm and Tg (refer Figure 4.18) probably aided by the lack of external consolidation pressure. This is assumed to result in a reduction in the compactness of the fibre network, thus reducing heat transfer via the carbon fibres. Since crystallisation continues until the temperature reaches Tg, it was possible that the differences in cooling rates might also influence the degree of crystallisation.

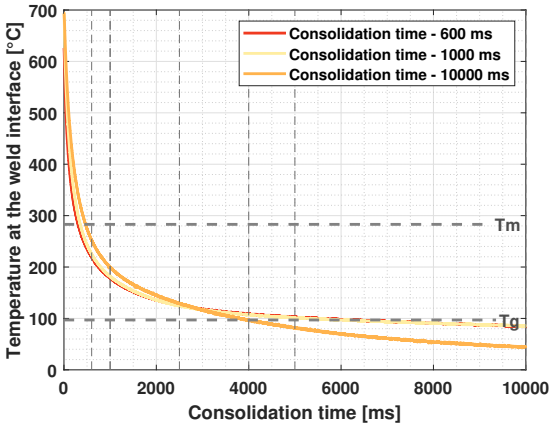

Figure 4.18: Dependency of cooling rate on consolidation time; Vibration amplitude (peak-to-peak): 80 µm, welding pressure: 1.6 MPa (500 N), consolidation pressure: 1.6 MPa, weld control - displacement to 0.07 mm

4.6. Effect of varying consolidation pressure on the consolidation of the welds

This section investigates how the consolidation pressure influences the consolidation of the weld interface in static USW of thermoplastic composites. The section initially discusses the methodology used for investigating how consolidation pressure influences the consolidation quality, which is followed by the results of the tests and concludes with the discussion of results obtained.

4.6.1. Methodology

The research started by investigating how cooling rates during consolidation are influenced by consolidation pressure. It was hypothesised that the effect of consolidation pressure on cooling rate would be minimal. Thermocouples were incorporated as stated in section 4.3.2 and specimens were welded at three different consolidation pressures of 0.4 MPa, 1.6 MPa and 4.7 MPa. Consolidation pressures were then chosen for the trials based on the welding pressure (two consolidation pressures each above and below the welding pressure). Seven specimens were welded in each configuration out of which five were subjected to LSS assessments, and one each for cross-sectional micrography and micro-CT scans. All characterisation techniques mentioned in section 4.5.1 (barring crystallisation tests) were carried out. Apart from these, the sonotrode displacement during welds with different consolidation pressures was plotted to identify if a method can be developed to control in-situ the consolidation process. A peak-to-peak amplitude of 80 µm, welding pressure of 1.6 MPa, and a consolidation time of 10000 ms was used. The vibrations were stopped once the vertical displacement of the sonotrode reached 0.07 mm in the downward direction.

To investigate the effect of varying consolidation pressure on consolidation, consolidation forces (or pressures) had to be initially defined. Welds were consolidated for 10000 ms post vibration to eliminate any effect that might arise due to the influence of consolidation time on the consolidation force. The inter-dependency of consolidation time and pressure are discussed in Appendix D. It was calculated that the minimum consolidation pressure possible with the weld overlap was 0.4 MPa (the machine had a lower force limit of 130 N). The higher limit was fixed as 4.7 MPa, thrice the welding pressure, which corresponds to a consolidation force of 1500 N (the higher limit of the machine). The welding pressure was kept at a constant 1.6 MPa throughout the process. The consolidation forces (and the corresponding consolidation pressure) thus chosen are tabulated below.

Table 4.7: Consolidation pressures chosen for study

Consolidation force [N]	Consolidation pressure [MPa]	Justification for choice
0	0	No consolidation
130	0.4	Lowest force possible with the static Hermann machine at TU Delft
200	0.6	Another low consolidation pressure trial
500	1.6	Same as the welding pressure
1000	3.1	A high consolidation pressure trial
1500	4.7	Highest force possible with the static Hermann machine at TU Delft

4.6.2. Experimental Results - Effect of consolidation pressure

Cooling rates for varying consolidation pressure

Trials were conducted to investigate how the consolidation pressure influences the cooling rate. Three consolidation pressures were chosen - same as the welding pressure (500 N - 1.6 MPa), a lower consolidation pressure (130 N - 0.4 MPa), and a higher consolidation pressure (1500 N - 4.7 MPa). Consolidation time was fixed at 10000 ms to eliminate any effect that might arise due to the removal of consolidation pressure before the temperature at the weld line drops below Tg. The corresponding cooling curves and an overlaid plot are shown in Figure 4.19 and Figure 4.20. Five different welds with a thermocouple placed in the weld interface were analysed for each configuration. The mean temperature was also plotted. For the welds, which had a consolidation pressure of 0.4 MPa and 1.6 MPa, the mean temperature almost overlaps. The individual temperature profiles for the welds at

0.4 MPa and 4.7 MPa consolidation pressures are more scattered than that of 1.6 MPa consolidation pressure. The weld interface cooled down the fastest when welded with a consolidation pressure of 4.7 MPa.

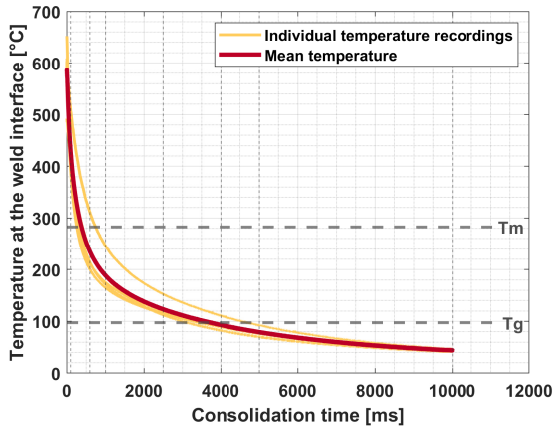

(a) Temperature drop at 0.4 MPa consolidation pressure

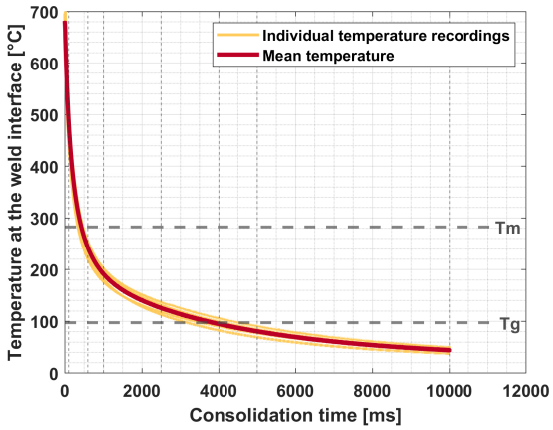

(b) Temperature drop at 1.6 MPa consolidation pressure

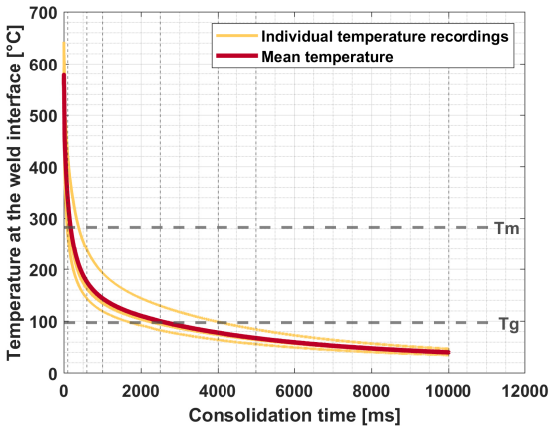

(c) Temperature drop at 4.7 MPa consolidation pressure

Figure 4.19: Dependency of cooling rate on consolidation pressure; Vibration amplitude (peak-to-peak): 80 µm, welding pressure: 1.6 MPa (500 N), consolidation time: 10000 ms, weld control - displacement to 0.07 mm

Effect of varying consolidation pressures on (de)consolidation

Based on the consolidation pressures defined in Table 4.7, specimens were welded with a peak-to-peak amplitude of 80 µm, welding force of 500 N and a consolidation time of 10000 ms. The vibrations were stopped once the vertical displacement of the sonotrode reached 0.07 mm in the downward direction.

Lap shear strength

Single LSS values for the specimens consolidated at varying consolidation pressure are shown in Figure 4.21 and Table 4.8. Even at a consolidation pressure of 0.4 MPa, the strength of the welded joint was relatively high. However, the strength of the welded joint increased as the consolidation pressure increased. While the LSS of the welded joint at a consolidation pressure of 0.4 MPa was 29.48 ± 0.90 MPa, it rose to 36.08 ± 0.69 MPa at a consolidation pressure of 4.7 MPa. A one-way between-subjects ANOVA conducted to compare the effect of consolidation pressure on single LSS for 0.4 MPa, 0.6 MPa, 1.6 MPa, 3.1 MPa, and 4.7 MPa revealed that there is a significant effect of consolidation pressure on single LSS at the $p < 0.05$ level for the five conditions stated [$F(4,20) = 31.75$, $p = 2E\text{-}08$]. Post hoc comparisons indicated that the single LSS of welds varied significantly between the lower consolidation pressures (0.4 MPa and 0.6 MPa) and higher consolidation

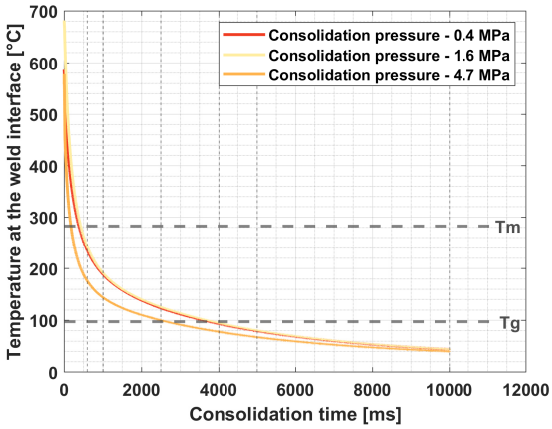

Figure 4.20: Overlaid plot of the interface temperature change with varying consolidation pressures during consolidation phase; Vibration amplitude (peak-to-peak): 80 µm, welding pressure: 1.6 MPa (500 N), consolidation time: 10000 ms, weld control - displacement to 0.07 mm

pressures (3.1 MPa and 4.7 MPa) but did not vary significantly between consolidation pressures of 1.6 MPa, 3.1 MPa and 4.7 MPa.

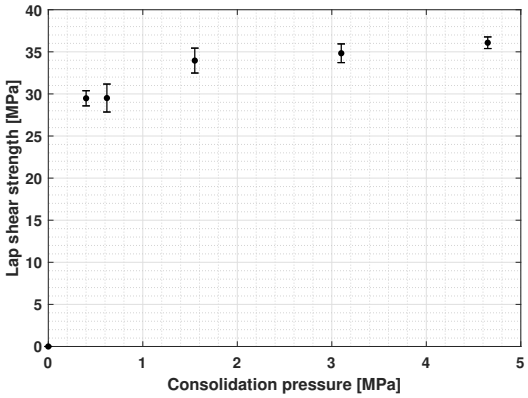

Consolidation Pressure (Force) [MPa] (N)	LSS (n=5) [MPa]
0 (0)	0
0.4 (130)	29.5 ± 0.9
0.6 (200)	29.5 ± 1.7
1.6 (500)	34.0 ± 1.5
3.1 (1000)	34.9 ± 1.1
4.7 (1500)	36.1 ± 0.7

Figure 4.21 & Table 4.8: Effect of consolidation pressure on LSS; Vibration amplitude (peak-to-peak): 80 µm, welding pressure: 1.6 MPa (500 N), consolidation time: 10000 ms, weld control - displacement to 0.07 mm

Fracture surface analysis

The fracture surfaces of the welded specimens are shown in Figure 4.22. No intact ED was found in the welds, and the ED was well melted. For welds with a consolidation pressure of 0.4 MPa and 0.6 MPa, resin accumulation can be found in the weld interface (see Figure 4.22). Not many differences were noticed in the fracture surfaces of welds with a consolidation pressure of 1.6 MPa or more.

Cross-sectional micrographs

The cross-sectional micrographs of the specimens welded at different consolidation pressures are shown in Figure 4.23. The cross-sectional micrographs of welds without consolidation was already discussed in section 4.5.2. The specimens welded with a consolidation pressure of 0.4 MPa showed the presence of voids in the weld line. The welds from 1.6 MPa consolidation pressure and above showed almost no voids in the weld line. The squeeze flow at higher consolidation pressures of 3.1 MPa and 4.7 MPa was comparatively higher than that seen at lower consolidation forces, though not quantified.

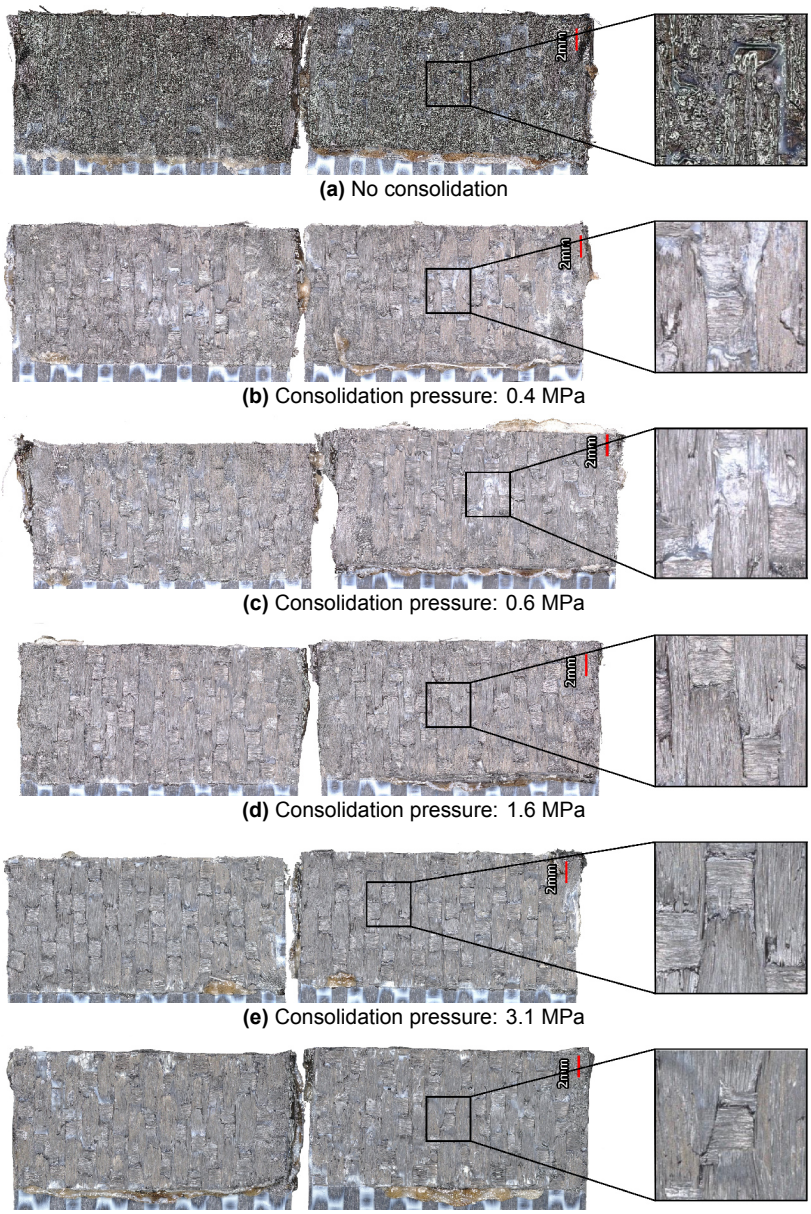

(a) No consolidation

(b) Consolidation pressure: 0.4 MPa

(c) Consolidation pressure: 0.6 MPa

(d) Consolidation pressure: 1.6 MPa

(e) Consolidation pressure: 3.1 MPa

(f) Consolidation pressure: 4.7 MPa

Figure 4.22: Fracture surface of samples welded at varying consolidation pressure; Vibration amplitude (peak-to-peak): 80 µm, welding pressure: 1.6 MPa (500 N), consolidation time: 10000 ms, weld control - displacement to 0.07 mm

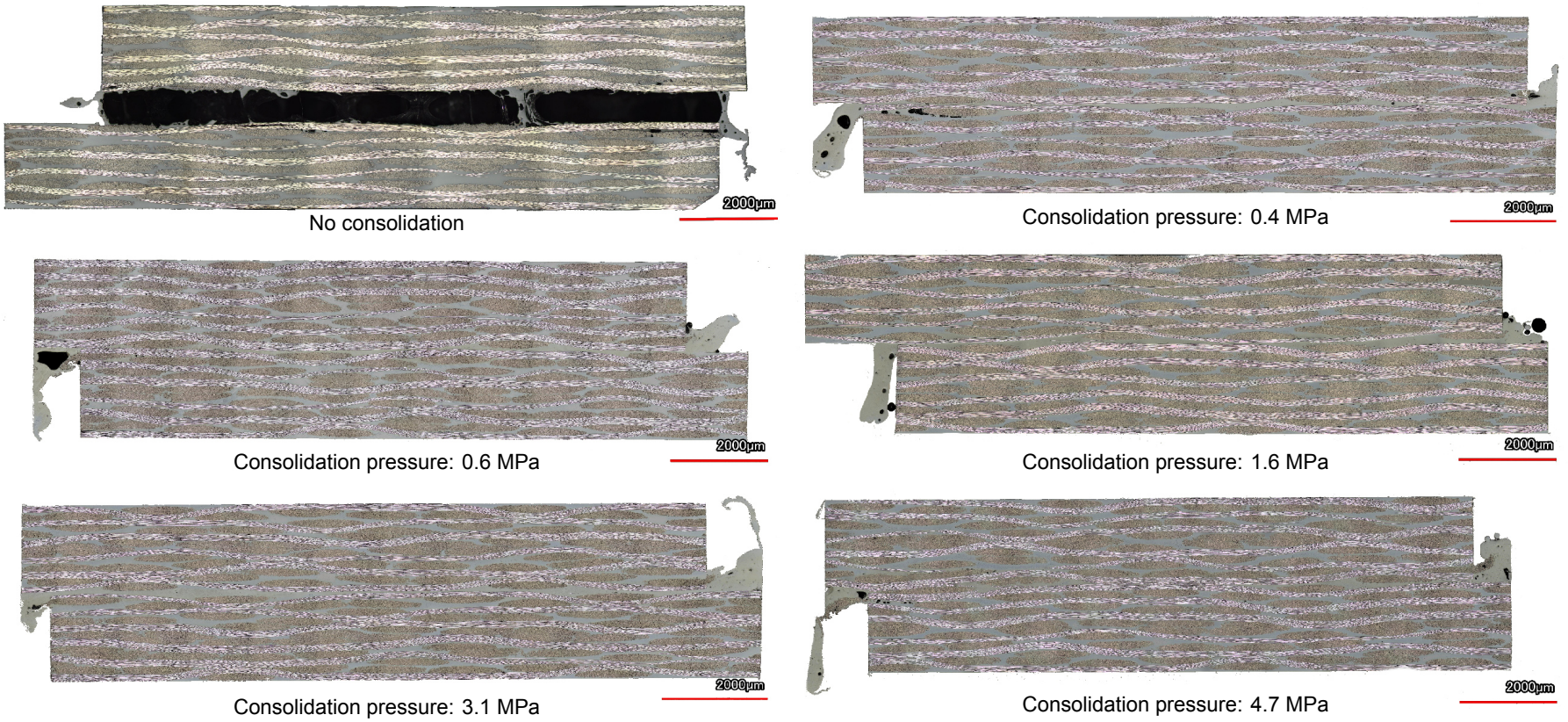

Figure 4.23: Cross-sectional micrographs of specimens welded at different consolidation pressure (observed at 10x magnification); The top adherend is on the top; Vibration amplitude (peak-to-peak): 80 µm, welding pressure: 1.6 MPa (500 N), consolidation time: 10000 ms, weld control - displacement to 0.07 mm

Micro-CT scans

Figure 4.24 shows the distribution of voids within the weld interface. Voids can be seen throughout the weld interface when welded with a consolidation pressure of 0.4 MPa. As the consolidation pressure was increased to 1.6 MPa and beyond, the voids in the weld interface were much lower. But as the pressure increased, the voids in the weld edges increased. Appendix E includes additional images from the micro-CT scans for better clarification.

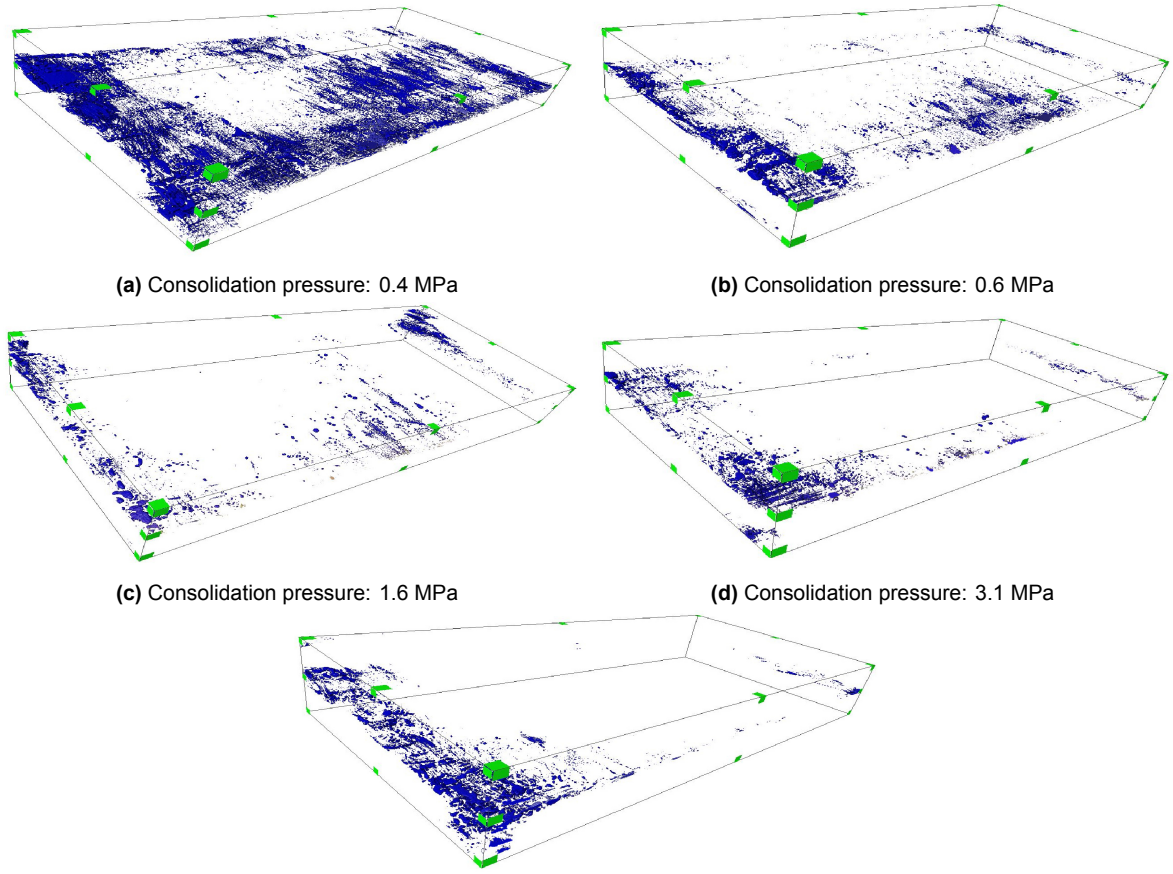

(a) Consolidation pressure: 0.4 MPa

(b) Consolidation pressure: 0.6 MPa

(c) Consolidation pressure: 1.6 MPa

(d) Consolidation pressure: 3.1 MPa

(e) Consolidation pressure: 4.7 MPa

Figure 4.24: CT scan image of specimens welded with varying consolidation pressures depicting the distribution of voids within the welded specimen; Vibration amplitude (peak-to-peak): 80 µm, welding pressure: 1.6 MPa (500 N), consolidation time: 10000 ms, weld control - displacement to 0.07 mm

Table 4.9 shows the volumetric void content of the welds at varying consolidation pressures. The average LSS calculated earlier (from Table 4.21) has also been tabulated for further clarity. Volumetric void content, in welds consolidated with a pressure of 0.4 MPa, was more than seven times the void content in welds consolidated with a pressure of 1.6 MPa. The void content, when welded with a consolidation pressure of 1.6 MPa or more, did not vary much and were close to 0.05-0.06%.

Weld line thickness measurement

The weld line thickness of the specimens welded with varying consolidation pressures is shown in Figure 4.25 and Table 4.10. There was a considerable decrease in weld line thickness as the consolidation pressure increased. Consolidation pressures of 0.4 MPa and below produced weld line thickness not lower than 40 µm. At pressures of 3.1 MPa and higher, the weld line was so barely visible that the thickness dropped to less than 5 µm. At consolidation pressure of 4.7 MPa or thrice the welding pressure, the excessive squeeze flow of the polymer resulted in negative weld line.

Table 4.9: Volumetric void content of specimens welded at varying consolidation pressure; Vibration amplitude (peak-to-peak): 80 µm, welding pressure: 1.6 MPa (500 N), consolidation time: 10000 ms, weld control - displacement to 0.07 mm

Consolidation pressure [MPa]	Volumetric void content [%]	Strength of the tested specimen [MPa]	Average LSS from Figure 4.21 [MPa]
0.4	0.46	27.2	29.5 ± 0.9
0.6	0.08	31.2	29.5 ± 1.7
1.6	0.06	33.5	34.0 ± 1.5
3.1	0.05	35.0	34.9 ± 1.1
4.7	0.06	35.0	36.1 ± 0.7

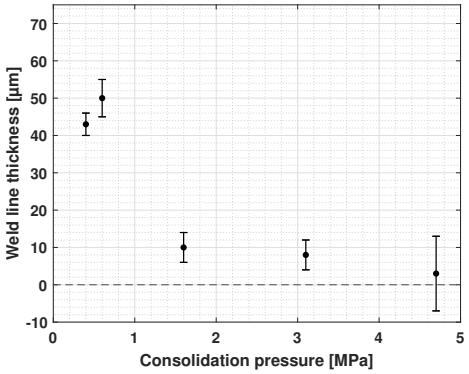

Consolidation pressure [MPa]	Weld line thickness [µm]
0.4	43 ± 3
0.6	50 ± 5
1.6	10 ± 4
3.1	8 ± 4
4.7	3 ± 10

Figure 4.25 & Table 4.10: Weld line thickness of specimens welded at varying consolidation pressure; Vibration amplitude (peak-to-peak): 80 µm, welding pressure: 1.6 MPa (500 N), consolidation time: 10000 ms, weld control - displacement to 0.07 mm

Displacement data from the microprocessor

The vertical displacement of the sonotrode under different consolidation pressures is presented in Figure 4.26. While consolidation pressure of 0.4 MPa showed a sonotrode vertical displacement of about 0.07 mm, it increased to 0.41 mm when a consolidation pressure of 4.7 MPa was used (the thickness of the ED was only 0.20 mm). The difference in the vertical displacement of the sonotrode between consolidation pressure of 0.4 MPa and 4.7 MPa was about 0.34 mm.

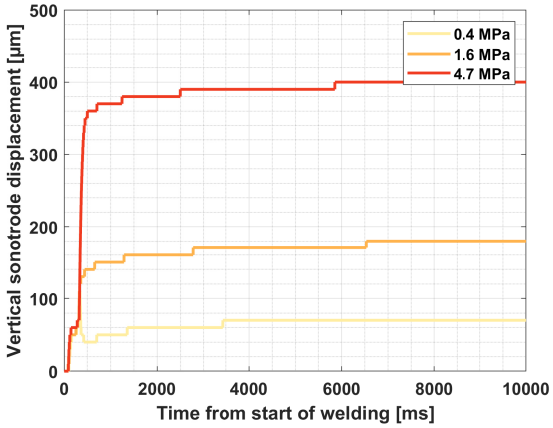

Figure 4.26: Vertical displacement of the sonotrode under varying consolidation pressure; Vibration amplitude (peak-to-peak): 80 µm, welding pressure: 1.6 MPa (500 N), consolidation time: 10000 ms, weld control - displacement to 0.07 mm

4.6.3. Discussion

This section discusses the results of the tests conducted to investigate the effect of consolidation pressures on the (de)consolidation of the weld interface. The research began with the definition of consolidation pressures or forces possible with the static welding machine, as shown in Table 4.1. The initial hypothesis was that a high consolidation pressure might result in excess squeeze flow of the resin and a low force might result in deconsolidation of the welded specimen.

The dependency of cooling rates on consolidation pressures

From Figure 4.20, the cooling rate was seen to increase with an increase in the consolidation pressure from 1.6 MPa to 4.7 MPa. The faster heat dissipation in welds consolidated at a higher consolidation pressure can be either due to the heat dissipated by the molten resin that was squeezed out, increased polymer flow [67] or an increased heat dissipation through the carbon fibres. Carbon fibres are good thermal conductors, and the higher consolidation forces might be resulting in compact fibre network aiding faster heat dissipation. The average temperature profile of 0.4 MPa consolidation pressure might seem to cool slightly quicker than that of 1.6 MPa consolidation pressure due to the scatter in the individual temperature profiles of welds with a consolidation pressure of 0.4 MPa.

Effect of consolidation pressure on the consolidation of the welds

A consolidation pressure as low as 0.4 MPa was found sufficient to provide welds with LSS of about 30 MPa. Despite this high strength, these welds showed the presence of voids in considerable quantities, as in Table 4.9. Welds with consolidation pressure of 0.4 MPa and 0.6 MPa also showed polymer accumulation at the weld interface, as seen in Figure 4.22. A consolidation pressure of 1.6 MPa (same as the welding pressure) had minimal void content and performed well in LSS. This was probably aided by the polymer flow and higher fibre compaction ensuring more heat dissipation via the carbon fibres compared to welds with consolidation pressure of 0.4 MPa and 0.6 MPa. These results were well supported by the weld line thickness observed. At higher consolidation pressures, the excess squeeze flow of resin away from the weld interface was seen to reduce the weld line thickness of the specimens, as is evidenced in Figure 4.25. This squeeze flow resulted in a weld line thickness of 3 ± 10 µm. A negative weld line indicates that the squeeze flow not only squeezed polymer from the ED but also the adherends.

The anomaly in the void content in the specimen welded with a consolidation pressure of 0.6 MPa was due to the higher strength of the specimen tested for void content. Nevertheless, the similarity in the average strength and the weld line thickness of specimens welded with a consolidation pressure of 0.4 MPa and 0.6 MPa are clear indications of deconsolidation.

Probable reasons for void formation

In section 4.5.3, it was seen that the significant factors that contribute to void formation were the shrinkage due to crystallisation, fibre decompaction, squeeze flow of the polymer and the retraction force exerted by the springs on the top adherend. The consolidation force was exerted until the interface temperature dropped below Tg; hence it should be able to hinder the formation of voids due to crystallisation shrinkage and fibre decompaction. But at lower pressures, voids were still observed in the weld interface, which meant that the pressure exerted was not adequate to prevent the formation of voids due to decompaction of the fibres. At higher pressures, the voids at the weld interface were comparatively lower, but these voids were concentrated more in the weld edges. These voids were most likely the result of squeeze flow of the polymers from both the molten ED and the adherends.

Displacement of the sonotrode during the consolidation process

Welds with different consolidation pressures showed a considerable deviation in the sonotrode vertical displacement at the end of the consolidation phase, as shown in Figure 4.26. This difference

might be due to the sudden surge in displacement at the end of the vibration phase that might be triggered by slack in the stiffness of the machine unit. After all, the machine unit is not infinitely stiff. This might result in the sonotrode bending during this phase, which might increase/decrease in the displacement data, as seen at the end of the vibration phase in Figure 4.26. This was further substantiated by the difference in weld line thickness for specimens with a consolidation pressure of 0.6 MPa and 4.7 MPa which was only about 40 µm while studies from the microprocessor displacement data showed a difference of 340 µm (refer Figure 4.26). Unlike the vibration phase, no distinct stages were found during the consolidation phase. A control measure of the consolidation phase using the vertical displacement of the sonotrode hence could not be formulated.

4.7. Ways to eliminate voids from the weld line

- The retraction force of the springs was determined by placing known weights on the springs until the springs were completely compressed. The force thus obtained was 18 N. This meant that the application of 18 N was sufficient to prevent void formation due to springs in the spring jig. It is known that the polymer can be considered to be solidified once the temperature drops below Tc while the onset temperature of the truly liquid melt of the amorphous phase also lies close to the Tc of the polymer. Thus, extending the consolidation pressure application until the interface temperature drops below Tc should be sufficient to eliminate the effect of retraction forces of the springs as the welded joint can overcome the retraction forces.
- Extending the consolidation force application until the interface temperature drops below Tc meant that the formation of crystallisation shrinkage voids is also controlled.
- The void formation due to fibre decompaction can be eliminated by the application of a pressure higher than the minimum threshold pressure required to prevent decompaction. From the results obtained from this thesis, this threshold pressure was about 1.6 MPa.
- The void formation due to excessive squeeze flow of the resin, which are predominantly seen at the weld edges, can be minimised by controlling the consolidation pressure. In the tests carried out in this thesis, maintaining the same consolidation pressure as the welding pressure was seen to reduce voids due to excessive squeeze flow of the resin.

4.8. Conclusions on consolidation in static USW process

Investigation on the effect of consolidation time and pressure on the (de)consolidation of statically welded specimens were carried out and were analysed via quality tools such as LSS, void content, and fractography. Tests were also carried out to determine the crystallinity while power-displacement data from the microprocessor were also used wherever necessary. Multiple conclusions were drawn based on the results obtained from the tests on consolidation in static USW and are listed below.

- When the consolidation pressure application was stopped before the interface temperature dropped below Tm, no consolidated joint was formed.
- Stopping the consolidation pressure application before the interface temperature dropped below Tc resulted in a weld of low LSS and high void content. Increasing consolidation until the temperature at the interface dropped below Tc resulted in a well-consolidated weld. Extending consolidation when the temperature drops below Tc hindered the formation of voids due to shrinkage due to crystallisation. The crystallisation of the polymer also most likely restricted chain mobility once the temperature drops below Tc of the polymer. The increased viscosity of the polymer due to crystallisation and the fact that the truly liquid onset temperature of the amorphous melt is almost 60-100 °C above Tg helped counteract the retraction force exerted by the springs of the spring jig.
- The voids in USW of thermoplastic composites were found to appear due to a combined effect of fibre decompaction, shrinkage in the polymer due to crystallisation, retraction forces exerted by the springs in the spring jig, and the excessive squeeze flow of the polymer from the weld edges.

- Increasing the duration of consolidation pressure application until the temperature at the interface dropped below Tg did not result in a significant increase of LSS or a considerable decrease in void content. This also meant that the pressure application should start when the polymer is in its melt stage and should extend at least until the temperature drops below the specimen's Tc.
- Consolidation pressure of 0.4 MPa and 0.6 MPa was found to be sufficient to produce welds with LSS of about 30 MPa. However, the void content for a specimen welded with consolidation pressure of 0.4 MPa was almost nine times than welds with consolidation pressures of 1.6 MPa. A consolidation pressure of 0.4 MPa was sufficient the prevent formation of voids due to the retraction forces exerted by the springs. But, the pressure of 0.4 MPa was not sufficient to prevent void formation due to shrinkage due to crystallisation or fibre decompaction.
- High consolidation pressures of 3.1 MPa and 4.7 MPa resulted in squeeze flow of the resin resulting in voids along the weld edges because of excessive resin flow. A lower consolidation pressure can thus result in voids due to crystallisation shrinkage or fibre decompaction while a higher consolidation force can lead to voids due to excessive squeeze flow of resins.
- The void content in all instances when consolidated until the interface temperature dropped below Tm, including in specimens consolidated for 600 ms, was less than 0.1% of the total weld volume, lower than the Aerospace industry standards of 1% [68, 69]. But, the resolution of the micro-CT scans was 14 µm due to which smaller voids whose diameter was less than 14 µm were not captured during the scan and was not computed.

5

Continuous Ultrasonic Welding (CUW)

5.1. Introduction

The study on static ultrasonic welding (USW) has culminated in multiple conclusions regarding the consolidation parameters, which are listed in section 4.8. This chapter seeks to answer how the knowledge obtained about the consolidation parameters in static USW can be used to define consolidation parameters in CUW of thermoplastic composites. Tests were carried out to relate the consolidation pressure and consolidation time in static USW to consolidation pressure and positioning of the consolidation device in CUW. The consolidation device or the consolidator is a separate block of material which is fitted along with the sonotrode unit that aids in consolidation pressure application in CUW.

Unlike static USW, the duration of consolidation pressure application cannot be controlled directly in CUW. The consolidator and the sonotrode in CUW are attached to a single unit which implies that the speed of the consolidator will be the same as the speed of the sonotrode. Since the speed of the sonotrode is fixed for a given welding configuration based on the optimum welding conditions [43], the consolidator speed cannot be changed to increase or decrease the duration of consolidation pressure application in CUW. The only parameter that can be modified is thus the consolidator length. The position of the consolidator behind the sonotrode determines the consolidation window, i.e. when during the consolidation process, does the consolidator pass over the adherends. So, the consolidation parameters for the continuous welding of thermoplastic composites can be summarised as the consolidation pressure, consolidator length, and position of the consolidator behind the sonotrode.

In this study, the welding speed was kept constant. Also, the consolidator length was not modified since changing consolidator length involved changing the consolidator block to another of a different length. Thus, the study was restricted to the effect of consolidator position behind the sonotrode and consolidation pressure on the (de)consolidation of continuous ultrasonic welded specimens.

5.2. Materials

The thermoplastic laminates were manufactured as per the procedure defined in section 4.2 of the previous chapter. The thermoplastic laminates were cut to dimensions of 101.6 mm x 220 mm in a water-cooled Proth grinding machine. The energy director (ED) used for the welding was state of the art in CUW - a 0.20 mm PPS mesh [43]. The consolidator was a block of copper of dimensions 40 mm x 25 mm.

5.3. Machines and parameters

5.3.1. Ultrasonic welding machine

The tests on CUW were conducted on the in-house built CUW machine at TU Delft, as shown in Figure 5.1. The ultrasonic stack (that consisted of the sonotrode, converter, and booster) and the consolidator was pneumatically controlled to press against the stack of adherends. The position of the consolidator behind the sonotrode was adjusted by a separation adjustment screw, which allowed for modifying the distance between the sonotrode and the consolidator. The length of the consolidator was 40 mm. The minimum distance possible between the sonotrode and the consolidator was 12 mm due to the geometry of both the components (see distance 'A' in Figure 5.1b). The curvature of the sonotrode meant that the effective distance between the sonotrode and the consolidator was an additional 6.4 mm (Refer Figure 5.1b). In this report, the distance between the sonotrode and the consolidator is reported as distance 'A' as in Figure 5.1b and not the effective distance. The sonotrode was so placed that the left edge of the sonotrode base coincided with the leftmost edge of the weld overlap (Weld direction shown in Figure 5.2). The weld stack was held in place by two aluminium clamps placed at the far end of the adherends, as shown in Figure 5.2. A spare adherend was placed beneath the top adherend to compensate for the differences in height. Two dummy adherend stacks were placed at either end of the welding stack to ensure uniform welding/consolidation pressure at the edges of the weld stacks (refer Figure 5.2). The consolidator thus started its pressure application, and movement from the dummy adherend stack 1 in Figure 5.2 and both the sonotrode and the consolidator moved beyond the far end of the welding stack into the dummy adherend stack 2 post welding. The dimensions of the sonotrode and other machine capabilities were similar to the static welding machine, as was detailed in section 4.3 in the previous chapter. The sonotrode and the consolidator stack remained stationary while the weld table moved in a direction opposite to the welding direction, as shown in Figure 5.2.

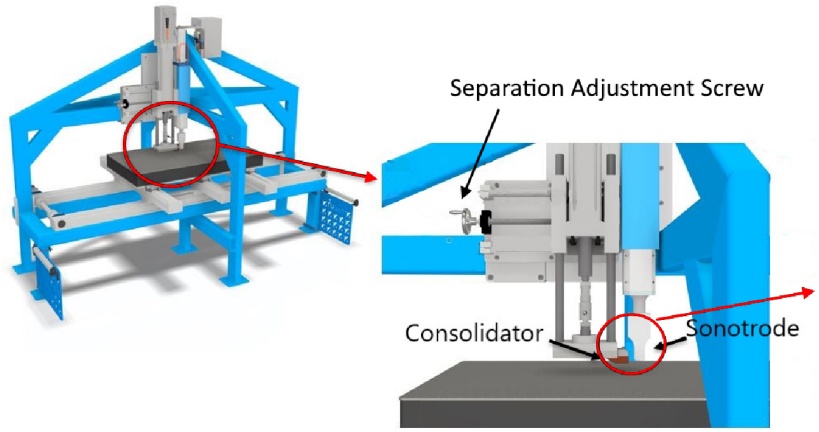

(a) Continuous ultrasonic welding machine at TU Delft

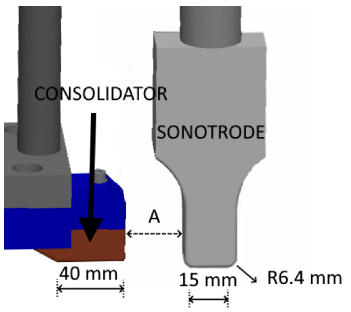

(b) Close up of the sonotrode-consolidator setup; the distance between the sonotrode and the consolidator reported throughout this report is the distance 'A'

Figure 5.1: (a) Setup of the continuous ultrasonic welding machine along with the (b) consolidator at TU Delft

5.3.2. Parameters used

To be comparable to static USW, a welding amplitude of 80 µm (peak-to-peak) and a welding force of 500 N were chosen. The welding speed was chosen as 35 mm/s [14, 44], which was reported to provide consistent optimal welds for the chosen welding parameters. The consolidator length of 40 mm ensured that the consolidation lasted for approximately 1100 ms at any given location within the weld with the chosen welding speed. This was close to the 1000 ms consolidation time, which was seen effective in static USW for similar welding parameters.

Two consolidation pressures - 0.6 MPa and 1.6 MPa that corresponds to a consolidation force of 315 N and 800 N respectively were used to study the effect of consolidation pressure on the consolidation of

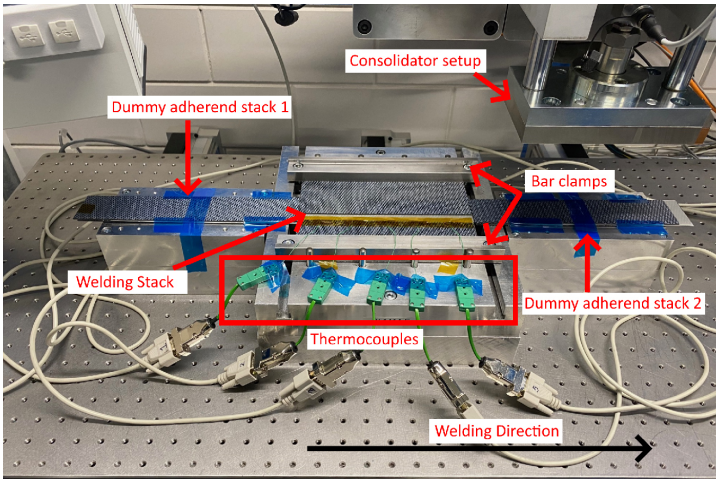

Figure 5.2: Stacking of the adherends, dummy adherend stacks and thermocouples for CUW

welds. The consolidator was placed at 12 mm, 56.6 mm and 80 mm away from the sonotrode to study the effect of consolidator positioning. Thermocouples were placed at five different locations along the weld line, as shown in Figure 5.2 and Figure 5.3 to investigate the development of temperature in the weld interface during the continuous welding process.

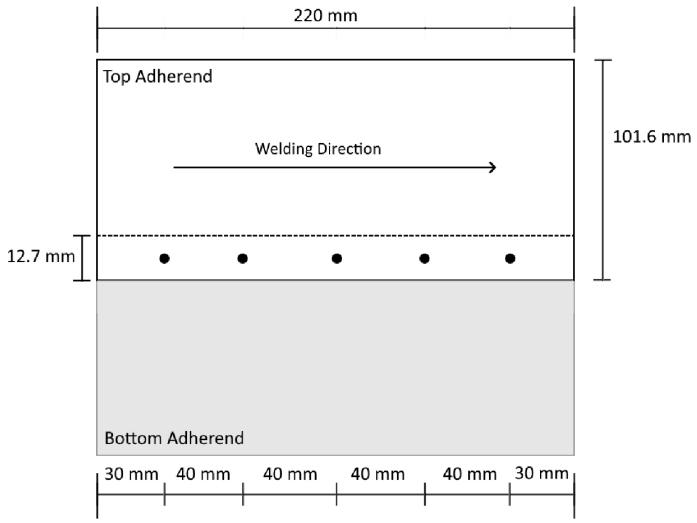

Figure 5.3: Depiction of the location of the thermocouples along the weld line (represented by the black dots). Figure not to scale.

5.4. Characterisation techniques

The characterisation techniques used for CUW were the same as used for static USW and as defined in section 4.4. Once the welding was completed, six lap shear samples were cut in water-cooled Proth grinding machine of overlap width of 25.4 mm from the welded specimen as seen in Figure 5.4. The samples at the start and end (L and R in Figure 5.4) were discarded. Samples 3 was used for cross-sectional micrographs, while sample 5 was used for micro-CT scans. The remaining samples were used for the computation of LSS.

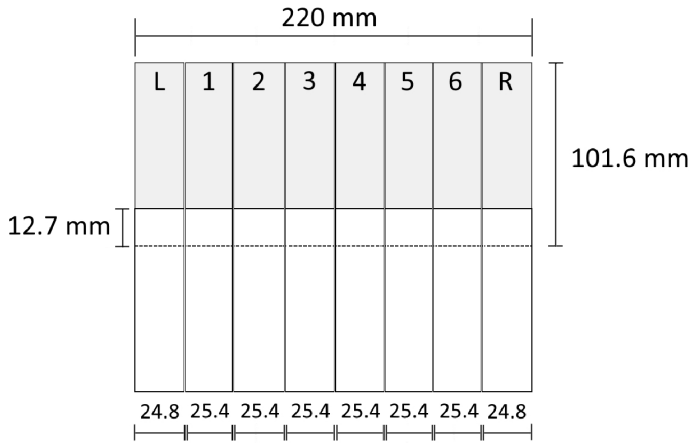

Figure 5.4: Depiction of the specimens cut from the continuously welded sample for quality testing

5.5. Effect of consolidator distance on the weld quality in CUW

5.5.1. Methodology

This section details the methodology used to determine the effect of consolidator positioning behind the sonotrode on the (de)consolidation of ultrasonic continuously welded specimens. Specimens were initially welded without consolidator to recreate the state-of-the-art welds in CUW under the chosen welding parameters. This was followed by welding with the consolidator placed 12 mm from the sonotrode to investigate how the presence of consolidator influence the cooling rates after welding. These welds were assumed to provide temperature profiles that could be used as a baseline to determine the position of the consolidator behind the sonotrode for further trials. Accordingly, the distance of the consolidator was increased to 56.6 mm and 80 mm. LSS of the specimens were assessed, as mentioned in section 5.4 to compare the weld strength when the consolidator was placed at different locations behind the sonotrode. The fracture surfaces were analysed for the failure mechanism and the void content. The cross-sectional micrographs and micro-CT scans enabled the visualisation of void content in the weld line and calculation of volumetric void content in the welded specimen, respectively. The term ”consolidator pass” is used to denote the movement of the consolidator over the top adherend during the consolidation phase.

5.5.2. Results

Temperature at the weld interface during CUW

Figure 5.5a shows the temperature profile at the weld interface from the start of the sonotrode movement when welded without the consolidator. The ”end of welding” in Figure 5.5a refers to the time when the sonotrode has completely welded the 220 mm long overlap joint and the vibrations stop. Thermocouple 4 provided erroneous data at the beginning of the vibration phase, which can be seen in Figure 5.5a.

To better understand the temperature distribution during the welding process, Figure 5.5b depicts the overlaid temperature profile from the first contact of sonotrode at the respective thermocouple location. The cooling rate at thermocouple location 5 was higher than the cooling rates at the other thermocouple locations. Since this study investigates the effect of consolidation parameters on (de)consolidation of welds, the temperature profiles henceforth in this chapter will only show the overlaid consolidation plots as depicted in Figure 5.5c which depicts the overlaid temperature profiles from the moment the sonotrode completely passes the respective thermocouple location.

The temperature profile at the weld interface of specimens welded with a consolidation pressure of 1.6 MPa and the consolidator at 12 mm from the sonotrode is as shown in Figure 5.6. The shaded region depicts the period during which the consolidator passes over the adherend. Interface

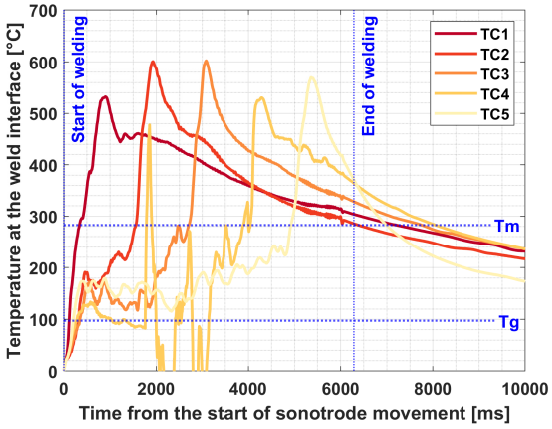

(a) From the start of sonotrode movement

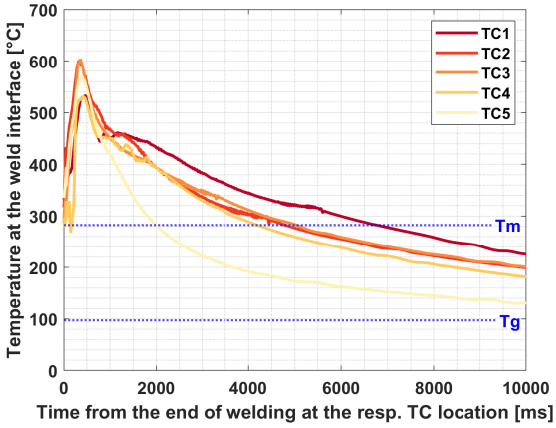

(b) Overlaid plot from the start of welding at the respective thermocouple location

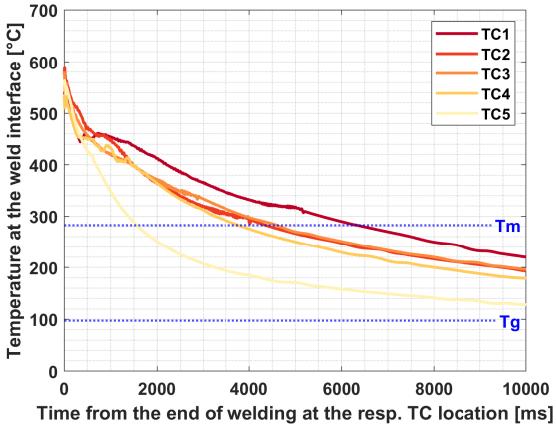

(c) Overlaid plot from the end of welding at the respective thermocouple location

Figure 5.5: Temperature profiles at the weld interface in CUW process without consolidator; Vibration amplitude (peak-to-peak): 80 µm, welding force: 500 N, Welding speed: 35 mm/s

temperatures along the whole weld line dropped below melting temperature in approximately 1600-2000 ms. Nevertheless, the temperature of the weld interface during the pass of the consolidator was above Tm.

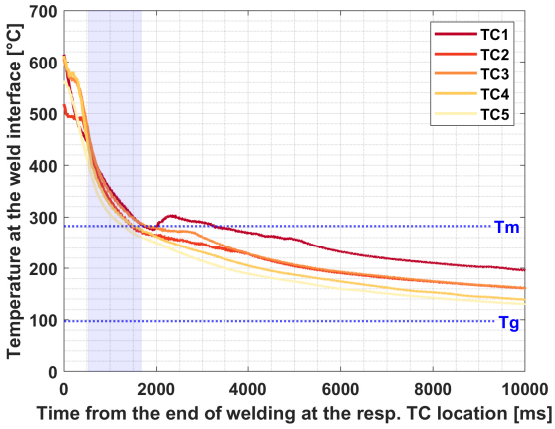

Figure 5.6: Temperature profiles at the weld interface in CUW process with consolidator placed12 mm from the sonotrode; Vibration amplitude (peak-to-peak): 80 µm, welding force: 500 N, welding speed: 35 mm/s, consolidation pressure: 1.6 MPa

The temperature profile at the weld interface of specimens welded with a consolidation pressure of 1.6 MPa and the consolidator 56.6 mm and 80 mm away from the sonotrode are shown in Figure 5.7a and Figure 5.7b. When the consolidator was placed 56.6 mm away from the sonotrode, the temperatures at the weld interface, when the consolidator first made contact with the thermocouple locations, were above Tm. At the end of the pass of the consolidator, the interface temperature at the respective location just dropped below Tm. In the case of 80 mm distance between the consolidator and the sonotrode, the temperature at all locations except thermocouple 1 dropped below melting temperature at the end of the consolidator pass. Nevertheless, the temperature in neither of the cases dropped below crystallisation temperature (160-190 °C) at the end of the consolidator pass. It was seen that the time it takes for the interface temperature to drop below Tm increases as the distance of the consolidator from the sonotrode increased.

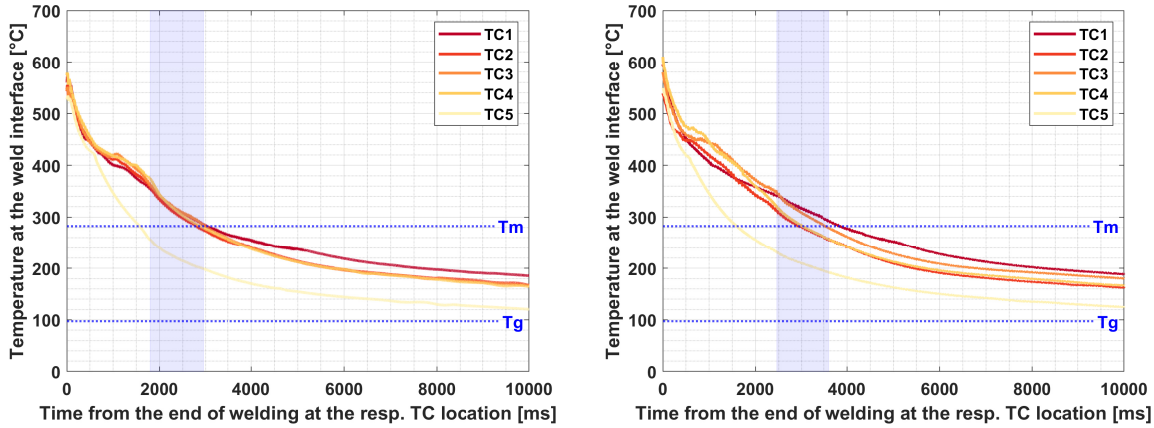

(a) Consolidator distance: 56.6 mm

(b) Consolidator distance: 80 mm

Figure 5.7: Temperature gradient at the weld interface in CUW under varying consolidator distances; Vibration amplitude (peak-to-peak): 80 µm, welding force: 500 N, welding speed: 35 mm/s, consolidation pressure: 1.6 MPa

Lap shear strength

As stated in section 5.3, the welded specimens were cut into six individual samples, out of which four samples were tested for LSS. Figure 5.8 and Table 5.1 compares the strength of joints which were welded without consolidator and with the consolidator placed 12 mm, 56.6 mm and 80 mm away from the sonotrode. The specimens welded with the consolidator placed close to the sonotrode was weaker in LSS than specimens welded without consolidator. Placing the consolidator at a further distance, i.e. at 56.6 mm and 80 mm produced joints of superior strength with LSS close to 40 MPa.

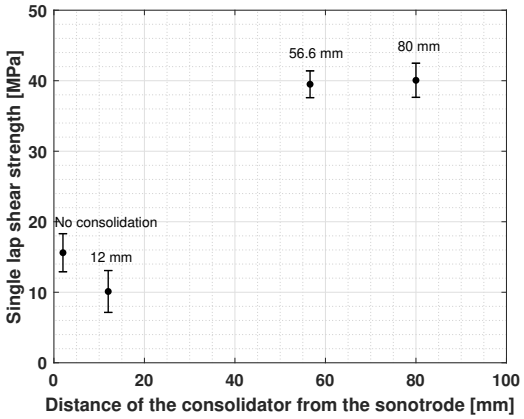

Distance between sonotrode and consolidator [mm]	LSS [MPa]
0	15.6 ± 2.7
12	10.1 ± 3.0
56.6	39.5 ± 1.9
80	40.1 ± 2.4

Figure 5.8 & Table 5.1: Single LSS of specimens that were continuously welded under different distances of consolidator from the sonotrode; Vibration amplitude (peak-to-peak): 80 µm, welding force: 500 N, welding speed: 35 mm/s, consolidation pressure: 1.6 MPa

Fracture surface analysis

The fracture surfaces of the welded specimens are shown in Figure 5.10. When welded without consolidator and when the consolidator was placed at 12 mm from the sonotrode, the fracture occurred at the weld interface as seen in Figure 5.9 and Figure 5.10a, respectively. These fracture surfaces reveal a resin-rich surface with resin accumulations in several areas within the weld interface. Increasing the distance of the consolidator further from the sonotrode to 56.6 mm and 80 mm resulted in a fracture in the adherends rather than the interface, as seen in Figure 5.10b and Figure 5.10c.

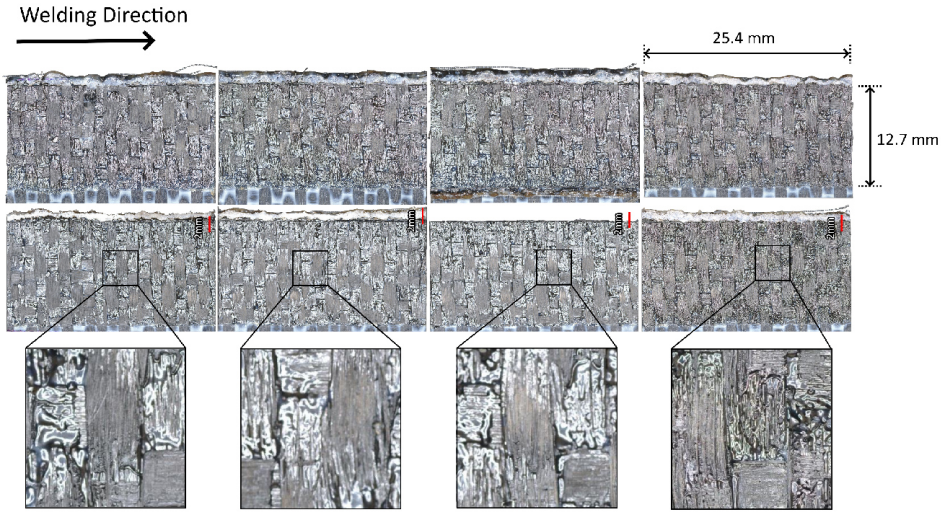

Figure 5.9: Fracture surface of specimens that were continuously welded without consolidator; Vibration amplitude (peak-to-peak): 80 µm, welding force: 500 N, welding speed: 35 mm/s

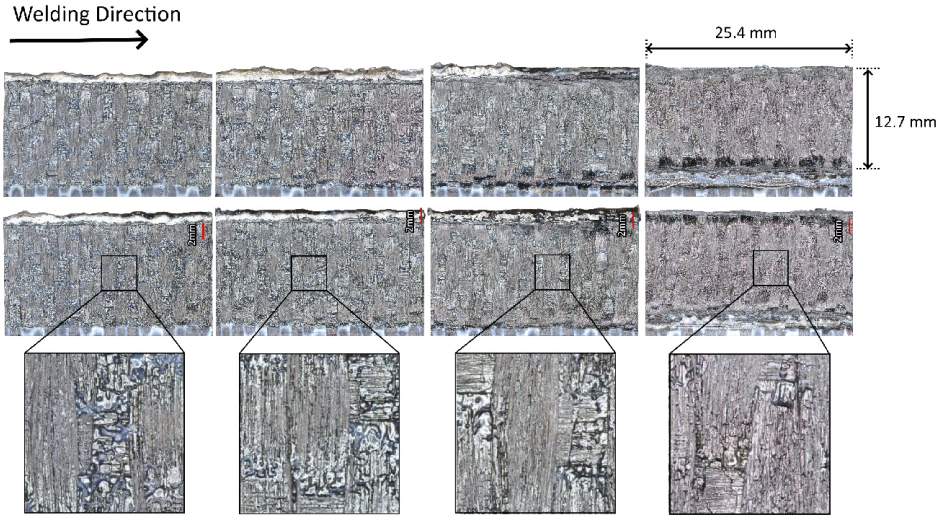

(a) consolidator placed12 mm from the sonotrode

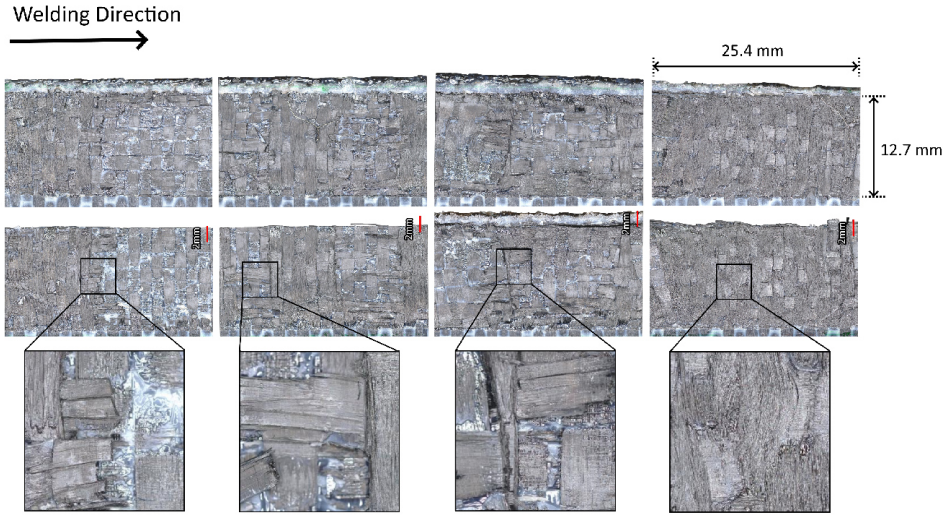

(b) Consolidator 56.6 mm from the sonotrode

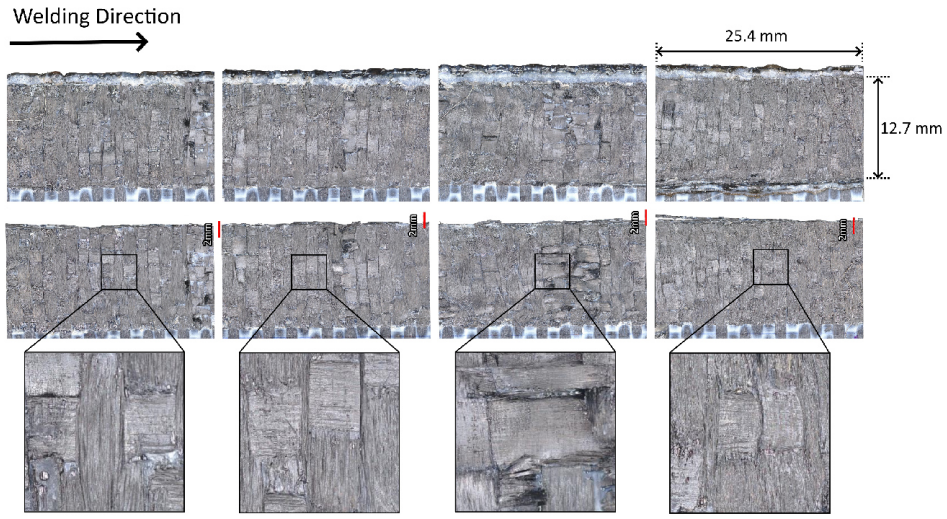

(c) Consolidator 80 mm from the sonotrode

Figure 5.10: Fracture surface of specimens that were continuously welded under different distances of consolidator from the sonotrode; Vibration amplitude (peak-to-peak): 80 µm, welding force: 500 N, welding speed: 35 mm/s, consolidation pressure: 1.6 MPa

Cross-sectional micrographs

The cross-sectional images of the specimens welded under varying distances of the consolidator from the sonotrode are shown in Figure 5.11 and Figure 5.12. The volumetric void content was high when welded without consolidator and when the consolidator was placed close to the sonotrode. As the distance of the consolidator from the sonotrode increased from 12 mm to 80 mm, the volumetric void content decreased. When the consolidator was placed 80 mm from the sonotrode, the voids were observed predominately in the layers rather than the weld line.

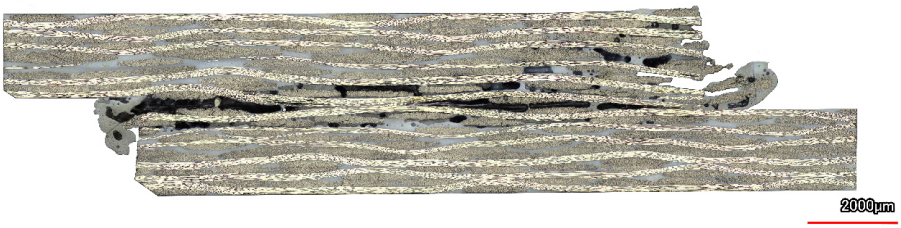

Figure 5.11: Cross-sectional micrographs of specimens that were continuously welded without consolidator; Vibration amplitude (peak-to-peak): 80 µm, welding force: 500 N, welding speed: 35 mm/s

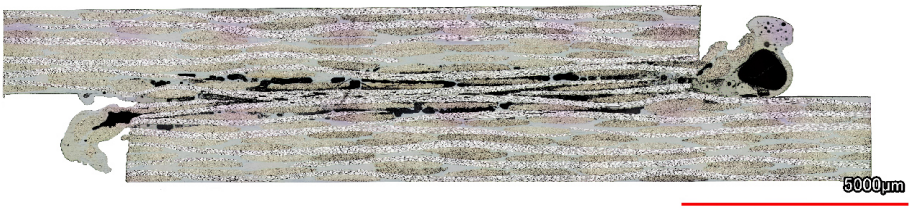

(a) consolidator placed12 mm from the sonotrode

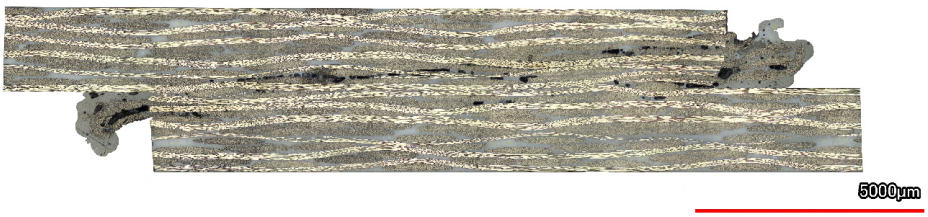

(b) Consolidator 56.6 mm from the sonotrode

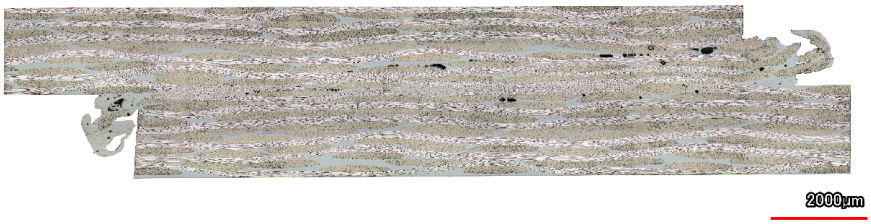

(c) Consolidator 80 mm from the sonotrode

Figure 5.12: Cross-sectional micrographs of specimens that were continuously welded under different distances of consolidator from the sonotrode; Vibration amplitude (peak-to-peak): 80 µm, welding force: 500 N, welding speed: 35 mm/s, consolidation pressure: 1.6 MPa

Micro-CT scans

The distribution of voids within the weld interface are shown in Figure 5.13 and Figure 5.14. While the voids in welds without consolidator was seen distributed towards the weld edges, they were more evenly distributed across the whole weld interface when welded with consolidator placed12 mm from

the sonotrode. The voids, when welded with consolidator 80 mm from the sonotrode, were comparatively lower and showed a void content of 1% against 7-8% when welded with no consolidation or consolidator close to the sonotrode as shown in Table 5.2. Appendix E includes additional images from the micro-CT scans for better clarification.

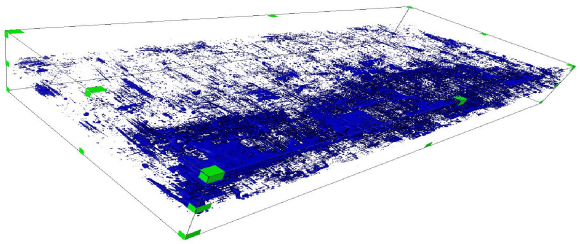

Figure 5.13: CT scan image of specimens that were continuously welded without consolidator; Vibration amplitude (peak-to-peak): 80 µm, welding force: 500 N, welding speed: 35 mm/s

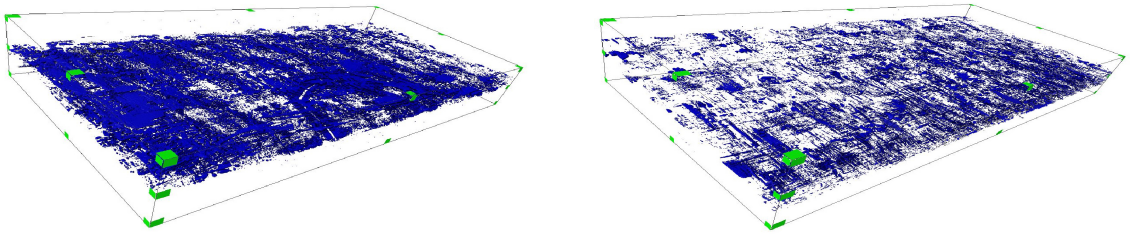

(a) consolidator placed12 mm from the sonotrode **(b)** Consolidator 80 mm from sonotrode

Figure 5.14: CT scan image of specimens that were continuously welded under different distances of consolidator from the sonotrode; Vibration amplitude (peak-to-peak): 80 µm, welding force: 500 N, welding speed: 35 mm/s, consolidation pressure: 1.6 MPa

Table 5.2: Volumetric void content of specimens that were continuously welded under different distances of consolidator from the sonotrode; Vibration amplitude (peak-to-peak): 80 µm, welding force: 500 N, welding speed: 35 mm/s, consolidation pressure: 1.6 MPa

Consolidator distance from sonotrode [mm]	Volumetric void content [%]	Strength of the tested specimen [MPa]	Average LSS from Table 5.1 [MPa]
No consolidator	7.80	13.2	15.6 ± 2.7
12	8.32	7.1	10.1 ± 3.0
80	1.01	38.0	40.0 ± 2.4

Weld line thickness measurement

Figure 5.15 and Table 5.3 depicts the weld line thickness of specimens welded with consolidator at different locations behind the sonotrode. When welded without consolidator and when the consolidator was placed 12 mm from the sonotrode, the weld line thickness was above 150 µm. When the consolidator was moved away from the sonotrode to 56.6 mm and 80 mm, a negative weld line thickness was observed.

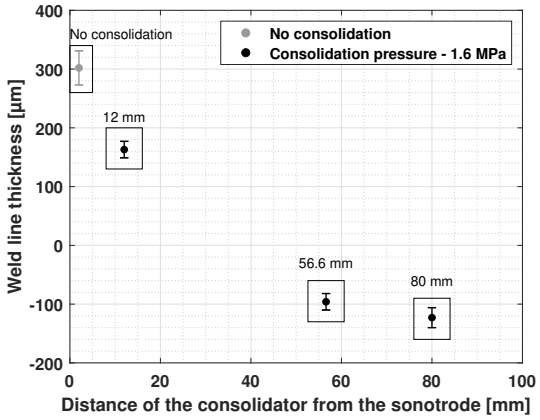

Consolidator distance from sonotrode [mm]	Weld line thickness [µm]
No consolidator	302 $\pm$ 29
12	163 $\pm$ 14
56.6	-96 $\pm$ 14
80	-123 $\pm$ 17

Figure 5.15 & Table 5.3: Weld line thickness of specimens that were continuously welded under different distances of consolidator from the sonotrode; Vibration amplitude (peak-to-peak): 80 µm, welding force: 500 N, welding speed: 35 mm/s, consolidation pressure: 1.6 MPa

5.5.3. Discussion

This section examines the results obtained from tests carried out to study the influence of the positioning of the consolidator behind the sonotrode on the (de)consolidation of welds. Vibration amplitude, welding force and consolidation pressure used were similar to that used for the tests in static USW. It was initially hypothesised that placing the consolidator too close to the sonotrode might result in vibration damping and thus a deconsolidated weld interface. Also placing the consolidator too far from the sonotrode was hypothesised to result in consolidation pressure application after the weld line solidified. This was assumed to produce deconsolidated joints since there might be no external pressure application when the interface temperature dropped below Tm.

Comparison with static welding

From Figure 5.5c, it was seen that the temperature at the weld interface stays above melting temperature for a longer duration in contrary to static USW. It took around 3700-6400 ms for the thermocouples 1-4 to cool down to temperatures below melting after the end of welding compared to around 340-470 ms in static USW, as shown in Table 5.4. The cooling rates in CUW were thus much slower than that observed in static ultrasonic welds. The slower cooling rates resulted in through-thickness heat dissipation into the adherends which resulted in melting of the additional thickness of the adherends during the continuous welding process. This increased size of the HAZ can be seen in Figure 5.11, where there are excessive voids and squeeze out of the resin in the edges of the top adherend as well. This increased HAZ was also reported in continuous induction welding of thermoplastic composites [70]. It can be thus assumed that the exposure of continuous ultrasonic welds to higher temperatures for a longer period in addition to the excessive squeeze flow contributes largely to void formation and deconsolidation in CUW.

Thermocouple 5 is not considered in Table 5.4, owing to its rapid cooling rate compared to other thermocouple locations. It is assumed that the thermocouple locations might still undergo vibrational amplitude due to transmission of the vibrations even when the sonotrode is not over it. These vibrations might also prevent the melted polymer from solidifying. Thermocouple 5, being the last thermocouple over which the sonotrode passes, melts last and may thus cool down faster since the polymer melt undergoes vibration transmissions from the sonotrode for a comparatively shorter time.

Effect of consolidator on cooling rates in the weld

Based on the temperature profile in Figure 5.5c, the consolidator should have been placed such that the consolidation should end around 8000-10000 ms after the pass of the sonotrode so that the consolidation extends until the temperature at the interface drops below the crystallisation temperature of the polymer (as concluded in chapter 4). With a welding speed of 35 mm/s, this would

Table 5.4: Comparison of cooling rate between static USW and CUW (without considering TC5 in CUW)

Welding configuration	Time for interface temperature to drop	
	From peak temperature to below Tm	From Tm till Tg
Static USW	340 - 470 ms	2800 - 4100 ms
CUW without consolidator	3700 - 6400 ms	20700 - 24000 ms
CUW- Consolidator 80 mm from sonotrode	3000 - 3900 ms	24500 - 27000 ms

mean placing the 40 mm long consolidator, 170-240 mm away from the sonotrode. However, as was seen in static USW, the presence of the consolidator was also seen to influence the temperature profile at the weld line. It is assumed that the presence of consolidator ensures more compact packing of the carbon fibre network, thus enabling more heat dissipation through the fibres and the resin, thus increasing the cooling rates at the weld interface. The excessive squeeze flow of the resin from the weld interface and the adherends also might result in a faster heat dissipation than when welded without consolidator.

Effect of varying consolidator distance on (de)consolidation and void formation

Three void formation mechanisms that were discussed in static USW were fibre decompaction, void formation due to crystallisation shrinkage, and the retraction forces of the springs of the spring jig. Since bar clamps were used for CUW, the void formation due to spring retraction forces is eliminated. From the temperature profiles of specimens welded continuously, it was seen that the pressure application by the consolidator did not extend until the interface temperature dropped below Tc in any of the cases discussed. This means that the void formation due to crystallisation shrinkage was prevalent in all cases discussed in this section. The lower cooling rate in CUW compared to static USW meant that the consolidation pressure application terminated either when the interface temperature was above Tm or just below Tm in all cases considered. Thus, the fibre decompaction due to a lack of external consolidation force was also a predominant void formation mechanism in CUW. The squeeze out of the resin is also a dominant void formation mechanism in CUW owing to the slow cooling rates and the consolidation window that was primarily in effect when the polymer was in a melt state.

The welds without consolidator showed a low LSS (refer Table 5.1) and numerous voids not only in the weld interface but also in the adherends (refer Figure 5.11 and Figure 5.13) due to the increased HAZ as mentioned previously. The results obtained bear a resemblance to the state-of-the-art continuous ultrasonic welded joints, which served as a motivation to this thesis project. The fracture surfaces also showed voids in the resin-rich weld interface, as is evident from Figure 5.9. The thermal deconsolidation was further substantiated by the increased weld line thickness, as observed in Figure 5.15. Fibre decompaction and crystallisation shrinkage can be considered as predominant factors contributing to void formation in this case.

Placing the consolidator close to the sonotrode proved to be more detrimental than welding without consolidator. One plausible reason for the reduced strength and increased voids is the excessive squeeze out of the polymer since the polymer in the weld interface when the consolidator passes over the adherends is a melt pool. The situation only aggravates as there is no consolidation when the temperature at the weld line drops below Tm. This might result in widespread decompaction of the fibres due to a lack of external pressure. The lack of pressure while the temperature at the weld interface drops below Tc also contributes significantly to void formation. These factors can, in combination, result in a weak weld line. The weld line thickness of specimens welded with no consolidation and consolidator placed 12 mm from the sonotrode was above 150 µm, as shown in Figure 5.15, confirming widespread decompaction within the welded specimen.

Based on the temperature profiles of the weld with no consolidation and with consolidator placed 12 mm from the sonotrode, 56.6 mm and 80 mm were chosen as distances between the sonotrode

and the consolidator for further trials. The consolidation, in these cases, started when the polymer interface temperature was above Tm and the consolidation continued until the temperature dropped below Tm. The LSS was almost four times higher and volumetric void content was eight times lower than when the consolidator was placed 12 mm from the sonotrode. The squeeze flow of the polymer was also observed in the adherend layers of the specimen when welded with the consolidator 80 mm from the sonotrode. The duration between the consolidator pass and the sonotrode pass when the consolidator was placed 12 mm from the sonotrode was about 500 ms which increased to about 2500 ms when the consolidator was placed 80 mm from the sonotrode. This difference most likely meant that the HAZ was larger (where the adherend layers might have melted as well) during the consolidator pass when the consolidator was placed 80 mm from the sonotrode. This increased the squeeze flow of the resin from the adherend layers might be the contributing factor towards the formation of voids observed in the adherend layers as seen in Figure 5.12c. The weld line thickness (refer Figure 5.15) further substantiated the claim that resin was squeezed out in excess from the weld interface and adherends. This also shifted the failure in LSS from the weld interface to the adherends as seen in Figure 5.10b and Figure 5.10c.

5.6. Effect of consolidation pressure in CUW

5.6.1. Methodology

Excessive squeeze flow of the resin was observed in CUW when welded with a consolidation pressure of 1.6 MPa, as seen in the previous sections. Hence, specimens were welded with a reduced consolidation pressure of 0.6 MPa (consolidation force of 315 N) to study the effect of consolidation pressure on (de)consolidation in CUW. Consolidator was placed at two different locations: 12 mm and 80 mm behind the sonotrode. Vibration amplitude of 80 µm, welding force of 500 N and a welding speed of 35 mm/s was used.

5.6.2. Results

Figure 5.16 shows the temperature profile at the weld interface of continuously welded specimens with consolidation pressure of 0.6 MPa and consolidator 12 mm and 80 mm behind the sonotrode. The temperature profiles and the consolidation window were similar to when welded with a consolidation pressure of 1.6 MPa. When consolidator was placed 12 mm away from the sonotrode, the movement of the consolidator over the thermocouple locations was when the polymer was still in a melt stage. Placing the consolidator 80 mm from the sonotrode meant that the consolidator pressure application started when the polymer was in its melt stage and ended almost when the temperature dropped below the melting temperature. Nevertheless, the temperature of the weld interface at the end of the consolidation did not drop below the crystallisation temperature.

Lap shear strength

The LSS when welded with a consolidation pressure of 0.6 MPa was slightly higher (but not significantly different) than the LSS when the consolidation pressure was 1.6 MPa as shown in Figure 5.17.

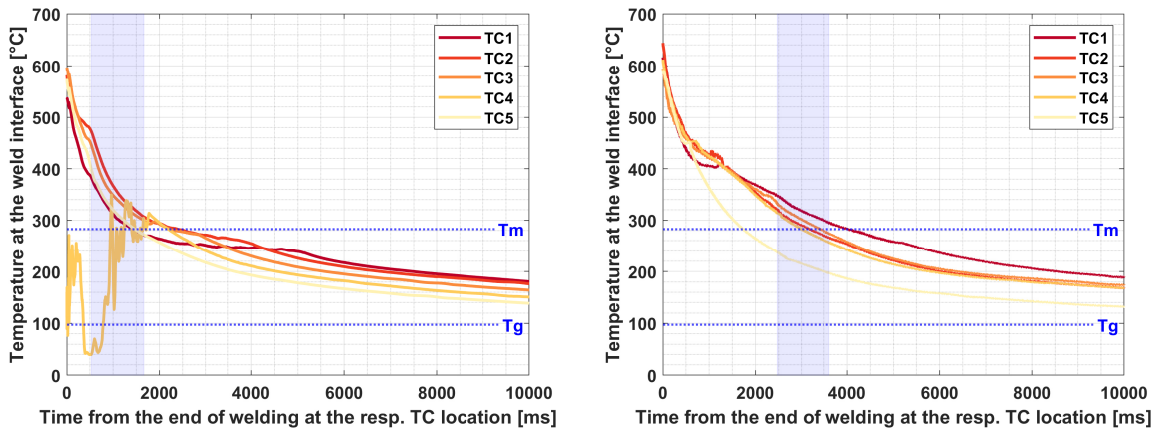

(a) Consolidator distance: 12 mm

(b) Consolidator distance: 80 mm

Figure 5.16: Temperature gradient at the weld interface during CUW; Vibration amplitude (peak-to-peak): 80 µm, welding force: 500 N, welding speed: 35 mm/s, consolidation pressure: 0.6 MPa

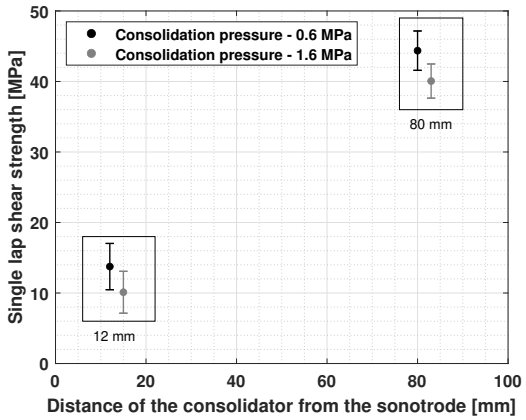

Distance between sonotrode and consolidator [mm]	Consolidation Pressure [MPa]	LSS [MPa]
12	0.6	13.8 ± 3.3
	1.6	10.1 ± 3.0
80	0.6	44.4 ± 2.8
	1.6	40.1 ± 2.4

Figure 5.17 & Table 5.5: Single lap shear strength for varying distances of the consolidator from the sonotrode under varying consolidation pressure; Vibration amplitude (peak-to-peak): 80 µm, welding force: 500 N, welding speed: 35 mm/s

Fracture surface analysis

The fracture surfaces of the specimens welded with a consolidation force of 0.6 MPa with the consolidator 12 mm and 80 mm from the sonotrode are as shown in Figure 5.18. The specimens welded with the consolidator placed 12 mm from the sonotrode failed in the weld interface while the welds with consolidator placed 80 mm from the sonotrode failed in the adherend. Resin rich areas can be seen in the weld with consolidator placed 12 mm from the sonotrode.

Cross-sectional micrographs

The cross-sectional micrographs of the welds are shown in Figure 5.19. These also bore a resemblance to the welds with a consolidation pressure of 1.6 MPa. Specimens consolidated by placing the consolidator 12 mm from the sonotrode showed voids both in the weld interface and in the adjacent layers. When the consolidator was placed 80 mm from the sonotrode, the squeeze flow was significant in the adherends as well, apart from the weld interface.

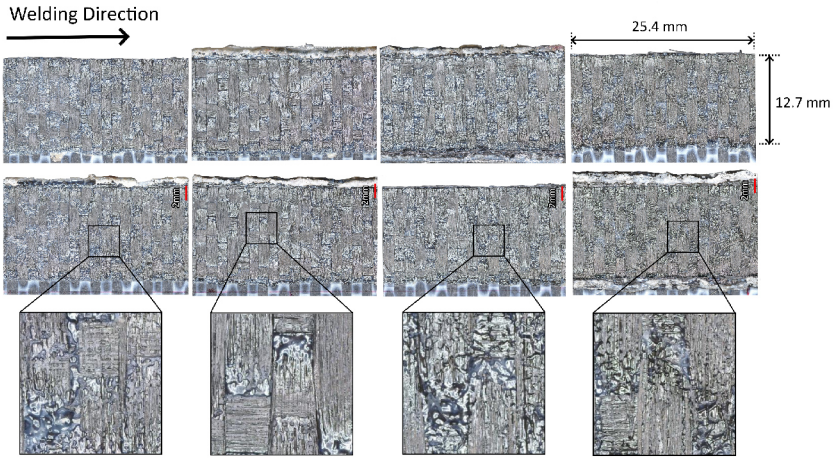

(a) Consolidator placed 12 mm from the sonotrode

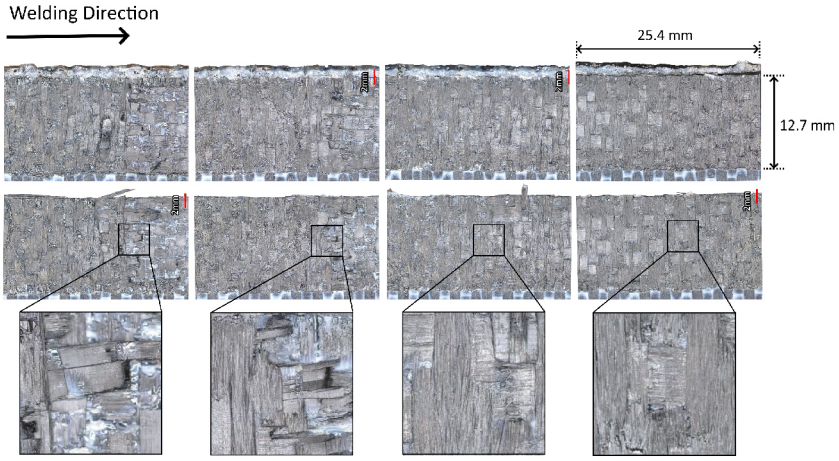

(b) Consolidator 80 mm from the sonotrode

Figure 5.18: Fracture surface of specimens that were continuously welded under different distances of consolidator from the sonotrode; Vibration amplitude (peak-to-peak): 80 µm, welding force: 500 N, welding speed: 35 mm/s, consolidation pressure: 0.6 MPa

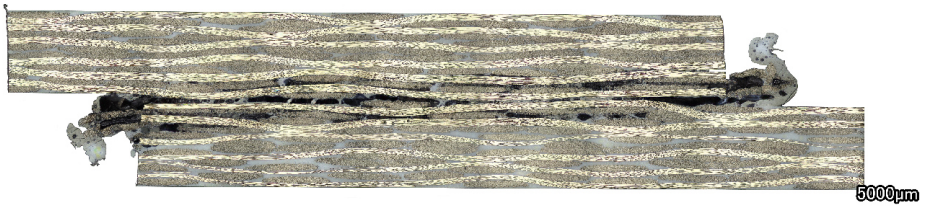

(a) Consolidator placed 12 mm from the sonotrode

(b) Consolidator placed 80 mm from the sonotrode

Figure 5.19: Cross-sectional micrographs of specimens that were continuously welded under different distances of consolidator from the sonotrode; Vibration amplitude (peak-to-peak): 80 µm, welding force: 500 N, welding speed: 35 mm/s, consolidation pressure: 0.6 MPa

Micro-CT scans

Figure 5.20 and Table 5.6 shows the results of the micro-CT scans of specimens welded with a consolidation pressure of 0.6 MPa. The specimen welded with consolidator placed 12 mm from the sonotrode showed a volumetric void content of 7.20% against a void content of 0.73% observed when welded with consolidator 80 mm away from the sonotrode. The volumetric void content of welds with a consolidation pressure of 0.6 MPa was slightly lower than welds with a consolidation pressure of 1.6 MPa. Appendix E includes additional images from the micro-CT scans for better clarification.

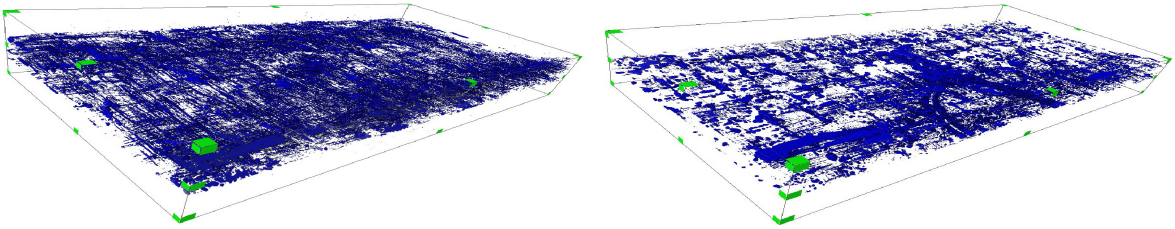

(a) Consolidator placed 12 mm from the sonotrode **(b)** Consolidator 80 mm from the sonotrode

Figure 5.20: CT scan image of specimens that were continuously welded under different distances of consolidator from the sonotrode; Vibration amplitude (peak-to-peak): 80 µm, welding force: 500 N, welding speed: 35 mm/s, consolidation pressure: 0.6 MPa

Table 5.6: Volumetric void content of specimens that were continuously welded under different distances of consolidator from the sonotrode; Vibration amplitude (peak-to-peak): 80 µm, welding force: 500 N, welding speed: 35 mm/s, consolidation pressure: 0.6 MPa

Consolidator distance from sonotrode [MPa]	Volumetric void content [%]	Strength of the tested specimen [MPa]	Average LSS from Table 5.5 [MPa]
12	7.20	11.4	13.8 ± 3.3
80	0.73	46.1	44.4 ± 2.8

Weld line thickness measurements

Figure 5.21 and Table 5.7 depicts the differences in the weld line thickness when welded under different consolidation pressures. As expected, welds with a lower consolidation pressure had a higher weld line thickness compared to welds with a higher consolidation pressure. Nevertheless, the weld line thickness of the specimen when welded with consolidator 80 mm from the sonotrode was still negative.

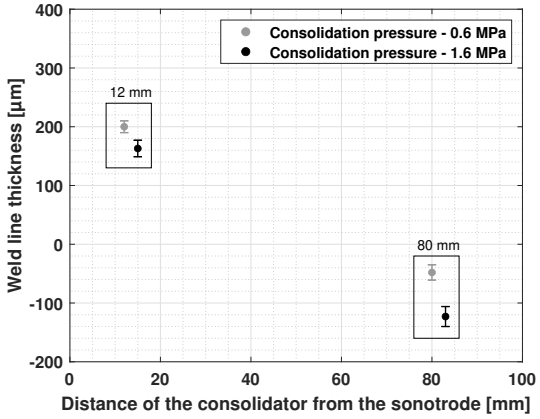

Consolidator distance from sonotrode [mm]	Consolidator pressure [MPa]	Weld line thickness [µm]
12	0.6	200 ± 10
	1.6	163 ± 14
80	0.6	-48 ± 13
	1.6	-123 ± 17

Figure 5.21 & Table 5.7: Weld line thickness of specimens that were continuously welded under different distances of consolidator from the sonotrode; Vibration amplitude (peak-to-peak): 80 µm, welding force: 500 N, welding speed: 35 mm/s; the weld line thickness of specimens welded with a consolidation pressure of 1.6 MPa has been shifted for more clarity

5.6.3. Discussion

The specimens welded with a consolidation pressure of 0.6 MPa showed higher LSS and lower volumetric void content in comparison to welds with a consolidation pressure of 1.6 MPa, as shown in Table 5.5 and Table 5.6, respectively. This was contrary to the results obtained in static USW where specimens welded with a consolidation pressure of 1.6 MPa had higher LSS than specimens welded with a consolidation pressure of 0.6 MPa. In section 5.5.3, it was shown that excessive consolidation pressure can result in the squeeze out of the resin contributing to void formation in the edges of the adherends and the weld interface. This resin squeeze out is aggravated by the low cooling rate in CUW since that the consolidator passes over the specimens mostly while the polymer is in its melt state. The higher consolidation pressure might result in higher polymer squeeze flow, thus resulting in higher volumetric void content (see Table 5.6) and lower LSS (see Figure 5.5). The increased matrix squeeze out in welds with higher consolidation pressure was also reported in continuous induction welding of carbon-fibre reinforced thermoplastics [71, 72].

The higher squeeze flow in welds with a consolidation pressure of 1.6 MPa was substantiated by the weld line thickness observed in Figure 5.21. The thickness of the weld line of the specimen welded with a consolidation pressure of 0.6 MPa was -50 µm while a consolidation pressure of 1.6 MPa produced welds with a weld line thickness of around -120 µm. The weld line in both cases was negative, implying that the squeeze flow was not just restricted to the weld line but also the adherends.

III

Conclusions and Recommendations

6

Research conclusions

This chapter summarises the conclusions made on the research questions detailed in chapter 3 based on the tests which were discussed in chapters 4 and 5. The effect of consolidation time and pressure on (de)consolidation of welds were studied in static ultrasonic welding (USW), and the knowledge was used to extend understanding of the effect of consolidation parameters on (de)consolidation of the welds in continuous ultrasonic welding (CUW). Various characterisation techniques were used to help answer the research questions, which included LSS assessment, fracture surface analysis and volumetric void content determination.

6.1. Effect of consolidation parameters on (de)consolidation of static ultrasonic welds

To study the effect of consolidation time on (de)consolidation of static ultrasonic welds, various consolidation times that best represented various stages of thermal physical changes in the polymer during the consolidation process were identified. Multiple test specimens were welded and consolidated at different consolidation times and were subjected to different characterisation tests. Once the effect of consolidation time on the (de)consolidation of welded specimens was investigated, studies were carried out to investigate the influence of consolidation pressure. Two consolidation pressures each below and above the welding pressure were identified, and specimens were thus welded. The research question, hypothesis and understanding obtained from the tests on static ultrasonic welding, as described in chapter 4 is recapitulated below.

1. **Research Question**
   What is the effect on the consolidation of the weld interface when the application of consolidation pressure is stopped (1) before the interface temperature drops below Tm, (2) when the interface temperature is between Tm and Tg, and (3) after the interface temperature drops below Tg.

   Hypothesis
   It was hypothesised that the consolidation pressure application should extend until the interface temperature drops below the melting temperature of the polymer to obtain a well-consolidated joint.

   Research findings

   - When the application of consolidation pressure was stopped before the interface temperature dropped below the melting temperature, no consolidated welds were obtained. The polymer was still in a melt state when the consolidation force application was stopped.

- Extending the consolidation pressure application until the interface temperature dropped below the crystallisation temperature (Tc) of the polymer was found to be adequate to provide a well-consolidated welded joint. In static welding, this meant that the consolidation could be stopped at an earlier time than previously known, thus reducing the cycle time of the welding process. Therefore, it was concluded that the pressure application should start when the polymer is in its melt state and should extend until the temperature drops below the Tc of the polymer.
- When the application of consolidation force was extended further after the temperature dropped below the crystallisation temperature, there was no significant difference in the strength of the welded specimens or the volumetric void content.
- The voids in ultrasonic welding of thermoplastic composites were most likely formed due to a combined effect of
  - shrinkage due to crystallisation,
  - Decompaction of the fibre reinforcement network,
  - Retraction forces of the springs of the spring jig,
  - Excessive squeeze out of the polymer from the energy director and the adherends

2. **Research Question**
   What is the minimum threshold for the consolidation pressure that can still provide a good consolidation at the interface? Does a high consolidation pressure lead to an improved consolidation of the interface?

   Hypothesis
   Deconsolidation of laminates after welding was assumed to occur if the applied pressure was below a defined critical pressure. A high consolidation pressure was assumed to provide higher strength but was assumed to squeeze out more resin from the joint.

   Research findings

   - A low consolidation pressure of 0.4 MPa produced welds with strengths close to 30 MPa. Despite the high strength, the volumetric void content was almost eight times the void content observed in welds consolidated at a pressure of 1.6 MPa.
   - A high consolidation pressure of 4.7 MPa produced welds with higher strength than welds consolidated with a consolidation pressure of 1.6 MPa. The voids were low and very concentrated in the weld edges hinting that visible voids were due to squeeze flow of the polymer at the weld edges. This excessive squeeze flow was substantiated by the weld line thickness, which was negative, indicating additional squeeze out of polymer from the adherends.

3. **Research Question**
   How does the presence of sonotrode influence the rate of cooling at the weld interface during the consolidation phase?

   Hypothesis
   The effect of consolidation pressure on cooling rate was assumed to be minimal. The sonotrode contact on the adherend was assumed to influence the cooling rate, which implies that the consolidation time might influence the cooling rate.

Research findings

- The cooling rate in the weld interface increased when welded with a consolidation pressure of 4.7 MPa compared to a weld with a consolidation pressure of 0.6 MPa or 1.6 MPa. The cooling rate at a higher consolidation pressure was most likely aided by increased polymer flow and higher compactness of the carbon fibres, thus resulting in increased heat dissipation. The retraction of the sonotrode was observed to slightly decrease the cooling rates at the weld interface.

4. **Research Question**
   Can the displacement data obtained from the microprocessor be used for in situ monitoring of the consolidation phase?

   Hypothesis
   The displacement of the sonotrode was assumed to show variations during the phase change of the material during consolidation which might aid in establishing a control method for the consolidation phase during the ultrasonic welding process.

   Research findings

   - No distinct stages were found, and hence a control measure using sonotrode vertical displacement could not be formulated. Additionally, the displacement data obtained from the microprocessor was found to be sensitive to the consolidation pressure used. A difference of 0.34 mm was found in the displacement data obtained between a consolidation pressure of 0.4 MPa and 4.7 MPa even though the weld line thickness differed by only 0.04 mm.

6.2. Effect of consolidation parameters on (de)consolidation of continuous ultrasonic welds

Based on the conclusions from static ultrasonic welding, the effect of consolidation parameters on (de)consolidation of continuously welded ultrasonic welds was investigated. This study was restricted to the investigation of the effect of consolidation pressure and the consolidator location behind the sonotrode on the (de)consolidation of ultrasonic welds. The conclusions thus made in chapter 5 are recapitulated below.

1. **Research Question**
   How far can the consolidator be placed away from the sonotrode such that a good consolidation is obtained?

   Hypothesis
   The distance of the consolidator from the sonotrode might depend on the temperature profiles at the weld line. Here again, the consolidator should be so placed that the consolidation extends until the interface temperature drops below Tg.

   Research findings

   - The consolidation pressure application could not be extended until the temperature at the interface dropped below Tc. Placing the consolidator such that consolidation started before the temperature dropped below Tm and continued until the interface temperature dropped below melting temperature meant that the LSS increased almost four times and voids decreased nearly eight times than that of welds which were welded without consolidator

(state-of-the-art continuous ultrasonic welded joints). The consolidation pressure application when the temperature dropped below melting temperature plausibly ensured that the decompaction voids were minimised.

- The use of bar clamps in continuous ultrasonic welding ensured that the voids due to the spring jigs, which was a dominant contributor for void formation in static ultrasonic welding, were eliminated. But, since consolidator pressure application did not extend until the interface dropped below the crystallisation temperature of the polymer meant that shrinkage due to crystallisation is a dominant void formation mechanism. Fibre decompaction were also observed in welds without consolidator and when the consolidator was placed close to the sonotrode. The lower cooling rates in continuous ultrasonic welding compared to static ultrasonic welding aggravated void formation due to excessive polymer squeeze flow.

2. **Research Question**
   Does the continuous ultrasonic welding process require the same consolidation pressure as that of static welding?

   Hypothesis
   It was hypothesised that the consolidation parameters required for continuous ultrasonic welding process might differ from that of the static USW process due to the differences in the boundary conditions of the process. Nevertheless, consolidation pressure application below a threshold value was assumed to lead to laminate deconsolidation. A high consolidation pressure was assumed to lead to excessive squeeze flow from the weld interface.

   Research findings

   - Contrary to static welding, a consolidation pressure of 0.6 MPa was found to give better results in continuous ultrasonic welding than a consolidation pressure of 1.6 MPa in terms of LSS and volumetric void content. This is most likely due to the lower squeeze flow of the polymer in the welds with lower consolidation pressure. The state-of-the-art CUW joints (welds without consolidator) showed a volumetric void content of about 8% which reduced to about 0.7% when welded with a consolidation pressure of 0.6 MPa and the consolidator 80 mm away from the sonotrode. While these results do not increase the process capability to a level where CUW can be industrialised, the observations can be used as a primary step towards improving the maturity levels or the TRLs of the technology.

3. **Research Question**
   How does the presence of the consolidator affect the cooling rates during continuous ultrasonic welding process of thermoplastic composites?

   Hypothesis
   It was hypothesised that the presence of consolidation might affect the cooling rates in CUW. The consolidator was assumed to conduct heat from the welds because of through-thickness heat dissipation, which might reduce the cooling rates in the presence of the consolidator.

   Research findings

   - The presence of the consolidator most likely ensures a more compact packing of the carbon fibre network, thus enabling more heat dissipation through the fibres and the resin, thus increasing the cooling rates at the weld interface. The heat dissipation might also be aided by the excessive squeeze flow of the polymer from the weld interface and the adherend layers.

7

Recommendations

The goal of this research was to develop an understanding regarding the consolidation parameters and their effect on the (de)consolidation in USW process. Studies were initially carried out on static USW and then on CUW with the consolidator behind the sonotrode. A few conclusions were made which have been listed in chapter 6.

This project does not assume to solve any industrialisation concerns but instead aims to bridge the gaps in the knowledge we currently have on the process. This research is just a baseline towards realising a robust industrialised CUW process and concludes with a plethora of opportunities for future work. This section discusses the potential studies that could be incorporated in future work that will further improve the technology readiness levels (TRL) of continuous ultrasonic welding (CUW).

- The welding time and consolidation time in CUW are indirectly controlled via the welding speed. The welding speed will be determined based on the weld quality [43], which implies that the only way by which the consolidation time can be varied is by changing the size of the consolidator. Trials should be carried out with consolidators of longer length to ensure that the consolidation starts before the interface temperature drops below the melting temperature and extend until it drops below crystallisation temperature of the polymer.

- The use of USW in the industry will require welding of intricate shapes, including curvatures. This might require designing roller sonotrode and consolidator. Since the contact area of the roller sonotrode is small, it is hypothesised that the welding speed should be drastically reduced to ensure optimal welding conditions. The lower welding speeds can be beneficial for consolidation, if the consolidator is efficiently designed. The use of pressure rollers is already demonstrated in continuous induction welding process [70, 71].

- The effect of placing a consolidator in front of the sonotrode is discussed in Appendix F. Though not conclusive, the consolidator in front of the sonotrode was observed to help isolate the vibrations and reduce the amount of time that the areas in front of the sonotrode stays above the glass transition temperature of the polymer. This also might help improve the consolidation quality by controlling the through-thickness heating of the specimen.

- New methods can be developed to incorporate active cooling if the cooling rates are to be increased. Separate tooling can be introduced, or the consolidator can be redesigned that would allow for active cooling of the interface during the weld. The use of compressed air ventilation along with the consolidator was already mentioned as a potential active cooling mechanism in continuous induction welding [70].

- The influence of welding parameters on consolidation parameters have not been studied in detail. A higher welding force and amplitude results in an increase in power requirements and faster welding [40] which reduces the heat affected zone. The higher welding parameters might be able to reduce the void formations in the adherend layers in CUW by containing the HAZ within the

weld line and adjacent adherend layers. At the same time, faster welding speeds in CUW implies lower durations of consolidation pressure application. A separate study should be formulated to relate the consolidation parameter requirements to welding force and amplitude.

- The experiments in this thesis were carried out at a coupon level which was assumed to give a primary insight into deconsolidation mechanisms. Nonetheless, industrial use of technology demands welding on larger areas with more intricate shapes and dimensions. This inevitably means that the industrialisation of this technology still needs further research, and the study should be further extended on longer weld lines in CUW. Multi-pass continuous ultrasonic welding might have to be developed to realise welding on thicker adherends and longer weld lines that might be able to contain the heat affected zone to within the weld interface and neighbouring adherend layers.
- Despite investigating the displacement of sonotrode during the consolidation phase in a bid to develop an in-situ control method for consolidation phase in USW, no control method was devised. Developing an in-situ control measure can help duly control the consolidation process.
- Since woven fabrics are known to store more elastic energy than that in a unidirectional fibre architecture, it is expected that the effect of deconsolidation is more pronounced in the woven fabrics. However, in CUW, the use of unidirectional fibre architecture might lead to higher distortion of the fibres and void content due to the motion of the consolidator over the specimens. The consolidation requirements in a unidirectional fibre architecture might be different from that of woven fabrics and needs to be investigated.
- In a carbon fibre reinforced amorphous polymer composite, the consolidation might have to be extended until the interface temperature drops below the Tg of the polymer to obtain a well-consolidated welded joint.

IV

Appendices

A

Weld Control - Optimum Displacement

The static USW process in this study was controlled using the vertical displacement of the sonotrode, i.e., the vibration phase was stopped once the sonotrode reached a predefined vertical displacement. The displacement of the sonotrode is triggered by the melting of the energy director during the welding process [31]. This method of weld control was first reported by Villegas [31] for in situ monitoring of the welding process. This appendix details the tests carried out to determine the optimum downward displacement of the sonotrode to control the static ultrasonic weld efficiently in this study. Considering the variability in the power displacement curves that arose due to the use of the PPS mesh, the optimum displacement was determined from the understanding of the polymer flow during melting of a mesh ED [43] and experimental trials. The reason for controlling the weld via displacement is because it is relatively unaffected by clamping conditions unlike controlling the welding by ”energy control” method [42].

A.1. Results

Figure A.1 shows a typical power displacement curve when welded until the sonotrode had a vertical displacement that corresponded to the thickness of the mesh ED. The displacement curve shows an initial significant increase in displacement until it plateaus at 0.05 mm. The displacement increased henceforth until the end of the vibration phase.

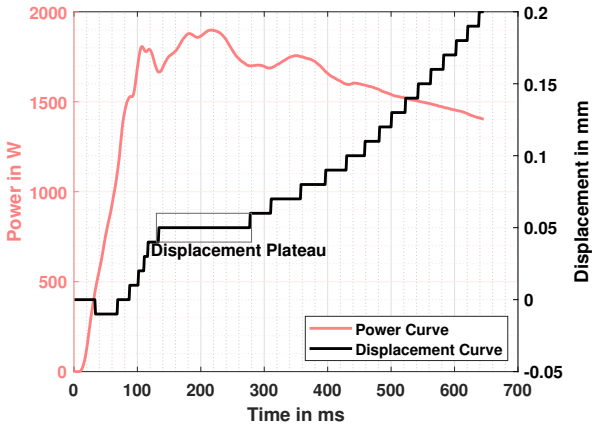

Figure A.1: Representative power displacement curve for an ultrasonically welded CF/PPS specimen; Vibration amplitude (peak-to-peak): 80 µm, welding pressure: 1.6 MPa (500 N), weld control - displacement to 0.20 mm

Specimens were then welded which were controlled by vertical sonotrode movement from 0.06 mm until 0.10 mm. For each displacement configuration of the sonotrode, four specimens were welded. A thermocouple was embedded in the weld interface, but the temperature details are not

considered as it is not the scope of this analysis. The welds were tested for LSS and were reported, as shown in Table A.1 and A.1. LSS was reported to be the highest when the sonotrode vertical displacement was 0.06 and 0.07 mm.

A one-way between subjects ANOVA showed significant effect of sonotrode displacement at $p<0.05$ levels on the single LSS of the welded samples [$F(4,15)=6.43$, $p=0.003$]. Individual t-tests were then carried out which showed no difference between welds welded at a displacement of 0.06 mm and 0.07 mm ($t(6)=-0.32$, $p=0.76$), between 0.07 mm and 0.08 mm ($t(4)=1.64$, $p=0.18$) and between 0.06 mm and 0.08 mm ($t(3)=-1.9$, $p=0.15$). However, the strength between 0.07 mm and 0.09 mm showed significant difference ($t(6)=4.09$, $p=0.006$).

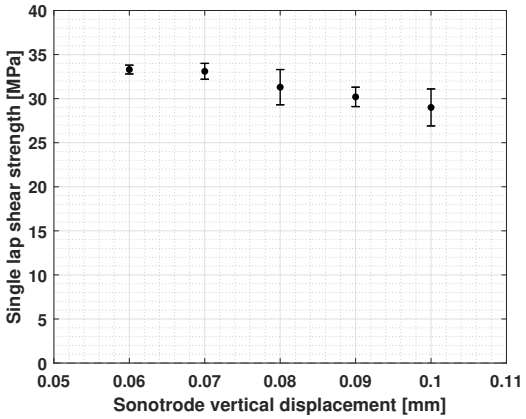

Vertical Displacement of the sonotrode [mm]	LSS [MPa]
0.06	33.3 ± 0.5
0.07	33.1 ± 0.9
0.08	31.3 ± 2.0
0.09	30.2 ± 1.1
0.10	29.0 ± 2.1

Figure A.2 & Table A.1: Lap shear strength for welds carried out with varying sonotrode vertical displacement; Vibration amplitude (peak-to-peak): 80 µm, welding pressure: 1.6 MPa (500 N), consolidation pressure: 1.6 MPa, consolidation time: 4000 ms

Figure A.3 shows the fracture surfaces of the samples welded to varying vertical sonotrode displacements. In specimens welded to displacements of 0.08 mm or more, the excess resin flow resulted in the fibres to distort at the weld edges. Traces of resin-rich areas were seen in the fracture surfaces of almost all welds.

A.2. Discussion

The optimum weld is obtained by controlling the welding process such that the highest LSS is obtained under the given welding parameters [31, 40]. The results obtained indicated that there is no significant difference in LSS between welds carried out at displacements of 0.06 mm, 0.07 mm and 0.08 mm. The LSS from Table A.1 has shown that the optimum displacement for the mesh ED for the given welding configuration is between 0.06 - 0.08 mm. Among these three, displacement of 0.08 mm was discarded due to its lower average strength, although it is not significantly different from 0.06 and 0.07 mm displacements. The fibre at the edges was also seemingly distorted more than when welded to displacements of 0.06 mm and 0.07 mm.

Since the flattening of the mesh ED only completes at the end of the displacement plateau, tests were not extended to 0.05 mm. Both vertical displacements of 0.06 and 0.07 mm showed the same LSS. However, the fracture surfaces showed that 0.06 mm had small traces of intact ED in the weld surface (depicted by the red arrow in Figure A.4a).

Considering that the displacement of 0.06 mm is closer to the displacement plateau and the fracture surfaces show traces of intact energy director, 0.07 mm was chosen as the optimum displacement for the given weld configuration. All static welds in this study were hence controlled by welding to a vertical sonotrode displacement of 0.07 mm.

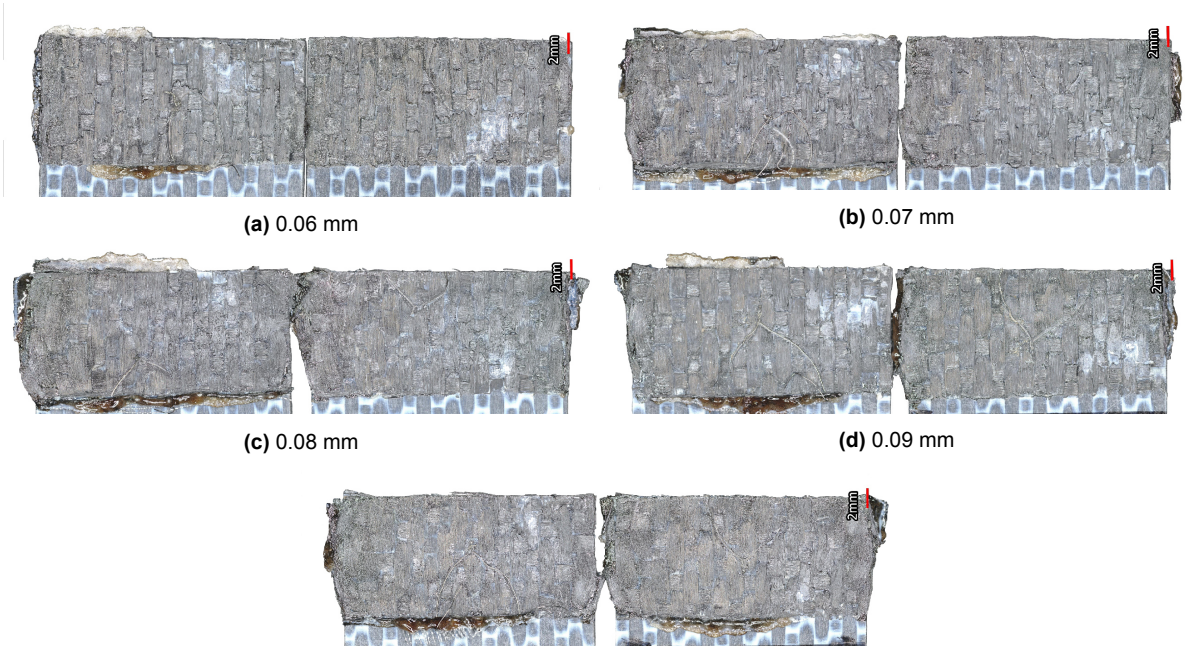

(a) 0.06 mm

(b) 0.07 mm

(c) 0.08 mm

(d) 0.09 mm

(e) 0.10 mm

Figure A.3: Representative fracture surface of specimens welded with varying vertical displacement of the sonotrode; Vibration amplitude (peak-to-peak): 80 µm, welding pressure: 1.6 MPa (500 N), consolidation pressure: 1.6 MPa, consolidation time: 4000 ms

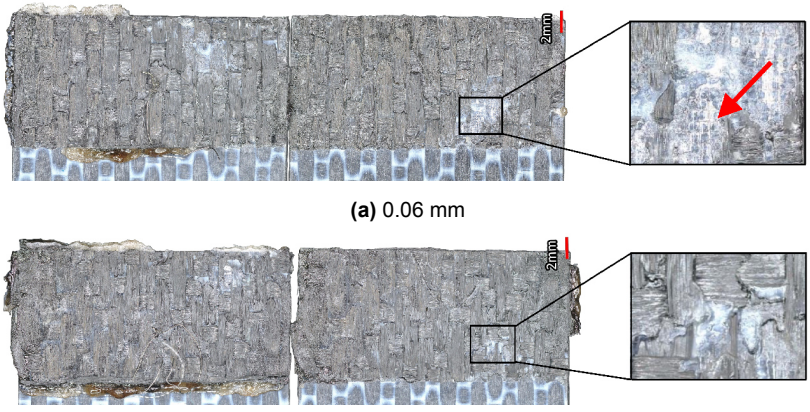

(a) 0.06 mm

(b) 0.07 mm

Figure A.4: Close up view of fracture surfaces welded at different vertical sonotrode displacements

B

Effect of different clamping configurations

The static welding experiments discussed in this study have mostly utilised the spring jig, which was defined in section 4.3. This jig has the added advantage of allowing the top adherend to move down once the energy director starts to flow while maintaining parallelity with the bottom adherend. This ensures that there is no misalignment in the adherends during welding. However, it is known that the welding process also depends on the boundary condition imposed on the weld specimen. Considering that the CUW uses the bar clamp jig, it was imperative to investigate how different clamping conditions influence the weld quality. Three clamping configurations were hence used to introduce different boundary conditions in the welded specimen.

1. The spring jig
2. The Bar clamp jig
3. No clamp configuration

The spring jig has already been discussed in detail in section 4.3 and is as shown in Figure B.1.

The no clamp configuration is a rather novel way of welding, where clamps were not used to hold the specimens in place, but rather by tapes and alignment pins (see Figure B.2). Two aluminium bar clamps were placed on either end to prevent any outward movement of adherends in the transverse direction. The top adherend rested freely on top of the bottom adherend. Additional tapes were used to avoid any untoward movement during welding. The energy director, too, was taped in place before the welding process.

The ”Bar clamp Jig” on the other hand, used two aluminium bar clamps to lock the adherends in place (see Figure B.3). In this case, the top adherend was placed on top of a scrapped piece of the PPS sample to compensate for the thickness of the bottom adherend. The clamps were placed over the adherends to keep them in check. The two metal bars thus prevented any upward or sideways movement during welding. This setup introduced a small misalignment between the two adherends, but the application of the sonotrode pressure was assumed to correct it though not completely.

B.1. Test Results

To investigate the effect of clamping on the consolidation quality, welds were carried out without consolidation. Vibration amplitude of 80 µm and a welding pressure of 1.6 MPa was used. The welds were controlled by sonotrode displacement to 0.07 mm and were stopped after the vibration phase, without allowing to consolidate under pressure. The three jigs, owing to the differences in their

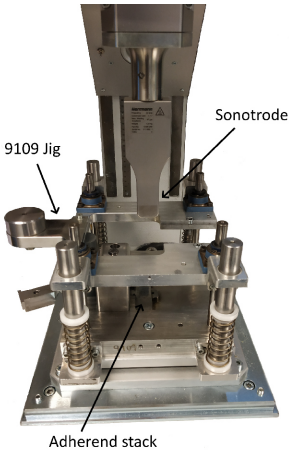

Figure B.1: Spring jig configuration

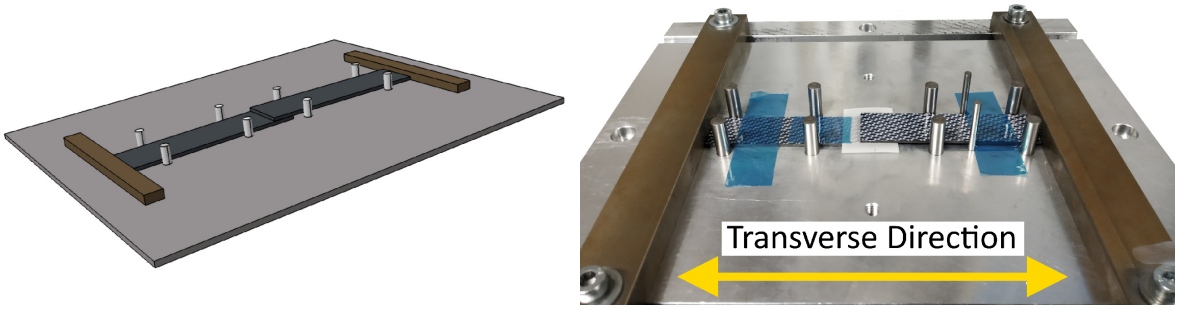

Figure B.2: No clamp configuration

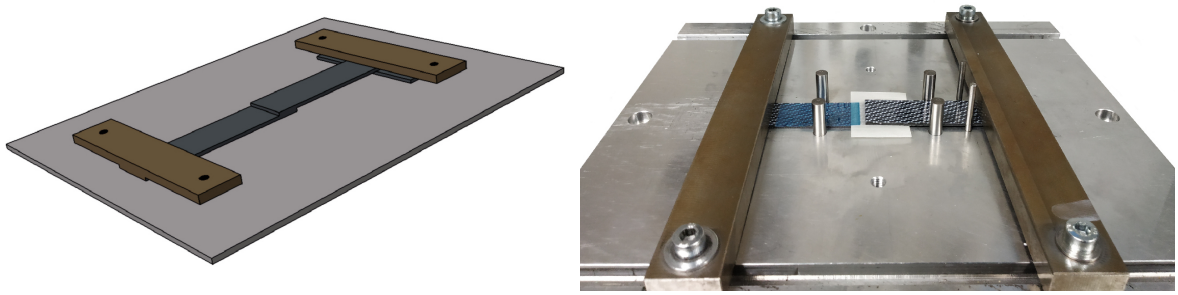

Figure B.3: Bar clamp configuration

clamping mechanism, was presumed to show differences in the consolidation quality. Three welds were carried out per each configuration.

The LSS obtained in all three cases is, as shown in Figure B.4 and Table B.1. The spring jig produced welds which were not consolidated and were separated as soon as it was taken out of the jig. The no clamp configuration produced a slightly better result producing welds with a strength of 6.55 ±0.56 MPa. The bar clamp jig produced welds of superior strength compared to the other clamping configurations.

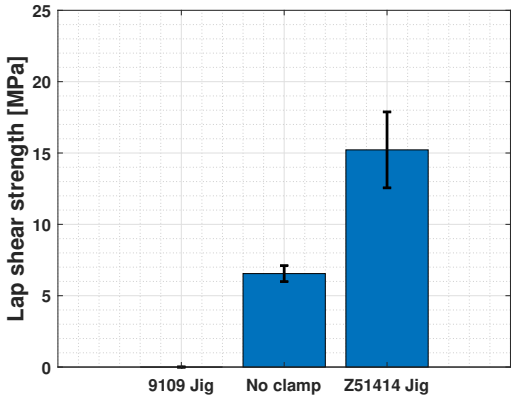

Clamping Mechanism	LSS [MPa]
Spring jig	0
No clamp configuration	6.6 ± 0.6
Bar clamp Jig	15.2 ± 2.7

Figure B.4 & Table B.1: Lap shear strength for welds carried out with different clamping configurations; Vibration amplitude (peak-to-peak) : 80 µm, welding pressure : 1.6 MPa (500 N), weld control - displacement to 0.07 mm

Figure B.5 shows the fracture surface of the welds under all three clamping configurations. As expected, voids were visible at the weld fracture surfaces. The fracture surface of the ”no clamp” configuration looks more uniformly welded than the other two. Intact energy director was found in the welds with bar clamp jig (depicted by the red arrow in Figure B.5c). Voids were visible throughout the weld interface in all three welds.

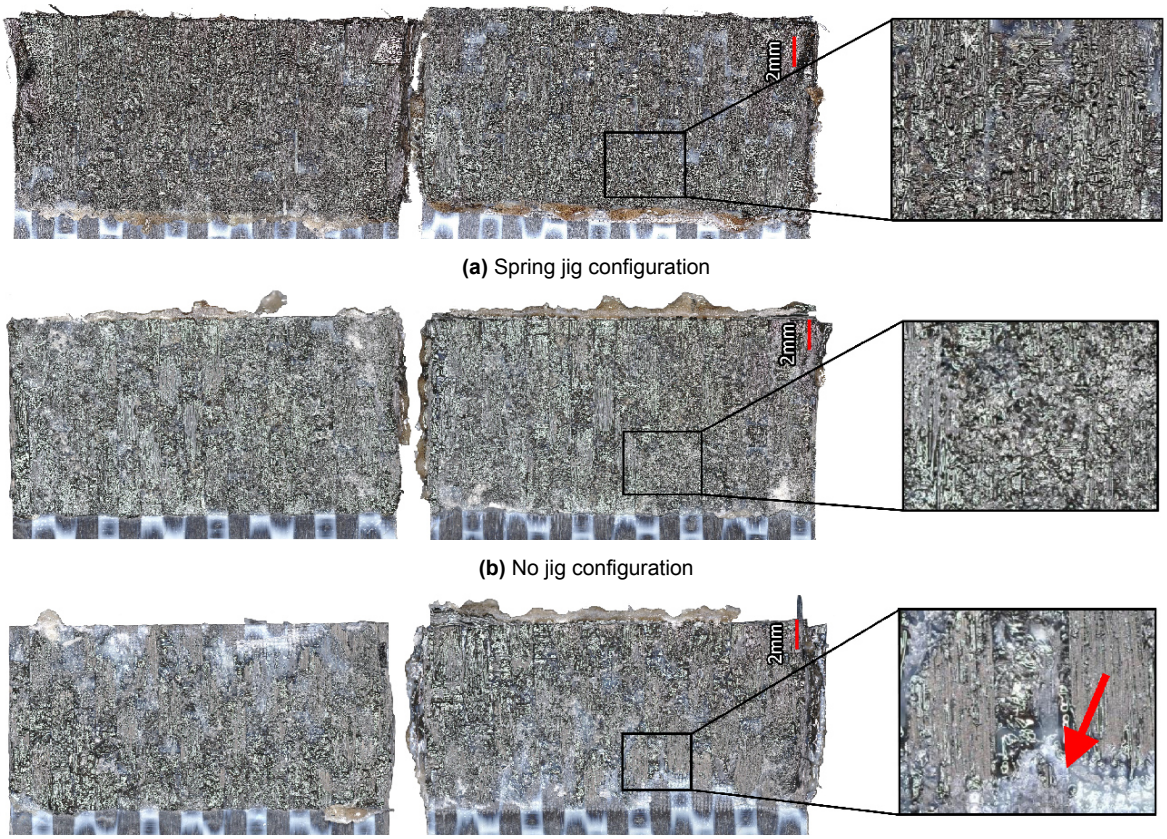

(a) Spring jig configuration

(b) No jig configuration

(c) Bar clamp jig

Figure B.5: Fracture surface of specimens welded without consolidation using three different jig configurations; the red arrow shows traces of intact energy director; Vibration amplitude (peak-to-peak) : 80 µm, welding pressure : 1.6 MPa (500 N), weld control - displacement to 0.07 mm

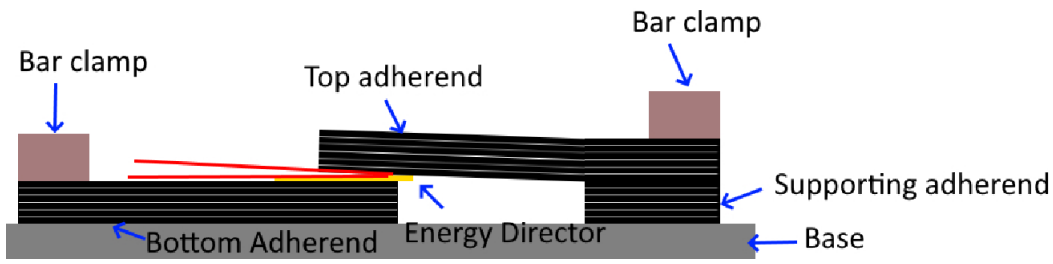

Figure B.6: Misalignment in the adherend positioning in bar clamp jig; the red lines indicate the misalignment in the adherends before welding

The energy utilised during the welding process was also studied. From Table B.2, it can be seen that the bar clamp jig uses higher weld energy when compared to the other two clamping configurations.

Table B.2: Welding energy requirement during welding under different jig configurations; Vibration amplitude (peak-to-peak) : 80 µm, welding pressure : 1.6 MPa (500 N), weld control - displacement to 0.07 mm

Clamping Mechanism	Welding energy [J]
Spring jig	461 ± 21
No clamp configuration	406 ± 24
Bar clamp Jig	632 ± 73

B.2. Discussion

In earlier research, it was observed that the boundary conditions imposed by jigs play a significant role in the welding energy requirements [42]. This was also observed in the tests that were carried out with the three different clamping mechanisms. The higher energy requirement is due to the higher resistance to adherend movement during the welding process. As expected, the bar clamp jig does indeed show the highest energy requirement which might be due to the less uniformity in the strain rates in the energy director due to its intricate design and misalignment in the adherend. In the no clamp configuration, there were no constraints whatsoever and hence shows a lower energy requirement. The spring jig, on the other hand, has a spring mechanism to allow for the vertical movement of the adherends. The spring stiffness might also offer a slight resistance in the vertical motion of the adherends during welding, which might have resulted in a slight increase in the welding energy requirements.

The bar clamp jig introduces additional pressure on the specimen during welding in addition to the welding pressure due to the misalignment between adherends, which is depicted in Figure B.6. This increased pressure might be the reason for the increased LSS compared to the other two jigs. This also meant that the optimum displacement of the sonotrode for the welding parameters so chosen could also vary when different clamps are used. The bar clamp jig also had traces of intact energy director, but these were mainly visible at the weld edges. This was expected as the misalignment between the two adherends would have resulted in a lack of contact at the weld edges. This is also aided by the fact that the displacement for the welding parameter so chosen might not be optimal. In CUW where the bar clamps were used, despite welding without consolidator, the strength was about 15 MPa. The weld in CUW was found to produce consolidated welds, similar in strength as seen in welds without consolidation in static USW when welded using the bar clamps.

The spring jig that was used in the entirety of this study did not produce a welded joint when it was not consolidated. Here, the spring system that is used to ensure parallelism between the specimens at all times during the welding process might be the reason for deconsolidation. The interface temperature at the end of welding is above melting temperature as was observed in part II. It was

already shown in section 4.5.3 that the retraction forces exerted by the springs in the spring jig contribute towards deconsolidation of the welds.

The no clamp configuration shows vast potential as alternate clamping for static welding processes. During the process, there is no additional pressure like in the case of bar clamp jig or deconsolidation aided by the spring system, like in the case of spring jig. The fracture surfaces in the case of spring jig and no clamp configuration showed uniform welded areas. The no clamp configuration neither did deconsolidate the weld nor produced joints with strengths as high as that exhibited by the bar clamp jig.

Hence, these observations only substantiate the claim that the welding jig (or boundary conditions) play a significant role in the consolidation of specimens and strength development.

C

Temperature variation across the weld interface

Due to the very high rate of heating and cooling, and unique boundary conditions of the USW, it was hypothesised that the temperature across the interface would not be uniform. To determine the temperature distribution within the weld interface, the weld area was divided into five different segments (see Figure C.1). All the thermocouples were placed between the energy director (ED) and the bottom adherend. The temperature was assumed to be symmetric along a midline drawn parallel to the length of the adherends. Thermocouple placed at location 1 and location 2 referred to a location at the edge of the bottom adherend, with 1 being at the middle and 2 at the corner respectively. Thermocouple 3 was at the middle of the overlap but the corner. The thermocouples 4 and 5 were placed at the edge of top adherend with 4 being at the corner and 5 at the centre of the overlap respectively. A thermocouple was placed in each one of these segments, and the adherends were welded.

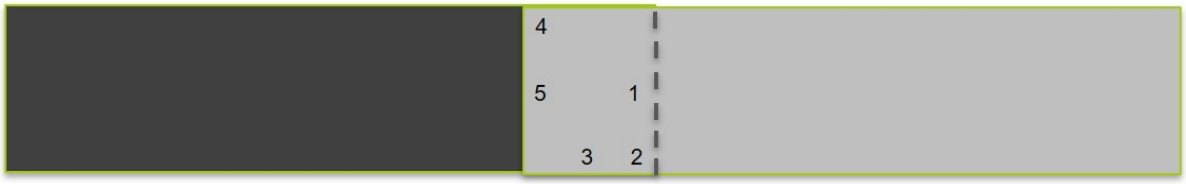

Figure C.1: Location of thermocouples within the weld interface; Bottom adherend is coloured dark

C.1. Test results

Figure C.2 shows a representative temperature curve with a thermocouple at five different locations within the weld interface. Thermocouple location 2 and 3 cooled down the slowest compared to the other thermocouple locations. It should be noted that slight changes in the thermocouple location can result in temperature curves different from the ones shown here. The minor variations can be either due to issues in the placement of the thermocouples before the start of welding or due to the flow of polymer while the ED melts. The order of temperature decrease in this section should hence not be assumed to be the actual temperature differences between the zones within the weld interface. Similar tests have revealed that thermocouple location 2 did indeed cool down slower than thermocouple location 3. At certain instances during consolidation, the difference in temperature within the weld interface was seen to be as high as 60-80 °C.

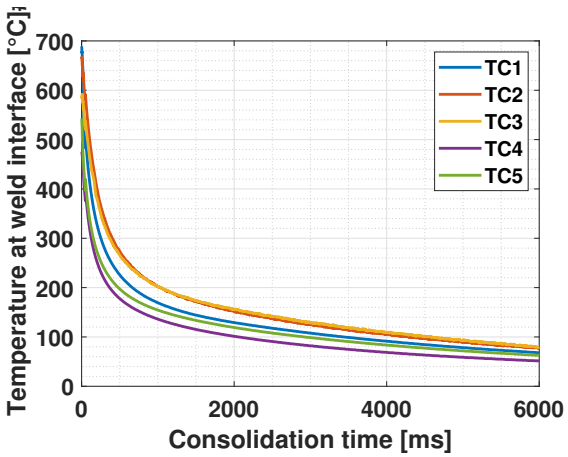

Figure C.2: A representative weld with thermocouples in five locations within the weld interface; Vibration amplitude - 80 µm, welding pressure - 1.6 MPa (500 N), consolidation pressure - 1.6 MPa, consolidation time - 6000 ms

C.2. Discussion

Heat dissipate from the weld interface predominantly through conduction via carbon fibre and polymer flow. Convective heat transfer to the environment surrounding the weld set up also results in heat dissipation but is significantly lower than conductive heat transfer. Carbon fibres being thermally conductive will dissipate heat better than the convective heat transfer. Hence the more a location is surrounded by carbon fibres or adherend material, the more it will dissipate heat faster to the adherend material via the carbon fibres.

Figure C.3 shows the directions through which the fibres can conduct heat away from the weld interface. Potential heat flux directions in top and bottom adherends are shown in Figure C.3. It is clear from the image that locations 2 and 4 should cool down the slowest since they offer the lowest possibility for heat conduction away from the interface. Figure C.3 though does not substantiate that claim about thermocouple location 4. This is most likely because of improper placement of the thermocouple in the weld interface or slight movement in the thermocouple during polymer flow during welding. It should also be noted that the presence of five thermocouples at the weld interface can lead to varying results since the thermocouples can act as energy directors [31].

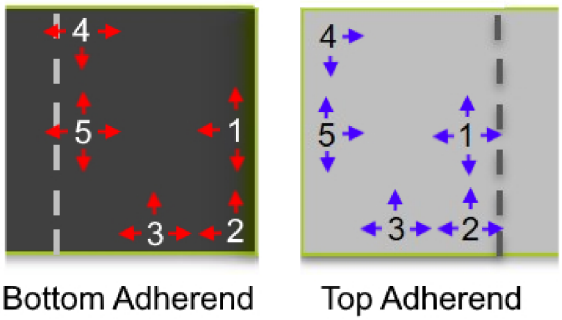

Figure C.3: Depiction of the direction through which the carbon fibres can conduct heat away from the weld interface at the different locations where thermocouple was placed

Nevertheless, based on experimental observations and a possible understanding of the heat conduction in the weld interface, it is assumed that thermocouple location 2 cools down the slowest. Hence this location should be considered while analysing the consolidation parameters since this will be the last zone to undergo any polymeric changes during the consolidation phase. This also ascertains that the cooling in the weld interface during consolidation is not homogeneous. Hence, the choice of thermocouple location within the weld line is of prime importance if the polymeric properties are to be studied.

D

Inter-dependency of consolidation time and consolidation pressure

Part II of this study have detailed the work carried out on the effect of consolidation time and pressure on the weld quality of static ultrasonic welds. In both cases, an effort was made to isolate the effect of one parameter on the other. Now that the effect of consolidation parameters on weld quality was investigated, it was imperative to investigate if the effect of consolidation pressure had an impact on consolidation time and vice versa.

D.1. Test Results

The single LSS of the specimens welded with consolidation pressures of 0.4 MPa, 1.6 MPa and 4.7 MPa with consolidation times of 1000 ms and 10000 ms is plotted in Figure D.1. The strength of the specimens with a consolidation pressure of 0.4 MPa, 1.6 MPa and 4.7 MPa with a consolidation time of 1000 ms follows the same trend as that welded with a consolidation time of 10000 ms. The strength development during welding with varying consolidation time did not show any significant difference in the strength of the welded specimens when welded for 1000 ms or above for consolidation pressures of 0.4 MPa and 1.6 MPa. T-tests carried out between specimens welded with the same consolidation pressure indicates that there is no significant difference in the LSS between specimens welded at different consolidation times at consolidation pressure of 0.4 MPa ($t(4)=-2.72$, $p=0.052$) and 1.6 MPa ($t(8)=-1.59$, $p=0.15$). But a significant difference was seen when welding at different consolidation times with a consolidation pressure of 4.7 MPa ($t(7)=-5.90$, $p=0.0005$).

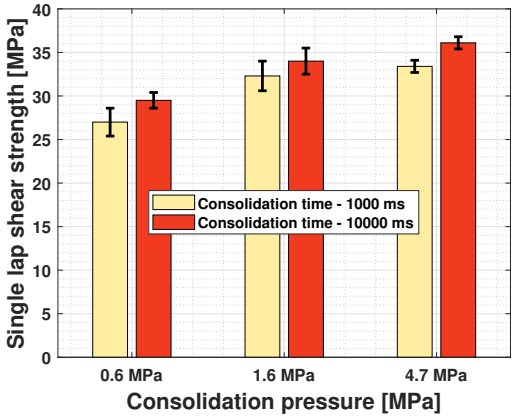

Consolidation time [ms]	Consolidation pressure [MPa]	LSS [MPa]
1000	0.4	27.0 ± 1.6
10000		29.5 ± 0.9
1000	1.6	32.3 ± 1.7
10000		34.0 ± 1.5
1000	4.7	33.4 ± 0.7
10000		36.1 ± 0.7

Figure D.1 & Table D.1: Lap shear strength of welds at varying consolidation pressure and time; Vibration amplitude - 80 µm, welding pressure - 1.6 MPa (500 N), weld control - displacement to 0.07 mm

The fracture surfaces of the configurations are shown in Figure D.2. The specimens welded at a consolidation pressure of 0.4 MPa showed a resin-rich weld interface. The specimen welded with a consolidation pressure of 0.4 MPa and 1000 ms consolidation time showed more resin-rich areas that when consolidated for 10000 ms. Voids were observed in welds consolidated for 1000 ms when compared to welds consolidated for 10000 ms. This was more prominent when the consolidation pressure of 4.7 MPa was used.

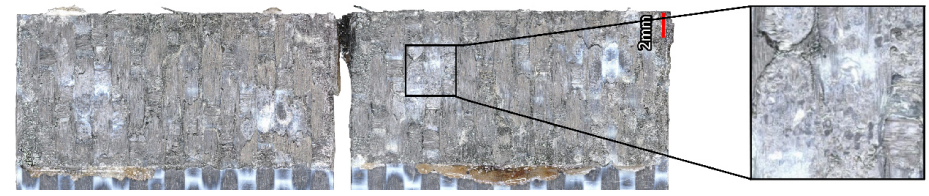

(a) 0.4 MPa; 1000 ms

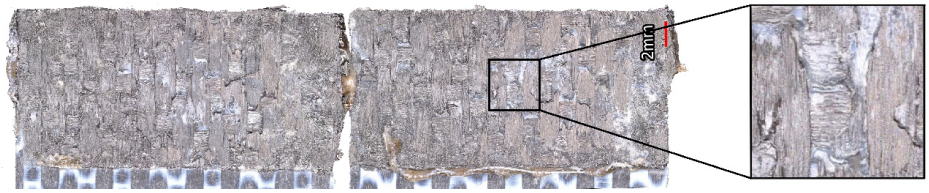

(b) 0.4 MPa; 10000 ms

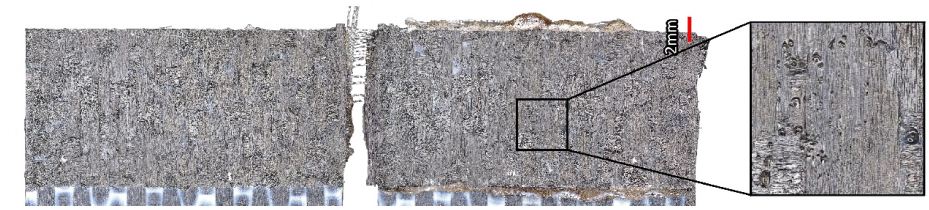

(c) 1.6 MPa; 1000 ms

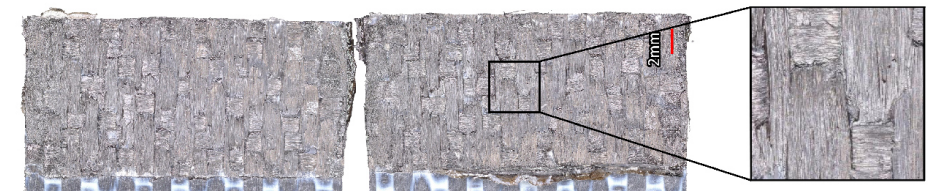

(d) 1.6 MPa; 10000 ms

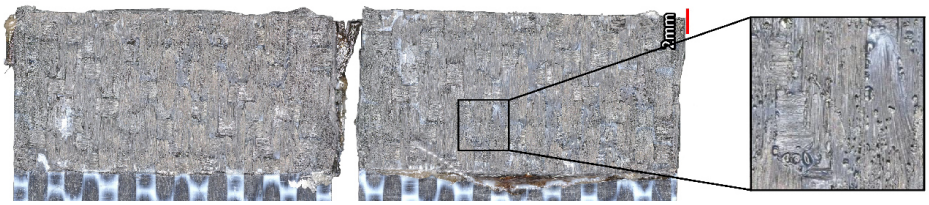

(e) 4.7 MPa; 1000 ms

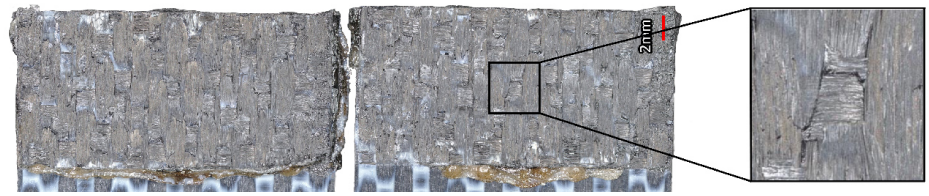

(f) 4.7 MPa; 10000 ms

Figure D.2: Fracture surface of welds at varying consolidation pressure and time; Vibration amplitude - 80 µm, welding pressure - 1.6 MPa (500 N), weld control - displacement to 0.07 mm

D.1.1. Discussion

In section 4.5.3 of chapter 4, it was ascertained that the crystallisation temperature of the specimen plays a significant role in defining what consolidation time would be sufficient to produce a uniformly consolidated welded joint. The cooling rates at varying consolidation pressures were also discussed in section 4.6.3, where a consolidation pressure of 4.7 MPa was found to cool faster than when consolidated with a consolidation pressure of 0.4 MPa or 1.6 MPa.

The results obtained at a consolidation pressure of 1.6 MPa were already discussed in section 4.5.3 of chapter 4. Hence detail discussion is not warranted.

The LSS of specimens consolidated with a consolidation pressure at 4.7 MPa for 1000 ms was slightly lower than that was observed in specimens consolidated with a consolidation pressure at 4.7 MPa for 10000 ms. One plausible reason can be related to the differences in the cooling rates as the consolidation pressure increases. Since the crystallisation decreases with increasing cooling rates, it is highly likely that the welds with high consolidation pressure of 4.7 MPa may have a lower degree of crystallinity than in welds consolidated at a pressure of 1.6 MPa. The lower crystallinity might mean that the influence of the crystal domains might decrease. Thus, the welds may not consolidate even after the interface temperature drops below Tc of the polymer. This might explain why despite the interface temperature falling below crystallisation temperature after 1000 ms of consolidation when consolidated at a pressure of 4.7 MPa, the LSS is still lower at 1000 ms than when welded with a consolidation time of 10000 ms. Besides, the sensitivity in the cooling rates due to the retraction of the sonotrode after 1000 ms of consolidation might be more profound at higher consolidation pressures, though this was not experimentally validated.

Despite the same, it can be safely stated within the scope of the parameters used in this experimental project, that the consolidation pressure does not influence the required consolidation time for obtaining a well-consolidated welded joint. This is also substantiated by the similarity in the fracture surfaces of welds consolidated at different consolidation pressures under the same consolidation time.

E

Distribution of voids - Additional images

This appendix includes a few images from the micro-CT scans that details the distribution of voids within the welded adherends. The yellow plane in Figure E.1, which is the midplane between the two adherends, depict the images in this appendix.

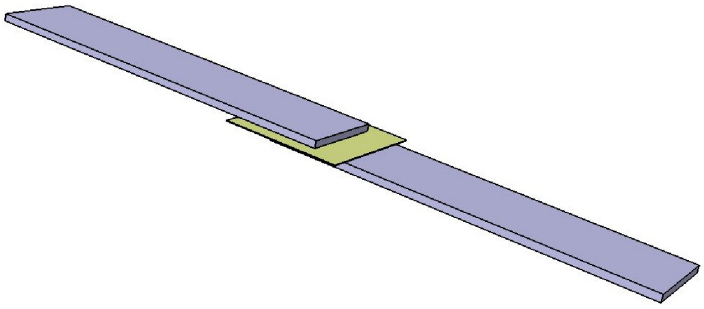

Figure E.1: Plane along the welded joint which has been shown in this appendix

The white areas in the images show the void within the weld interface. Representative images are shown in Figure E.2 to better identify the characteristics from the images in this appendix.

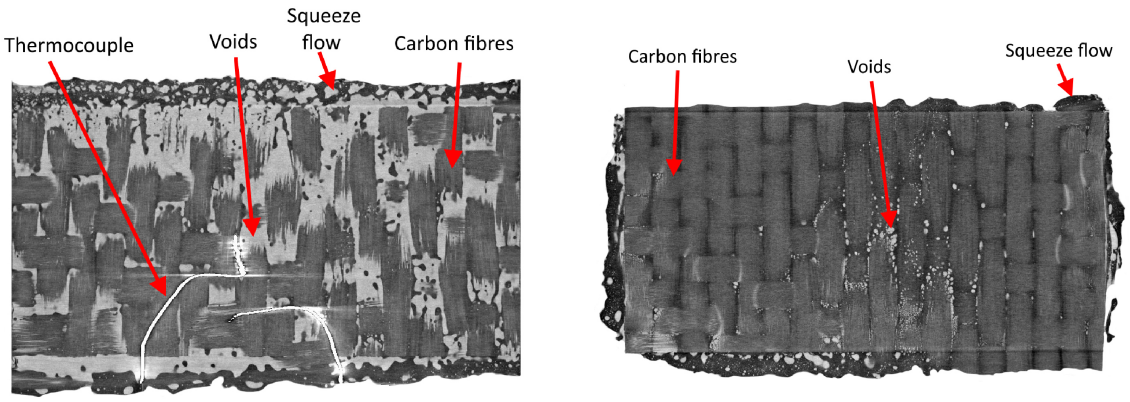

Figure E.2: Depiction of voids in the CT scan images in this appendix

E.1. Results

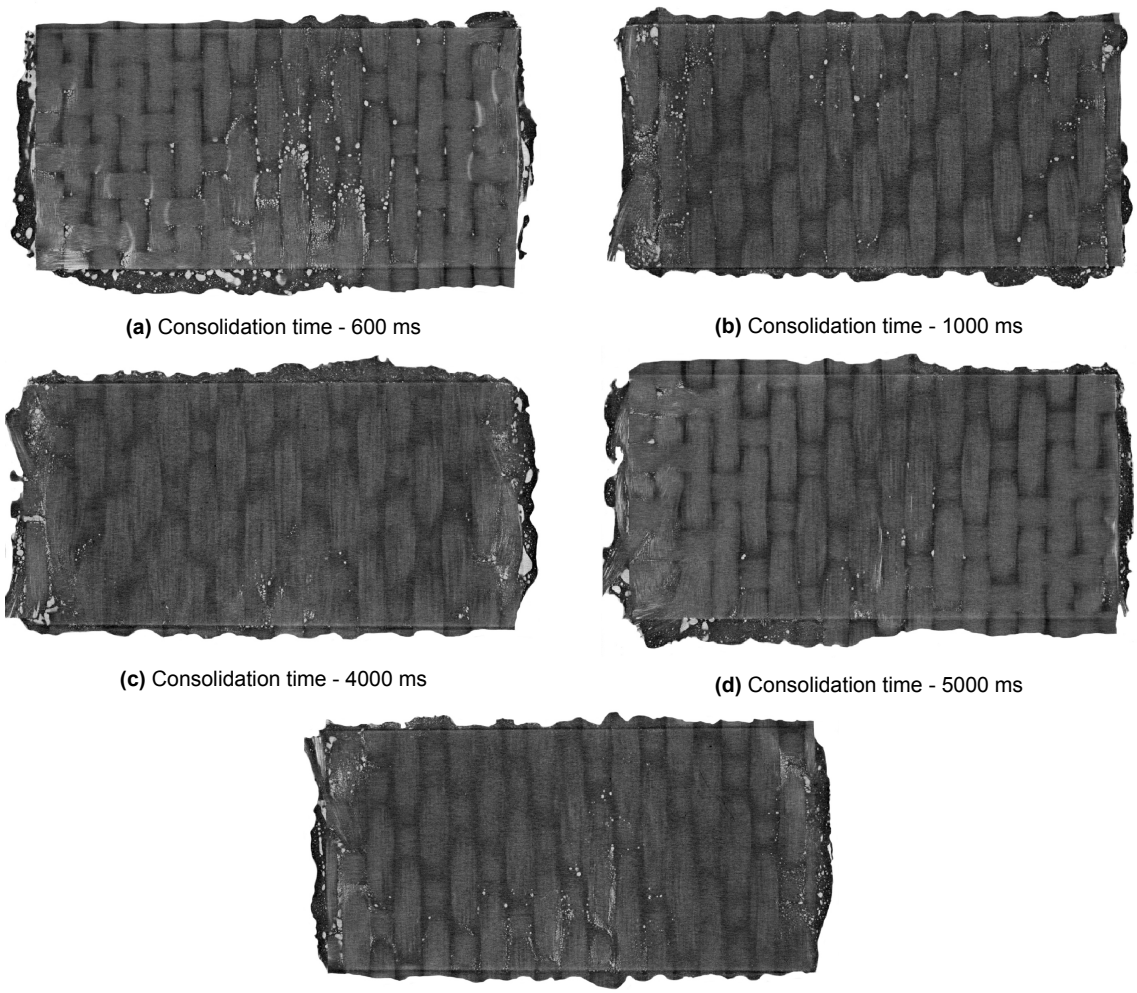

(a) Consolidation time - 600 ms

(b) Consolidation time - 1000 ms

(c) Consolidation time - 4000 ms

(d) Consolidation time - 5000 ms

(e) Consolidation time - 10000 ms

Figure E.3: CT scans of specimens welded with varying consolidation times depicting the distribution of voids within the welded specimens; Vibration amplitude (peak-to-peak) : 80 µm, welding force : 500 N, consolidation pressure : 1.6 MPa, weld control - displacement to 0.07 mm

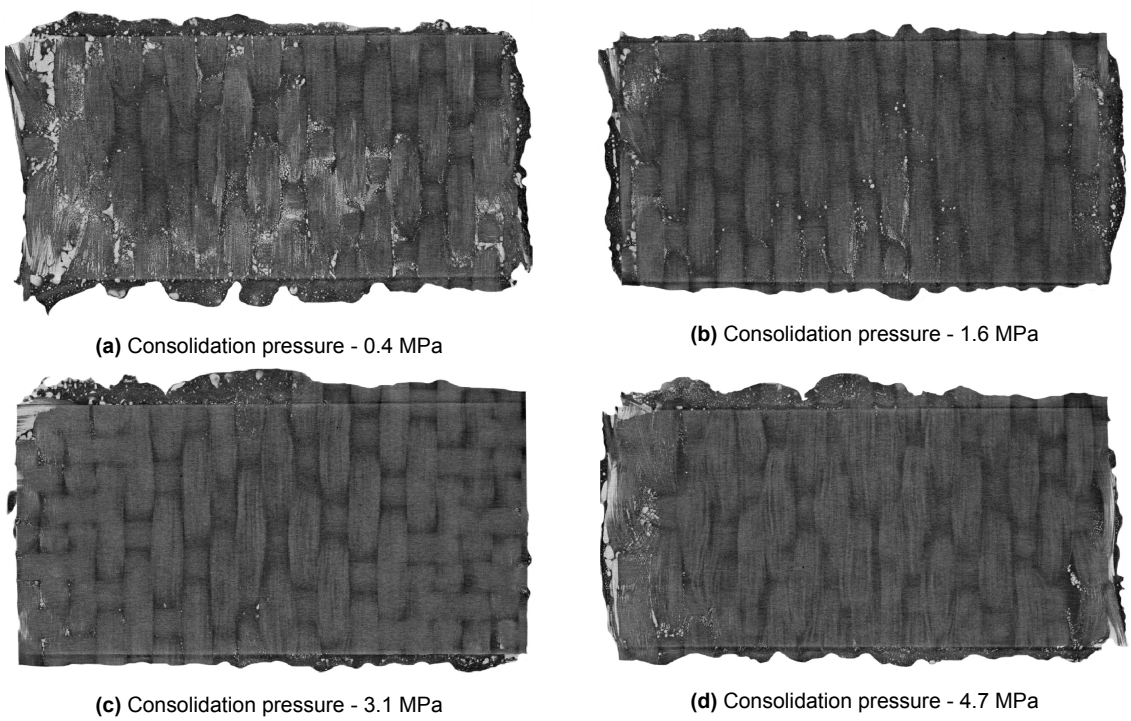

(a) Consolidation pressure - 0.4 MPa

(b) Consolidation pressure - 1.6 MPa

(c) Consolidation pressure - 3.1 MPa

(d) Consolidation pressure - 4.7 MPa

Figure E.4: CT scans of specimens welded with varying consolidation pressures depicting the distribution of voids within the welded specimen; vibration amplitude (peak-to-peak) : 80 µm, welding force : 500 N, consolidation pressure : 1.6 MPa, weld control - displacement to 0.07 mm

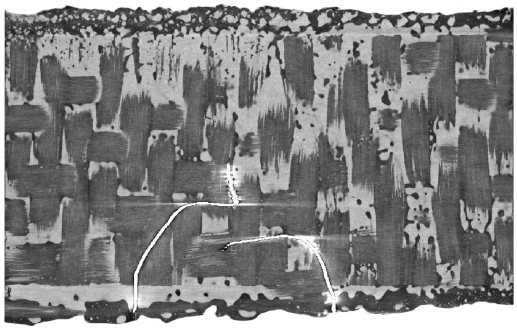

(a) Without consolidation

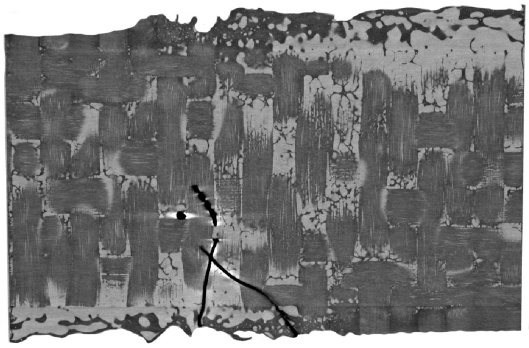

(b) Consolidator 12 mm from the sonotrode; consolidation pressure : 0.6 MPa

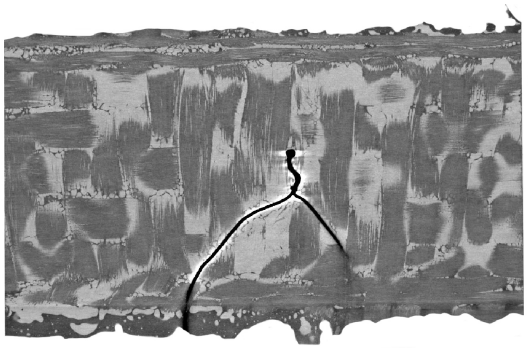

(c) Consolidator 12mm from sonotrode; consolidation pressure : 1.6 MPa

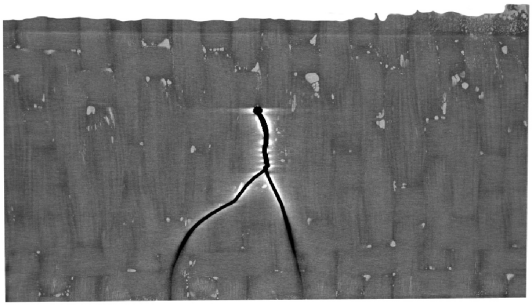

(d) Consolidator 80 mm from the sonotrode; consolidation pressure : 0.6 MPa

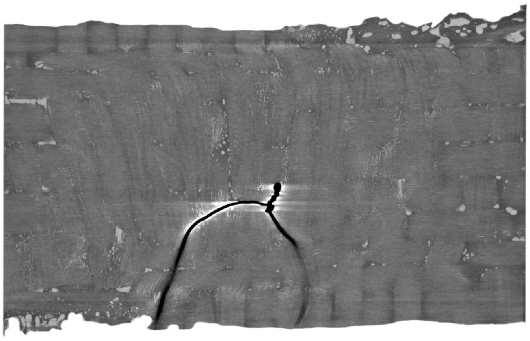

(e) Consolidator 80 mm from the sonotrode; consolidation pressure : 1.6 MPa

Figure E.5: CT scans of specimens welded continuously with varying consolidation parameters; Vibration amplitude (peak-to-peak) : 80 µm, welding force : 500 N, welding speed : 35 mm/s

F

Placing consolidator at the front of the sonotrode

It was initially hypothesised that placing the consolidator close to the sonotrode might result in restraining the transmission of amplitude to further areas aft of the sonotrode. This appendix investigates the effect of placing the consolidator ahead of the sonotrode, as opposed to placing it aft of the sonotrode as was discussed throughout this thesis.

F.1. Test results

Figure F.1 shows the temperature profiles of welds with different positioning of the consolidator near the sonotrode. Three configurations are discussed here - consolidator 12 mm behind the sonotrode, 12 mm in front of the sonotrode and welds without consolidator. The shaded region indicates the duration during which the sonotrode passes over each of the thermocouples.

The temperature profiles of the welds with the consolidator in front of the sonotrode were similar to the other two cases mentioned here. The primary difference though was the amount of time that the weld interface was above Tg when the consolidator was placed in front of the sonotrode. To observe the effect of amplitude transmission to thermocouple locations in front of the sonotrode, the temperature profile at thermocouple location 5 in all three cases can be analysed. When welded without consolidator, the temperature at thermocouple location 5 increased above Tg within 500-1000 ms. Thereafter it stayed above Tg until the sonotrode first made contact with thermocouple location 5 (after about 5000 ms from the start of sonotrode movement) where the interface temperature rose over Tm. When the consolidator was placed behind the sonotrode, the interface temperature increased above Tg in about 2000-2500 ms. When the consolidator was placed in front of the sonotrode, the interface temperature only increased above Tg after almost 4500 ms.

F.2. Discussion

Though the results are not conclusive to ascertain that the presence of consolidator in front of the sonotrode play a significant role in improving the weld quality, the observations are an indication that the presence of consolidator in front of the sonotrode does indeed influence the temperature profiles in the weld interface. The duration of time that the polymer is above Tg when the consolidator is placed in front of the sonotrode is lower than when the consolidator is placed behind the sonotrode or when the welds are made without consolidator. This is indicative of the fact that the presence of consolidator in front of the sonotrode might restrict the transmission of vibrations to areas in front of the sonotrode during welding. Placing a consolidator in front of the sonotrode might also aid the welding of intricate shapes by isolating the vibrations and its transmission to areas between the consolidators at the front and back of the sonotrode.

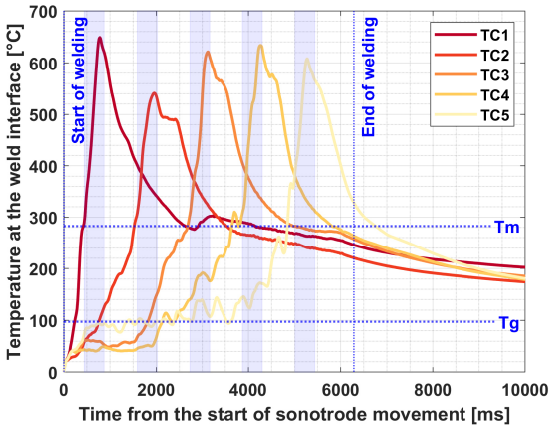

(a) Consolidator 12 mm behind the sonotrode

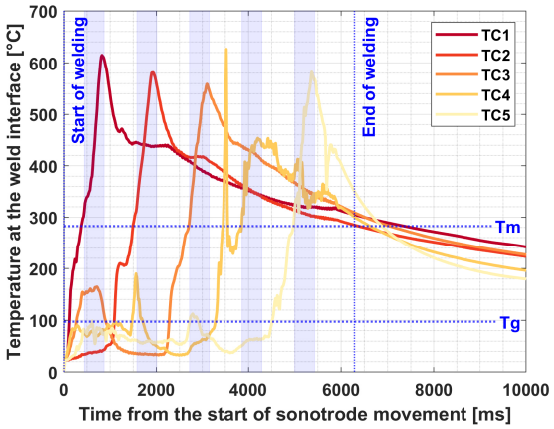

(b) Consolidator 12 mm in front of the sonotrode

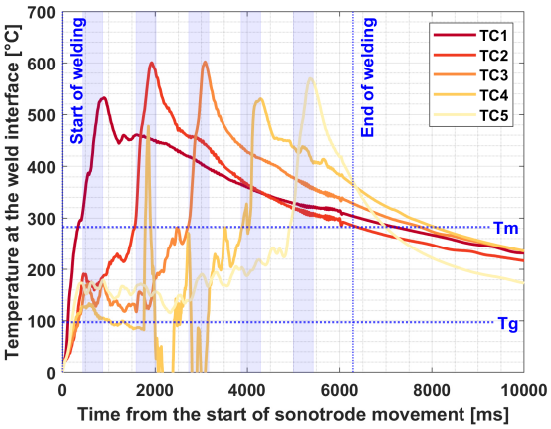

(c) No consolidator

Figure F.1: Temperature gradient at the weld interface in CUW under varying consolidator distances; Vibration amplitude (peak-to-peak): 80 µm, welding force: 500 N, welding speed: 35 mm/s, consolidation pressure: 1.6 MPa

Bibliography

[1] F. Habashi, “History of Metallurgy”, in *Encyclopedia of Materials: Science and Technology*. Dec. 2001, pp. 5537–5541.

[2] *Boeing 747-8: One plane, six million parts: Lufthansa magazine*. [Online]. Available: https://magazin.lufthansa.com/xx/en/fleet/boeing-747-8-en/one-plane-six-million-parts.

[3] J. W. van Ingen, A. Buitenhuis, M. Wijngaarden, and F. Simmons, “Development of the Gulfstream G650 induction welded thermoplastic elevators and rudder”, May 2010.

[4] G. Gardiner, “Thermoplastic composites gain leading edge on the A380”, *High-Performance Composites*, vol. 14, pp. 50–55, Mar. 2006.

[5] *Strategic Research and Innovation Agenda (SRIA), Advisory Council for Aviation Research and Innovation in Europe*. [Online]. Available: https://www.acare4europe.org/sria.

[6] I. F. Villegas, “Ultrasonic Welding of Thermoplastic Composites”, *Frontiers in Materials*, vol. 6, p. 291, 2019.

[7] *The next generation Multifunctional Fuselage Demonstrator - leveraging thermoplastics for cleaner skies*. [Online]. Available: https://www.cleansky.eu/the-next-generation-multifunctional-fuselage-demonstrator-leveraging-thermoplastics-for-cleaner.

[8] *Sprouting growth of Thermoplastic Composites in Aerospace*. [Online]. Available: https://www.stratviewresearch.com/articles/Sprouting-growth-of-Thermoplastic-Composites-in-Aerospace.

[9] I. F. Villegas, L. Moser, A. Yousefpour, P. Mitschang, and H. E. Bersee, “Process and performance evaluation of ultrasonic, induction and resistance welding of advanced thermoplastic composites”, *Journal of Thermoplastic Composite Materials*, vol. 26, no. 8, pp. 1007–1024, 2013. eprint: https://doi.org/10.1177/0892705712456031.

[10] M. Brzeski and P. Mitschang, “Deconsolidation and its Interdependent Mechanisms of Fibre Reinforced Polypropylene”, *Polymers and Polymer Composites*, vol. 23, no. 8, pp. 515–524, 2015. eprint: https://doi.org/10.1177/096739111502300801.

[11] L. Ye, Z.-R. Chen, M. Lu, and M. Hou, “De-consolidation and re-consolidation in CF/PPS thermoplastic matrix composites”, *Composites Part A: Applied Science and Manufacturing*, vol. 36, no. 7, pp. 915–922, 2005.

[12] J. Wolfrath, V. Michaud, and J.-A. Månson, “Deconsolidation in glass mat thermoplastic composites: Analysis of the mechanisms”, *Composites Part A: Applied Science and Manufacturing*, vol. 36, no. 12, pp. 1608–1616, 2005.

[13] L. Ye, M. Lu, and Y.-W. Mai, “Thermal de-consolidation of thermoplastic matrix composites—i. Growth of voids”, *Composites Science and Technology*, vol. 62, no. 16, pp. 2121–2130, 2002.

[14] F. Köhler, B. Jongbloed, T. Filipe, A. Herrmann, I. Villegas, and R. Benedictus, “A Roadmap for developing an Industrial Continuous Ultrasonic Welding Process for Thermoplastic Composites”, in *5th International Conference and Exhibition on Thermoplastic Composites, Bremen, Germany*. Oct. 2018.

[15] *Guide to Ultrasonic Plastics Assembly*, ser. Dukane Intelligent Assembly Solutions. 2011.

[16] T. Zhao, G. Palardy, I. F. Villegas, C. Rans, M. Martinez, and R. Benedictus, “Mechanical behaviour of thermoplastic composites spot-welded and mechanically fastened joints: A preliminary comparison”, *Composites Part B: Engineering*, vol. 112, pp. 224–234, 2017.

[17] T. Zhao, C. Rans, I. F. Villegas, and R. Benedictus, “On sequential ultrasonic spot welding as an alternative to mechanical fastening in thermoplastic composite assemblies: A study on single-column multi-row single-lap shear joints”, *Composites Part A: Applied Science and Manufacturing*, vol. 120, pp. 1–11, 2019.

[18] I. F. Villegas and R. van Moorleghem, “Ultrasonic welding of carbon/epoxy and carbon/PEEK composites through a PEI thermoplastic coupling layer”, *Composites Part A: Applied Science and Manufacturing*, vol. 109, pp. 75–83, 2018.

[19] I. F. Villegas and P. V. Rubio, “On avoiding thermal degradation during welding of high-performance thermoplastic composites to thermoset composites”, *Composites Part A: Applied Science and Manufacturing*, vol. 77, pp. 172–180, 2015.

[20] I. F. Villegas, B. V. Grande, H. Bersee, and R. Benedictus, “A comparative evaluation between flat and traditional energy directors for ultrasonic welding of CF/PPS thermoplastic composites”, *Composite Interfaces*, vol. 22, no. 8, pp. 717–729, 2015. eprint: https://doi.org/10.1080/09276440.2015.1053753.

[21] A. Benatar and T. G. Gutowski, “Ultrasonic welding of PEEK graphite APC-2 composites”, *Polymer Engineering & Science*, vol. 29, no. 23, pp. 1705–1721, 1989. eprint: https://onlinelibrary.wiley.com/doi/pdf/10.1002/pen.760292313.

[22] G. Palardy and I. F. Villegas, “On the effect of flat energy directors thickness on heat generation during ultrasonic welding of thermoplastic composites”, *Composite Interfaces*, vol. 24, no. 2, pp. 203–214, 2017. eprint: https://doi.org/10.1080/09276440.2016.1199149.

[23] N. Tateishi, T. North, and R. Woodhams, “Ultrasonic welding using tie-layer materials. part i: Analysis of process operation”, *Polymer Engineering & Science*, vol. 32, no. 9, pp. 600–611, 1992.

[24] A. Levy, S. Le Corre, and I. F. Villegas, “Modeling of the heating phenomena in ultrasonic welding of thermoplastic composites with flat energy directors”, *Journal of Materials Processing Technology*, vol. 214, no. 7, pp. 1361–1371, 2014.

[25] A. Benatar, “Ultrasonic welding of plastics and polymeric composites”, in *Power Ultrasonics*, J. A. Gallego-Juárez and K. F. Graff, Eds., Oxford: Woodhead Publishing, 2015, pp. 295–312.

[26] V. G. Gutnik, N. V. Gorbach, and A. V. Dashkov, “Some Characteristics of Ultrasonic Welding of Polymers”, *Fibre Chemistry*, vol. 34, no. 6, pp. 426–432, Nov. 2002.

[27] Z. Zhang, X. Wang, Y. Luo, Z. Zhang, and L. Wang, “Study on Heating Process of Ultrasonic Welding for Thermoplastics”, *Journal of Thermoplastic Composite Materials*, vol. 23, no. 5, pp. 647–664, 2010. eprint: https://doi.org/10.1177/0892705709356493.

[28] Z. Zhang, X. Wang, Y. Luo, Z. Zhang, and L. Wang, “Study on heating process of ultrasonic welding for thermoplastics”, *Journal of Thermoplastic Composite Materials*, vol. 23, no. 5, pp. 647–664, 2010. eprint: https://doi.org/10.1177/0892705709356493.

[29] F. Awaja, “Autohesion of polymers”, *Polymer*, vol. 97, pp. 387–407, 2016.

[30] A. Yousefpour, M. Hojjati, and J.-P. Immarigeon, “Fusion Bonding/Welding of Thermoplastic Composites”, *Journal of Thermoplastic Composite Materials*, vol. 17, no. 4, pp. 303–341, 2004. eprint: https://doi.org/10.1177/0892705704045187.

[31] I. F. Villegas, “In situ monitoring of ultrasonic welding of thermoplastic composites through power and displacement data”, *Journal of Thermoplastic Composite Materials*, vol. 28, no. 1, pp. 66–85, 2015.

[32] H. Lu, A. Benatar, and F. He, “Sequential ultrasonic welding of PEEK/graphite composite plates”, in *Proceedings of the annual technical conference ANTEC, Montreal, Quebec, Canada*, 1991.

[33] A. Benatar, R. V. Eswaran, and S. K. Nayar, “Ultrasonic welding of thermoplastics in the near-field”, *Polymer Engineering Science*, vol. 29, no. 23, pp. 1689–1698, eprint: https://onlinelibrary.wiley.com/doi/pdf/10.1002/pen.760292311.

[34] C. Nonhof and G. Luiten, “Estimates for process conditions during the ultrasonic welding of thermoplastics”, *Polymer Engineering & Science*, vol. 36, no. 9, pp. 1177–1183, 1996.

[35] A. Levy, S. Le Corre, and A. Poitou, “Ultrasonic welding of thermoplastic composites: A numerical analysis at the mesoscopic scale relating processing parameters, flow of polymer and quality of adhesion”, *International journal of material forming*, vol. 7, no. 1, pp. 39–51, 2014.

[36] T. Ahmed, D. Stavrov, H. Bersee, and A. Beukers, “Induction welding of thermoplastic composites—an overview”, *Composites Part A: Applied Science and Manufacturing*, vol. 37, no. 10, pp. 1638–1651, 2006.

[37] N. Koutras, J. Amirdine, N. Boyard, I. F. Villegas, and R. Benedictus, “Characterisation of crystallinity at the interface of ultrasonically welded carbon fibre PPS joints”, *Composites Part A: Applied Science and Manufacturing*, vol. 125, p. 105 574, 2019.

[38] R. P. Wool and K. M. O’Connor, “A theory crack healing in polymers”, *Journal of Applied Physics*, vol. 52, no. 10, pp. 5953–5963, 1981. eprint: https://doi.org/10.1063/1.328526.

[39] B. Harras, K. C. Cole, and T. Vu-Khanh, “Optimization of the Ultrasonic Welding of PEEK-Carbon Composites”, *Journal of Reinforced Plastics and Composites*, vol. 15, no. 2, pp. 174–182, 1996. eprint: https://doi.org/10.1177/073168449601500203.

[40] I. F. Villegas, “Strength development versus process data in ultrasonic welding of thermoplastic composites with flat energy directors and its application to the definition of optimum processing parameters”, *Composites Part A: Applied Science and Manufacturing*, vol. 65, pp. 27–37, 2014.

[41] I. F. Villegas and G. Palardy, “Ultrasonic welding of CF/PPS composites with integrated triangular energy directors: Melting, flow and weld strength development”, *Composite Interfaces*, vol. 24, no. 5, pp. 515–528, 2017. eprint: https://doi.org/10.1080/09276440.2017.1236626.

[42] T. Zhao, C. Broek, G. Palardy, I. F. Villegas, and R. Benedictus, “Towards robust sequential ultrasonic spot welding of thermoplastic composites: Welding process control strategy for consistent weld quality”, *Composites Part A: Applied Science and Manufacturing*, vol. 109, pp. 355–367, 2018.

[43] B. Jongbloed, J. Teuwen, G. Palardy, I. F. Villegas, and R. Benedictus, “Continuous ultrasonic welding of thermoplastic composites: Enhancing the weld uniformity by changing the energy director”, *Journal of Composite Materials*, vol. 54, no. 15, pp. 2023–2035, 2020. eprint: https://doi.org/10.1177/0021998319890 40.

[44] B. Jongbloed, J. Teuwen, I. F. Villegas, and R. Benedictus, “Investigation on the melting of the weld interface in continuous ultrasonic welding of thermoplastic composites”, in *22nd International Conference on Composite Materials, Melbourne, Australia*. Aug. 2019.

[45] F. Senders, M. van Beurden, G. Palardy, and I. F. Villegas, “Zero-flow: A novel approach to continuous ultrasonic welding of CF/PPS thermoplastic composite plates”, *Advanced Manufacturing: Polymer & Composites Science*, vol. 2, no. 3-4, pp. 83–92, 2016. eprint: https://doi.org/10.1080/20550340.2016.1253968.

[46] F. Senders, “Continuous Ultrasonic Welding of Thermoplastic Composites”, Master Thesis, Delft University of Technology, 2016.

[47] F. Henninger, L. Ye, and K. Friedrich, “Deconsolidation behaviour of glass fibre-polyamide 12 composite sheet material during post-processing”, *Plastics rubber and composites processing and applications*, vol. 27, no. 6, pp. 287–292, 1998.

[48] C. Ageorges, L. Ye, and M. Hou, “Experimental investigation of the resistance welding of thermoplastic-matrix composites. part ii: Optimum processing window and mechanical performance”, *Composites Science and Technology*, vol. 60, no. 8, pp. 1191–1202, 2000.

[49] C. Ageorges, L. Ye, Y.-W. Mai, and M. Hou, “Characteristics of resistance welding of lap shear coupons.: Part ii. Consolidation”, *Composites Part A: Applied Science and Manufacturing*, vol. 29, no. 8, pp. 911–919, 1998.

[50] M. Lu, L. Ye, and Y.-W. Mai, “Thermal de-consolidation of thermoplastic matrix composites-ii. ”Migration” of voids and ”re-consolidation””, English, *Composites Science and Technology*, vol. 64, no. 2, pp. 191–202, 2004.

[51] Y. Leterrier and C. G’Sell, “Formation and elimination of voids during the processing of thermoplastic of matrix composites”, *Polymer Composites*, vol. 15, no. 2, pp. 101–105, 1994. eprint: https://onlinelibrary.wiley.com/doi/pdf/10.1002/pc.750150203.

[52] V. Michaud and A. Mortensen, “Infiltration processing of fibre reinforced composites: Governing phenomena”, *Composites Part A: Applied Science and Manufacturing*, vol. 32, no. 8, pp. 981–996, 2001.

[53] R. M. Ogorkiewicz, *Thermoplastics: properties and design*. John Wiley & Sons, 1974.

[54] R. I. Tanner, *Engineering rheology*. OUP Oxford, 2000, vol. 52.

[55] X. Xiao, S. Hoa, and K. Street, “Processing and Modelling of Resistance Welding of APC-2 Composite”, *Journal of Composite Materials*, vol. 26, no. 7, pp. 1031–1049, 1992. eprint: https://doi.org/10.1177/002199839202600705.

[56] A. Benatar, “Ultrasonic welding of advanced thermoplastic composites”, PhD. Thesis, Massachusetts Institute of Technology, 1987.

[57] X. Xiao, S. V. Hoa, and K. N. Street, “Repair of thermoplastic resin composites by fusion bonding”, in *Composites bonding*, ASTM International, 1994.

[58] H. Shi, I. F. Villegas, and H. E. Bersee, “Analysis of void formation in thermoplastic composites during resistance welding”, *Journal of Thermoplastic Composite Materials*, vol. 30, no. 12, pp. 1654–1674, 2017. eprint: https://doi.org/10.1177/0892705716662514.

[59] G. Palardy, H. Shi, A. Levy, S. L. Corre, and I. F. Villegas, “A study on amplitude transmission in ultrasonic welding of thermoplastic composites”, *Composites Part A: Applied Science and Manufacturing*, vol. 113, pp. 339–349, 2018.

[60] B. Jongbloed, J. Teuwen, G. Palardy, I. F. Villegas, and R. Benedictus, “Improving weld uniformity in continuous ultrasonic welding of thermoplastic composites”, in *ECCM18 - 18th European Conference on Composite Materials Athens, Greece*. Jun. 2018.

[61] T. Slange, L. Warnet, W. Grouve, and R. Akkerman, “Deconsolidation of C/PEEK blanks: On the role of prepreg, blank manufacturing method and conditioning”, *Composites Part A: Applied Science and Manufacturing*, vol. 113, pp. 189–199, 2018.

[62] J.-F. Lamèthe, P. Beauchêne, and L. Léger, “Polymer dynamics applied to peek matrix composite welding”, *Aerospace Science and Technology*, vol. 9, no. 3, pp. 233–240, 2005.

[63] C. O. Horgan and D. A. Polignone, “Cavitation in Nonlinearly Elastic Solids: A Review”, *Applied Mechanics Reviews*, vol. 48, no. 8, pp. 471–485, Aug. 1995. eprint: https://asmedigitalcollection.asme.org/appliedmechanicsreviews/article-pdf/48/8/471/5437345/471_1.pdf.

[64] A. N. Gent, “Cavitation in Rubber: A Cautionary Tale”, *Rubber Chemistry and Technology*, vol. 63, no. 3, pp. 49–53, Jul. 1990. eprint: https://meridian.allenpress.com/rct/article-pdf/63/3/49/1943276/1_3538266.pdf.

[65] C.-C. M. Ma, C.-L. Lee, M.-J. Chang, and N.-H. Tai, “Hygrothermal behavior of carbon fiber-reinforced poly(ether ether ketone) and poly(phenylene sulfide) composites. i”, *Polymer Composites*, vol. 13, no. 6, pp. 448–453, eprint: https://onlinelibrary.wiley.com/doi/pdf/10.1002/pc.750130608.

[66] C.-C. M. Ma and S.-W. Yur, “Environmental effects on the water absorption and mechanical properties of carbon fiber reinforced pps and peek composites. part ii”, *Polymer Engineering & Science*, vol. 31, no. 1, pp. 34–39, 1991. eprint: https://onlinelibrary.wiley.com/doi/pdf/10.1002/pen.760310107.

[67] M. Balasubramanian, *Composite Materials and Processing*. CRC Press, 2013.

[68] D. Zhang, D. Heider, and J. John W Gillespie, “Void reduction of high-performance thermoplastic composites via oven vacuum bag processing”, *Journal of Composite Materials*, vol. 51, no. 30, pp. 4219–4230, 2017. eprint: https://doi.org/10.1177/0021998317700700.

[69] D. [Vajari], C. González, J. Llorca, and B. N. Legarth, “A numerical study of the influence of microvoids in the transverse mechanical response of unidirectional composites”, *Composites Science and Technology*, vol. 97, pp. 46–54, 2014.

[70] P. Mitschang, R. Rudolf, and M. Neitzel, “Continuous induction welding process, modelling and realisation”, *Journal of Thermoplastic Composite Materials*, vol. 15, no. 2, pp. 127–153, 2002.

[71] T. Ahmed, D. Stavrov, H. Bersee, and A. Beukers, “Induction welding of thermoplastic composites—an overview”, *Composites Part A: Applied Science and Manufacturing*, vol. 37, no. 10, pp. 1638–1651, 2006.

[72] R. Rudolf, P. Mitschang, M. Neitzel, and C. Rueckert, “Welding of high-performance thermoplastic composites”, *Polymers and Polymer Composites*, vol. 7, no. 5, pp. 309–315, 1999.